UNIVERSITÉ DE MONTRÉAL

PATIENT POSITIONING FOR SURGERIES OF THE SPINE: HOW DOES IT IMPACT SPINAL GEOMETRY AND HOW CAN IT BE EXPLOITED TO IMPROVE SURGICAL PROCEDURES

CHRISTOPHER DRISCOLL

INSTITUT DE GÉNIE BIOMÉDICAL

ÉCOLE POLYTECHNIQUE DE MONTRÉAL

THÈSE PRÉSENTÉE EN VUE DE L'OBTENTION

DU DIPLÔME DE PHILOSOPHIAE DOCTOR (Ph.D.)

(GÉNIE BIOMÉDICAL)

DÉCEMBRE 2010

UNIVERSITÉ DE MONTRÉAL

ÉCOLE POLYTECHNIQUE DE MONTRÉAL

Cette thèse intitulée:

PATIENT POSITIONING FOR SURGERIES OF THE SPINE: HOW DOES IT IMPACT SPINAL GEOMETRY AND HOW CAN IT BE EXPLOITED TO IMPROVE SURGICAL PROCEDURES

présentée par : DRISCOLL Christopher

en vue de l'obtention du diplôme de: Philosophiae doctor

a été dûment acceptée par le jury d'examen constitué de:

M. MATHIEU Pierre A., Ph.D., président

M. AUBIN Carl-Éric, Ph.D., membre et directeur de recherche

M. DANSEREAU Jean, Ph.D., membre et codirecteur de recherche

M. MAC-THIONG Jean-Marc, MD, Ph.D., membre

M. GAGNON Denis, Ph.D., membre

DEDICATION

I would like to dedicate this thesis to my wife Julie and kids Silver, Samara, and Stryker who have made all of my life's works worth doing.

ACKNOWLEDGEMENTS

I would like to first thank Carl-Éric Aubin, my research director, who had the biggest impact on my work, providing me with many good ideas and insights over the duration of this project and more importantly showing me what it takes to be a good researcher. I would also like to thank my co-research director Jean Dansereau for his support in establishing research objectives and providing ways to reach them. I would like to thank my colleagues working in the laboratories at Sainte-Justine University Hospital and École Polytechnique for all their technical help and for making the last few years enjoyable ones. I would like to thank Fanny Canet with whom I performed the experimental testing. I would like to thank all the patients and volunteers who participated in the experimental testing as well as Mickaël Cademartoni for coming in at all hours to take x-rays, Julie Joncas for helping me get patients and Souad Rhalmi for helping with the use of the experimental surgery room. I would like to thank the Sainte-Justine and Emory University Hospital orthopaedic surgeons Drs. Hubert Labelle, William Horton, Stefan Parent, and Jean-Marc Mac-Thiong for their input and perspective. I would like to thank my family for encouraging me to take a risk and go back to school. I could never have done it without you. Finally, I would like to thank our financial partners, the Natural Sciences and Engineering Research Council of Canada and Medtronic, especially Scott Drapeau for his input and help in building the positioning system.

RÉSUMÉ

Les cas les plus graves de déformation rachidienne, telles que la scoliose, nécessitent une intervention chirurgicale afin de traiter les symptômes et de réaligner la colonne vertébrale. Au cours de l'intervention chirurgicale, les patients sont habituellement maintenus dans une position en décubitus ventral et une instrumentation est utilisée pour corriger et fixer la géométrie de la colonne. Il a été démontré que le positionnement des patients sur des cadres chirurgicaux a un impact sur la géométrie rachidienne, mais ceci n'est pas exploité afin de faciliter et améliorer les procédures chirurgicales. Les cadres disponibles commercialement ont des capacités limitées de positionnement du patient qui puisse être modifiable durant l'intervention. Aussi, afin d'exploiter éventuellement les diverses possibilités de positionnement, on doit connaître l'impact de ces positions sur la modulation de la géométrie de la colonne vertébrale du patient opéré.

Ce projet a été effectué en parallèle avec la conception et la construction d'un nouveau cadre de positionnement multifonctionnel (MFPF) pour les chirurgies du rachis qui permet le positionnement des membres inférieurs ainsi que le déplacement vertical du thorax. Le MFPF lui-même était une combinaison de deux cadres précédents permettant le positionnement chirurgical: le DPF (permettant le réglage de coussins sur le tronc et l'application de forces correctives) et le "leg positionner" (permettant la flexion et l'extension des membres inférieurs). La modélisation par éléments finis (MEF) a été utilisée pour étudier le positionnement de patient sur le DPF.

Les objectifs spécifiques de ce projet étaient: 1) d'adapter et développer une MEF de la colonne vertébrale, cage thoracique, bassin, et des membres inférieurs qui soit capable de simuler les effets géométriques sur la colonne vertébrale résultant du positionnement en décubitus ventral et de l'ajustement des capacités de positionnement du MFPF; 2) effectuer des essais expérimentaux sur le positionnement en décubitus ventral et les capacités de positionnement du MFPF et utiliser les résultats pour valider le MFF; 3) exploiter le MEF pour développer de nouvelles possibilités de positionnement sur le MFPF permettant de moduler la géométrie de la colonne vertébrale et évaluer ces nouvelles positions expérimentalement avec des accessoires construit pour le MFPF; et 4) exploiter la MEF afin d'étudier l'impact de la combinaison des

capacités de positionnement du MFPF sur la géométrie du rachis, ainsi que développer une méthode pour son optimisation.

Les hypothèses étaient les suivantes: 1) une MEF de la colonne vertébrale, de la cage thoracique, du bassin et des structures adjacentes permet de simuler les effets géométriques, sur la colonne vertébrale, résultant du positionnement en décubitus ventral sur le MFPF avec une précision de 5° pour les angles de Cobb des courbes segmentaires coronale et sagittale; 2) le positionnement des jambes sur le MFPF a un impact significatif sur la géométrie de la colonne vertébrale (i.e. modification de la lordose lombaire de +25%, -40%, la cyphose dorsale de +20%, -10%, et réduction de l'angle de Cobb coronal primaire de 10% par rapport à la position neutre de référence); et 3) l'utilisation combinée des capacités de positionnement du MFPF a un impact significatif sur la géométrie de la colonne vertébrale qui peut être utilisée intra-opératoirement pour faciliter les procédures d'instrumentation rachidienne (i.e. modification de la lordose lombaire de +30%, -60%, la cyphose dorsale de +60%, -30%, et réduction de l'angle de Cobb coronal primaire de 25% par rapport à la position neutre de référence).

Dans le cadre du premier objectif, les membres inférieurs, y compris les muscles, les ligaments et les articulations ont été ajoutés à une MEF déjà développée de la colonne vertébrale, cage thoracique et bassin. La géométrie des membres inférieurs peut être personnalisée à un patient spécifique basé sur des mesures directes ou par mise à l'échelle en utilisant des équations anthropométriques.

Dans le cadre du second objectif, des essais expérimentaux du positionnement en décubitus ventral et des membres inférieurs ont été réalisés avec 10 sujets sur le MFPF, qui ont ensuite été reproduits avec la MEF spécifique à ces sujets pour tester sa validité. La MEF a ensuite été exploitée pour une étude plus approfondie du positionnement en décubitus ventral (par exemple l'impact de la configuration des coussins thoraciques) et le positionnement des membres inférieurs (par exemple, des positions plus extrêmes et intermédiaires des jambes) qui n'auront pas été possibles avec uniquement des tests expérimentaux. De plus, le déplacement vertical du thorax sur le MFPF a été expérimentalement évalué pour son impact sur les courbures sagittales sur 6 sujets.

Dans le cadre du troisième objectif, trois nouveaux concepts de positionnement chirurgical ont été développés (rotation latérale des jambes, torsion du bassin, et déplacement latéral du thorax) basés sur des simulations effectuées a priori avec la MEF. Des prototypes de ces nouveaux concepts de positionnement ont été fabriqués et expérimentalement évalués sur 10 sujets pour leur capacité de réduire les déformations scoliotiques.

Dans le cadre du quatrième et dernier objectif, l'impact combiné de toutes les capacités du MFPF a été étudié avec un plan d'expériences effectué avec la MEF dont les résultats ont été utilisés pour développer des méthodes d'optimisation pour les paramètres géométriques individuels et globaux de la colonne vertébrale.

Les essais expérimentaux ont donné les résultats suivants:

- Le positionnement en décubitus ventral sur le MFPF a induit une réduction significative des courbes scoliotiques coronales, telles que mesurées par les angles de Cobb MT et TL/L, ainsi qu'une réduction significative de la lordose lombaire et de la cyphose thoracique.
- Le positionnement des membres inférieurs sur le MFPF a eu un impact significatif sur les courbures sagittales de la colonne vertébrale. La flexion de la hanche a entraîné une réduction de lordose et cyphose et l’extension de la hanche a entraîné une augmentation de la lordose et de la cyphose.
- Le déplacement vertical du sternum par le MFPF a eu un impact significatif sur les courbures sagittales de la colonne vertébrale. Lever le sternum a causé une augmentation significative de la cyphose et de la lordose ainsi qu’un augmentation de l’espace intervertébrale dans la zone apical du segment thoracique.
- Le déplacement latéral des jambes sur le MFPF a permis une réduction significative de l'angle de Cobb et de la rotation vertébrale apicale (RVA) dans la courbure structurale inferieure quand les jambes sont fléchies du côté de la convexité scoliotique.
- La torsion pelvienne sur le MFPF a permis une réduction significative des angles de Cobb et de la RVA de la courbure structurale inférieure en levant le bassin sur le côté concave de la courbure scoliotique et le coussin thoracique opposé.

Des simulations avec la MEF du positionnement en décubitus ventral, flexion/extension des jambes, et positionnement combiné incluant le déplacement vertical du thorax, déplacement latéral du thorax, déplacement latéral des jambes, et torsion pelvienne a donné les résultats suivants:

- La MEF a été en mesure de reproduire la réduction des courbes segmentaires lors du positionnement en décubitus ventral sur le MFPF avec une précision de 5°.
- Les courbes segmentaires de la colonne vertébrale du patient en position debout et la position relative verticale des coussins thoraciques et pelviens du MFPF ont eu un impact important sur les changements géométriques de la colonne lors du positionnement en décubitus ventral. La position relative longitudinale des coussins thoraciques et pelviens du MFPF n'a pas eu d'impact sur la géométrie de la colonne.
- La MEF a été capable de reproduire les changements géométriques de la colonne vertébrale dû au positionnement des membres inférieurs sur le MFPF avec une précision de 5°.
- Le positionnement des membres inférieurs entre les limites physiologiques (30° d'extension à 90° de flexion) a causé une diminution linéaire de la lordose et cyphose (en moyenne 84% (59°) et 34% (13°)) qui est influencée principalement par la flexibilité des ischio-jambiers.
- L'utilisation combinée des différents systèmes de positionnement du MFPF a permis une plus grande possibilité d'ajustement de la géométrie intra-opératoire de la colonne vertébrale que leur utilisation individuelle. L'impact du positionnement combiné sur le MFPF était dépendant du type de courbe scoliotique.
- Une méthode a été développée afin de déterminer le positionnement optimal du patient sur le MFPF pour à la fois les paramètres géométriques de la colonne vertébrale individuelle et la géométrie globale en fonction des besoins de chaque chirurgien.

L'utilisation des capacités de positionnement du MFPF permet de manipuler un grand nombre de paramètres géométriques de la colonne vertébrale. Plusieurs des capacités de positionnement nouvelles ont un potentiel pour l'amélioration des procédures d'instrumentation rachidienne en offrant aux chirurgiens une large gamme d'ajustements de la géométrie du rachis pendant l'opération. La MEF développée a permis l'étude détaillée des positions opératoires

existantes ainsi qu’à en développer des nouvelles. Enfin, la MEF a permis d'optimiser l'utilisation combinée de plusieurs positions opératoires.

ABSTRACT

The most severe cases of spinal deformity, such as scoliosis, require surgical intervention in order to treat symptoms and re-align the spine. During surgical procedures, patients are typically kept in the prone position while surgical instrumentation is utilized to manipulate and fix spinal geometry. Patient positioning on surgical frames has been shown to have an impact on spinal geometry which can be exploited in order to facilitate and improve upon surgical procedures. Current commercial surgical frames have no or limited patient positioning capabilities. In order to best take advantage of a surgical frame's positioning capabilities, knowledge must be gained on how they will impact a given patient's spinal geometry.

This project was done in parallel with the design and construction of a new Multi-Functional Positioning Frame (MFPF) for spinal surgeries which allowed for lower limb positioning and thoracic vertical displacement. The MFPF itself was a combination of two previously developed surgical positioning devices: the Dynamic Positioning Frame (DPF) (allowing thoracic cushion adjustment and corrective force application) and the "leg positioner" (allowing hip flexion and extension). Finite element modeling (FEM) was previously used to study patient positioning on the DPF.

The global objective of this thesis was to study how patient positioning on a frame can be used in order to improve scoliosis instrumentation procedures through the intra-operative manipulation of spinal geometry. The specific objectives of this project were: 1) adapt and develop a FEM of the spine, thoracic cage, pelvis, and adjacent structures that is able to simulate the geometric effects on the spine resulting from prone positioning and feature adjustment on the MFPF; 2) experimentally test the impact of prone positioning and feature adjustment on the MFPF and utilize the results to validate the FEM; 3) exploit the FEM in order to study additional surgical positions allowing modification of spinal geometrical parameters not possible on the original MFPF design and experimentally assess these new positions using proof of concept features constructed for the MFPF; and 4) exploit the FEM in order to study the impact of combined MFPF positioning parameters on the geometry of the spine (especially the leg positioning and thoracic components) including developing a method allowing for individual and

global optimization of spinal geometrical parameters.

It was hypothesized that: 1) a FEM of the human spine, thoracic cage, pelvis, and relevant adjacent structures can simulate the geometric effects, on the spine, resulting from a patient moving from a standing position to a prone position on the MFPF with a coronal and sagittal plane Cobb angle accuracy of 5° for a segmental curve; 2) leg positioning has an important impact on the geometry of the spine. Manipulation of a patient's leg position while on the MFPF can modify lumbar lordosis by +25%, -40%, thoracic kyphosis by +20%, -10%, and reduce the primary coronal plane Cobb by 10% relative to a neutral prone position; and 3) the combined use of the MFPF positioning features has an important impact on the geometry of the spine which can be utilised intra-operatively to facilitate spinal instrumentation procedures. Combined use of the MFPF positioning features can modify lumbar lordosis by +30%, -60%, thoracic kyphosis by +60%, -30%, and reduce the primary coronal plane Cobb angle by 25% relative to the neutral prone position.

In the context of the first objective, lower limbs including muscles, ligaments, and joints were added to a previously developed FEM of the spine, ribcage and pelvis. Lower limb geometry can be personalized to a specific patient based on direct measurement or by scaling using anthropometric equations.

In the context of the second objective, experimental testing of prone positioning and hip flexion/extension was performed on the MFPF with 10 subjects which was reproduced with patient-specific FEMs in order to test validity. The FEMs were then exploited to further study aspects of prone positioning (e.g. impact of thoracic cushion configuration) and lower limb positioning (e.g. more extreme and intermediate leg positions) which were not possible through experimental testing alone. Thoracic vertical displacement was also experimentally tested with 6 subjects.

In the context of the third objective, three novel surgical positions on the MFPF were developed (lateral leg rotation, pelvic torsion and lateral thoracic displacement) based on FEM

simulations. Prototype features were fabricated and experimentally tested on 10 subjects for their impact of scoliotic deformity parameters.

In the context of the fourth and final objective, the combined impact of all the MFPF positioning features were studied through a design of experiment using the FEM the results of which were used to develop methods of optimization for both individual spinal geometrical parameters and global spinal geometry.

Experimental testing yielded the following results:

- Prone positioning on the MFPF resulted in a significant loss in Main Thoracic (MT) and Thoraco-Lumbar/Lumbar (TL/L) Cobb angles, a significant loss in lordosis and an important loss in kyphosis.
- Lower limb positioning on the MFPF had a significant impact on both sagittal curves of the spine. Hip flexion resulted in reduction of lordosis and kyphosis and hip extension resulted in increases in lordosis and kyphosis.
- Vertical displacement of the sternum on the MFPF had a significant impact on both sagittal curves of the spine. Raising the sternum resulted in a significant increase in kyphosis and lordosis in addition to an increase in intervertebral disc space in the apical thoracic segment.
- Lateral leg displacement on the MFPF allowed for a significant reduction of Cobb angle and Apical Vertebral Rotation (AVR) in the lowest structural curve by lateral displacement of the lower limbs towards the scoliotic spine convexity.
- Pelvic torsion on the MFPF allowed a significant reduction in Cobb angles and important reductions in AVR by raising the pelvis on the concave side of their lowest structural curve and opposite thoracic cushion

FEM simulations of prone positioning, hip flexion/extension, and combined positioning including thorax vertical displacement, thorax lateral displacement, lower limb lateral displacement and pelvic torsion yielded the following results:

- The FEM developed was able to reproduce segmental curve reductions due to prone positioning on the MFPF within 5°.

- Patient and surgical frame parameters such as standing segmental curves and relative vertical position of thoracic cushions had an important impact of spinal geometrical changes due to prone positioning while the relative longitudinal position of the thoracic cushions had no impact.
- The FEM developed was able to reproduce sagittal curve changes due to lower limb positioning on the MFPF within 5°.
- Lower limb positioning between limit physiological positions (30° of extension to 90° of flexion) resulted in a relatively linear decrease in lordosis and kyphosis (an average of 84% (59°) and 34% (13°)) which is most influenced by flexibility of the hamstrings during flexion.
- Combined use of the MFPF features offered a wider range of possible intra-operative spinal geometrical manipulation as compared to their individual use which was dependent on scoliotic curve type.
- A method for determining patient positioning on the MFPF allowed for global optimization of spinal geometry based on the needs of individual surgeons.

Use of the MFPF positioning features allowed for a wide range of spinal geometrical parameters to be manipulated. Several of its novel positioning features have great potential for the improvement of spinal instrumentation procedures by offering surgeons a wider range of possible intra-operative geometries. The FEM developed allowed for the detailed study of existing surgical positions as well as aided to develop some new ones. Finally, the FEM allowed for optimization of the combined use of multiple surgical positions.

CONDENSÉ EN FRANÇAIS

Une colonne vertébrale normale est droite dans le plan coronal et courbée dans le plan sagittal (avec des lordoses cervicale et lombaire et des cyphoses thoracique et coccygienne). Cette géométrie permet entre autre une mobilité intervertébrale et l'absorption de chocs. Il y a plusieurs pathologies qui causent une déformation de la colonne vertébrale, notamment la scoliose qui cause des courbes dans le plan coronal et des rotations vertébrales dans le plan transversal. Pour les cas de déformations sévères, une intervention chirurgicale est requise. Des vis et/ou crochets sont installés sur les vertèbres qui sont ensuite interconnectés avec des tiges qui permettent l'application de forces correctives. Ces interventions sont relativement empiriques et nécessitent de faire des compromis au niveau de la correction. Par ailleurs, d'importantes forces sont requises, ce qui peut engendrer la défaillance ou l'arrachement des implants.

Pendant les opérations par approche postérieure, les patients sont disposés en position décubitus ventral sur une table opératoire. Plusieurs différents types de tables opératoires sont commercialement disponibles comme la table Relton-Hall et la table Jackson. Ces tables permettent quelques ajustements de la position, principalement dans le plan sagittal. Une nouvelle table opératoire a été développée au CHU Sainte-Justine et à l'École Polytechnique, à partir de deux projets antérieurs : la table de positionnement dynamique (« dynamic positioning frame ») qui permettait la réduction de déformations scoliotiques avec des coussins pouvant appliquer des forces correctives et le dispositif de positionnement des membres inférieurs (« leg positioner ») qui permettait une flexion et extension des jambes. Cette nouvelle table, le « Multi-Functional Positioning Frame » ou MFPF, a plusieurs composantes permettant le positionnent du patient dans le plan sagittal notamment la flexion et extension des jambes de -50° à +20° et le déplacement vertical du sternum de ±15 cm.

La modélisation par éléments finis (MEF) permet l'étude biomécanique de la colonne vertébrale. Par exemple, une MEF personnalisée des structures osséo-ligamenteuses de la colonne, cage thoracique et bassin a été développée au CHU Sainte-Justine et à l'École

Polytechnique, basée sur une reconstruction 3D à partir de radiographies biplanaires de patients et les propriétés matérielles tirées de la littérature.

Des études antérieures ont étudié l'impact du positionnement opératoire sur la géométrie de la colonne vertébrale. Elles ont trouvé que le positionnement en décubitus ventral cause une réduction significative des courbes coronales. Des résultats contradictoires ont cependant été trouvés pour l'impact du positionnement en décubitus ventral sur les courbes sagittales; certaines ont documenté une augmentation des courbes alors que d'autres ont trouvé une réduction. La flexion des hanches réduit la lordose mais seulement pour quelques positions des jambes et l'impact sur la cyphose et les courbes coronales n'a pas été considéré. Des pressions d'interfaces importantes entre le patient et les coussins de positionnement ont été relevées. L'utilisation combinée des composantes du MFPF et son impact sur la géométrie de la colonne vertébrale de chaque patient demeurent à être explorés de même qu'une méthode pour l'optimisation du positionnement.

L'objectif global de ce projet était l'étude de l'impact du positionnent sur le MFPF sur la géométrie de la colonne vertébrale et comment peut-il être exploité pour améliorer les interventions chirurgicales. Les objectifs spécifiques de ce projet étaient: 1) d'adapter et développer un MEF de la colonne vertébrale, cage thoracique, bassin et membres inférieurs qui soit capable de simuler les effets sur la colonne vertébrale résultant du positionnement en décubitus ventral et de l'ajustement selon les composantes de positionnement du MFPF; 2) effectuer des essais expérimentaux sur le positionnement en décubitus ventral, évaluer les capacités de positionnement du MFPF et utiliser les résultats pour valider le MFF; 3) exploiter le MEF pour développer de nouvelles possibilités de positionnement sur le MFPF permettant de moduler la géométrie de la colonne vertébrale et évaluer ces nouvelles positions expérimentalement; et 4) utiliser le MEF afin d'exploiter les capacités de positionnement du MFPF pour optimiser l'effet sur la géométrie du rachis et les forces nécessaires lors de l'instrumentation chirurgicale.

Les hypothèses de ce projet étaient les suivantes: 1) une MEF de la colonne vertébrale, de la cage thoracique, du bassin et des structures adjacentes permet de simuler les effets

géométriques, sur la colonne vertébrale, résultant du positionnement en décubitus ventral sur le MFPF avec une précision de 5° pour les angles de Cobb des courbes segmentaires coronale et sagittale; 2) le positionnement des jambes sur le MFPF a un impact significatif sur la géométrie de la colonne vertébrale (i.e. modification de la lordose lombaire de +25%, -40%, la cyphose dorsale de +20%, -10%, et réduction de l'angle de Cobb coronal primaire de 10% par rapport à la position neutre de référence); et 3) l'utilisation combinée des capacités de positionnement du MFPF a un impact significatif sur la géométrie de la colonne vertébrale qui peut être utilisée intra-opératoirement pour faciliter les procédures d'instrumentation rachidienne (i.e. modification de la lordose lombaire de +30%, -60%, la cyphose dorsale de +60%, -30%, et réduction de l'angle de Cobb coronal primaire de 25% par rapport à la position neutre de référence).

Trois types de positionnement sur le MFPF original ont été évalués expérimentalement : le positionnement en décubitus ventral avec 6 patients scoliotiques, la manipulation des membres inferieurs avec 4 volontaires sains, et le déplacement vertical du sternum avec 6 volontaires sains. Des radiographies ont été prises dans les divers positions soit: debout, en décubitus ventral sur le MFPF, et en décubitus ventral intra-opératoire sur le Relton-Hall, avec les jambes en extension et en flexion, et finalement avec le sternum en bas ou déplacé verticalement vers le haut. Les changements géométriques de la colonne vertébrale entre les diverses positions ont été mesurés. Divers tests de flexibilités ont aussi été effectués avec ces sujets. Un MEF des structures osséo-ligamenteuses de la colonne vertébrale, cage thoracique et bassin a été adapté pour ce projet. Les membres inférieurs ont été ajoutés ainsi que les muscles qui les relient au bassin. Leurs géométrie et déplacements limites ont été personnalisés avec des mesures directes sur les sujets. Des propriétés mécaniques publiées ont été attribuées. De plus, les poids et centres de masses de chaque segment vertébral ont été calculés. Des simulations préliminaires ont été effectuées avec le MEF pour identifier les muscles sous tension durant la flexion et extension des jambes ainsi que sa sensibilité de réponse lors de la flexion des genoux, de la modification de la tension initiale des muscles des membres inférieurs et de la superficie transversale des muscles des membres inférieurs. Des simulations avec les MEF personnalisés des 6 patients scoliotiques et 4 volontaires sains ont reproduit les positionnements expérimentaux en décubitus ventral et la flexion/extension des membres inférieurs. Ceci a été effectué avec des propriétés de base pour les

disques et muscles respectivement ainsi qu'avec leurs propriétés optimisées à l'aide de plans d'expériences. Suite à l'optimisation, les MEF ont été exploités pour étudier les facteurs qui peuvent influencer la géométrie de la colonne vertébrale durant le positionnement en décubitus ventral. Ils ont aussi été exploités pour étudier l'impact du positionnement des jambes sur une plus grande amplitude de mouvement que possible avec le MFPF, de 30° en extension à 90° en flexion par intervalle de 20°.

Trois nouvelles composantes ont été développées pour le MFPF pour le positionnement de patients avec déformations scoliotiques. Le « lateral limb displacer » permet d'effectuer une flexion latérale du rachis en déplaçant les jambes latéralement de 60°, le « pelvic torsion device » permet une rotation pelvienne dans le plan transversal de 30°, et le « lateral thoracic displacer » permet un déplacement latéral du thorax de 15 cm. Les deux premières composantes ont été évaluées expérimentalement avec 12 patients scoliotiques. Des radiographies ont été prises en position décubitus latéral neutre sur le MFPF et en utilisant les composantes pour réduire les déformations scoliotiques. Les jambes ont été tirées vers la convexité de la courbe structurale inférieure et le bassin a été levé du côté de la concavité de la courbe structurale inferieure. Les changements géométriques de la colonne vertébrale entre ces positions ont été mesurés et les patients questionnés sur leur niveau de confort.

L'utilisation combinée des différentes composantes du MFPF a été étudiée avec les MEF de patients avec trois types de courbes scoliotiques différentes. Les positions limites des 5 composantes du MFPF ont été simulées. À partir des résultats, des équations de régressions quadratiques ont permis de décrire chaque paramètre géométrique en terme de positionnement sur le MFPF. Ces équations étaient ensuite optimisées pour atteindre une valeur de correction désirée (par exemple : 0° de Cobb ou une cyphose physiologique de 37°). L'utilisation de toutes les composantes du MFPF a été comparée à l'utilisation de seulement la composante la plus influente. Les équations décrivant l'effet de chaque paramètre géométrique ont été combinées dans deux équations globales qui tenaient en compte de leur valeur désirée et leur importance relative : une équation normalisée et une équation avec un facteur d'échelle relatif permettant la comparaison de différentes mesures (angles de courbes, angle de rotations et des distances). Les équations globales ont été optimisées pour trois conditions opératoires différentes.

Les 6 patients scoliotiques avaient des flexibilités de colonne vertébrale variées (réductions de Cobb entre 0% et 70%) mais ont tous eu une réduction des courbes scoliotiques dû au positionnement en décubitus ventral sur le MFPF entre 12% et 26%. Les réductions intra-opératoires sur le Relton-Hall étaient en moyenne 16% plus grande que celles sur le MFPF. Pour les 4 sujets volontaires sains, passer de la position des jambes en extension à celle en flexion a causé une réduction de la lordose (42% à 65%) et de la cyphose (8% à 18%). Ces réductions étaient hautement corrélées (r=-1) aux flexibilités des ischio-jambiers et moyennement corrélées (r=-0.63) aux largeurs des cuisses. Une équation a été développée afin de prédire la réduction de lordose en fonction de la rotation de la hanche et la flexibilité des ischio-jambiers. Le déplacement vertical du sternum des 6 sujets volontaires sains a causé une augmentation des courbes sagittales ainsi que la hauteur des disques intervertébraux à l'apex de la cyphose. Ce déplacement était accompagné d'une translation du thorax (8 cm) et une légère (<1 cm) compression de la cage thoracique. Les modifications de la géométrie du rachis n'étaient pas reliées aux tests de flexibilité. Les trajectoires des capteurs optoélectroniques ont montré que le déplacement du haut du thorax suivait celui du « sternum vertical displacer » et qu'il y avait un déplacement postérieur de la tête. Les pressions d'interfaces mesurées entre le tronc et le MFPF ont passé de 26 mmHg (coussins thoraciques en position neutre) à 111 mmHg (coussin du sternum) lors du déplacement vertical.

Les simulations effectuées avec le MEF ont permis d'identifier que les muscles des ishio-jambiers étaient sous tension pendant la flexion des jambes tandis que les muscles des cuisses étaient sous tension pendant l'extension des jambes. Elles ont aussi démontré que le niveau de flexion des genoux a un impact important sur les changements de lordose pendant la flexion des hanches et que la tension initiale des muscles des membres inferieures est le facteur le plus influant sur les modifications de courbes sagittales pendant la flexion et extension des hanches. Avec les propriétés mécaniques des disques intervertébraux de base, les MEF des 6 patients scoliotiques avaient une précision en moyenne inférieure à 5° pour reproduire les changements géométriques de la colonne vertébrale durant le positionnement en décubitus ventral pour toutes les courbes segmentaires sauf l'angle de Cobb thoracique et la cyphose qui avaient des erreurs moyennes respectives de 14° et 6°. L'optimisation à partir des radiographies en inflexion latérale a amélioré légèrement la précision du MEF (10° erreur pour le Cobb thoracique). L'optimisation

à partir des radiographies en position décubitus ventral a permis d'atteindre une précision moyenne inférieure à 5° pour toutes le courbes segmentaires. Les MEF des 4 volontaires sains, avec les tensions des muscles des membres inférieurs de base, ont sous-estimé la perte de lordose pour les cas d'ischio-jambiers non-souples. Suite à l'optimisation, ils ont atteint une précision de 5° pour les changements géométriques des courbes sagittales.

L'exploitation des MEF des 6 patients scoliotiques a montré que plus les courbes segmentaires étaient importantes en position debout, plus la réduction était importante pendent le positionnement en décubitus ventral. La position relative des coussins thoraciques et pelviens a eu un impact important sur la réduction des courbes sagittales. La modification de la position verticale des coussins thoraciques par rapport aux coussins du bassin sur le MFPF a entraîné respectivement une augmentation ou réduction de la lordose et cyphose. L'exploitation des MEFs des 4 volontaires sains a montré que les changements de lordose et cyphose, sur la plus grande amplitude de mouvement, étaient approximativement linéaires. Des simulations additionnelles de flexion et extension des jambes avec des MEFs de patients scoliotiques ont démontré qu'il n'avait pas d'impact sur les courbes scoliotiques (<4° de réduction).

Pour 6 patients scoliotiques, le déplacement de leurs jambes vers la convexité de leurs courbes structurales distales a réduit en moyenne les angles de Cobb et les rotations vertébrales apicales de 39% et 33% respectivement. Pour 4 patients scoliotiques, lever le bassin du côté de la concavité de la courbe structurale distale a réduit en moyenne les angles de Cobb et les rotations vertébrales apicales de 19% et 48% respectivement. Dans les deux cas, les réductions étaient hautement corrélées aux réductions obtenues lors des tests de flexion latérale. Tous les patients ont trouvé le MFPF assez confortable.

L'optimisation du positionnement combiné des 5 composantes du MFPF a permis d'améliorer les paramètres géométriques (21% plus proche de leur valeur cible) par rapport à l'utilisation de seulement la composante la plus influente. Ceci a permis, pour les trois types de courbes, d'obtenir des courbes sagittales <2° de leurs valeurs physiologiques, une réduction de Cobb de 49% à 66%, le rétablissement de la balance sagittale et coronale, une augmentation de la

hauteur des disques intervertébraux de 18% à 29%, et une réduction de la rotation apicale vertébrale thoracique de 71%.

Les paramètres géométriques de la colonne vertébrale étaient en moyenne manipulés d'une manière significative par 3 composantes du MFPF. La composante du MFPF qui influençait le plus de paramètres géométriques était le « lateral thoracic displacer » et celui qui influençait le moins de paramètres géométriques était le « lower limb positioner ». Les positions dans lesquelles les différents paramètres géométriques ont été optimisées sur le MFPF étaient différents pour les différentes types de courbes, cependant, il y avait certaines tendances qui se répétaient.

L'utilisation de la deuxième équation globale d'optimisation (avec le facteur d'échelle relatif) durant les simulations de positionnement combinées sur le MFPF a permis une meilleure adéquation des paramètres géométriques de la colonne vertébrale avec leurs valeurs désirées (comparativement a l'équation normalisé). Dans le position globalement optimisée, les paramètres géométriques étaient plus loin de leurs valeurs désirées comparativement à l'optimisation individuelle avec toutes les composantes du MFPF mais plus proche de leurs valeurs désirées comparativement à l'optimisation individuelle avec seulement la composante du MFPF le plus influent. Finalement, les positions optimales globales étaient différentes pour les différents stages opératoires.

Avec les nouvelles techniques chirurgicales, certains chirurgiens sous-estiment l'importance du positionnement opératoire des patients. Les instrumentations modernes sont puissantes, et l'utilisation adéquate du positionnement sur une table comme le MFPF pourrait offrir des avantages comme l'amélioration de l'accès aux éléments vertébraux postérieurs, la réduction des déformations scoliotiques au moment de l'insertion des tiges et l'atténuation de la perte de courbes sagittales durant le positionnent en décubitus ventral. Pour les nouvelles chirurgies minimalement invasives, durant lesquelles l'application de forces de correction avec l'instrumentation est limitée, des corrections des déformations scoliotiques peuvent être obtenues avec le positionnement opératoire qui peuvent ensuite être maintenues (exemple avec des agrafes). Ce projet a démontré l'utilité de la MEF. Elle a permis l'étude et le développement de nouvelles composantes de positionnement. La MEF a aussi permis l'étude de positionnements

plus complexes exploitant les nouvelles possibilités offertes par le MFPF, qui seraient difficiles expérimentalement en raison du grand nombre d'essais requis. Finalement, la MEF a offert une possibilité de personnalisation et prédiction pour un patient spécifique.

La MEF avait certaines limites en raison des hypothèses simplificatrices utilisées pour sa construction. Les simplifications géométriques peuvent avoir impacté la précision des résultats et n'ont pas permis l'étude de la distribution de contraintes dans les disques intervertébraux pour les divers positions du MFPF. Des améliorations peuvent être apportées au MFPF comme : la combinaison de toutes les composantes des membres inférieures sur un support de bassin avec joint universel, et un support thoracique qui permet une rotation transversale.

Les conclusions relatives aux hypothèses posées dans cette thèse sont les suivantes. Une précision de 5° en moyenne a été atteinte pour le positionnement en décubitus ventral. La flexion et extension des membres inferieures ont permis la manipulation de la lordose de +18%, -76% et de la cyphose de +10%, -28%. Les valeurs ciblées d'augmentation n'ont pas été atteintes à l'aide de la manipulation des jambes, mais elles sont possibles avec le « sternum vertical displacer ». La flexion et extension des membres inferieures n'ont pas permis une modification des courbes scoliotiques mais tirer les jambes latéralement a permis une réduction supérieure aux valeurs ciblées de 10%. Finalement, l'utilisation combinée des composantes du MFPF a permis d'atteindre ou de se rapprocher des valeurs ciblées (lordose +32%, -56%; cyphose +55%, -52%; et Cobb -19% a 27%) .

Ce travail de thèse a permis de générer des connaissances utiles pour le positionnement opératoire lors des chirurgies de la scolioses. Des essaies expérimentaux et des simulations avec un MEF ont permit le développement et évaluation de plusieurs nouvelles composantes d'une table opératoire. Une méthode pour l'optimisation de l'utilisation combinée de plusieurs composantes d'une table opératoire a été développé.

TABLE OF CONTENT

LIST OF TABLES

LIST OF FIGURES

LIST OF ANNEXES

INTRODUCTION

Patient positioning is an important step in spinal surgeries (Schonauer et al. 2004). Proper patient positioning should facilitate exposure, minimize bleeding, minimize chance of damage to vital structures, allow proper ventilation, avoid post-operative morbidity, and preserve sagittal alignment. Patient positioning also has an impact on spinal geometry. Studies have shown the relationship between hip flexion and loss of lumbar lordosis (Stephen et al. 1996 and Benfanti et al. 1997), prone positioning and the reduction in Cobb angles (Delorme et al. 2000) and sagittal curves (Jackson et al. 2005), back flexion/extension and degree of spondylolisthesis vertebral slip (Luk et al. 2003), and lateral force application on the deformity apex and the reduction in rib hump (Duke et al. 2002). It has been hypothesized that surgical effort (forces applied during instrumentation manoeuvres) can be reduced, and in some cases surgical results improved, if the spinal geometry is in the desired configuration for a given spinal surgery (Duke et al. 2005). Despite this, current operating tables used in spinal instrumentation/fusion procedures, such as the Relton-Hall and Orthopaedic Systems Inc. frames (Jackson, Wilson, and Andrews) allow limited spinal geometry modification through patient positioning.

A new multi-functional positioning frame (MFPF) has been developed at École Polytechnique and CHU Sainte-Justine (US Patent 7,234,180) (Canet 2008). It incorporates a mobile support for easy transportation, a static head rest, two movable arm rests, a leg positioning system that allows for hip movement from 60° flexion to 20° extension while maintaining the tibias at an angle of 20° above horizontal, a pelvic support cushion which is adjustable in height, thoracic cushions which are adjustable in height and horizontal direction, and a sternum vertical displacer which can rise 15 cm above the neutral plane established by linking the femoral heads and C7. Spine surgeries that are envisioned to utilize the MFPF are: scoliosis, spondylolisthesis, hyper-kyphosis, degenerative and herniated discs, and spinal trauma.

Finite element models (FEMs) allow for detailed analysis on displacement, stress, strain, and reaction forces to be computed by breaking down solids into finer simplified pieces known as elements which are interconnected by nodes. They have been used for several studies related to the spine such as the study of surgical techniques (Lafage et al. 2004; Grealou et al. 2002),

pathology development and progression (Villemure et al. 2004; Lin et al. 2010), brace treatment (Clin et al. 2007), etc. One previous finite element model was used to investigate the impact of surgical positioning on the geometry of the spine (Duke et al. 2005, 2008). This wireframe model contains 2974 elements and 1440 nodes. Patient specific 3D geometry of the spine, pelvis, and ribcage was obtained using a bi-planar reconstruction technique (Delorme et al. 2003). Material properties were obtained from literature and personalized using side bending radiographs (Petit et al. 2004). Interface with the surgical frame was represented by the application of nodal displacements and forces. Firstly, the model was used to simulate prone patient positioning on a surgical frame then to study the impact of different positioning parameters: pelvic incidence (+/-15°), chest cushion location (under ribs 3-6 or 6-9), chest cushion height (0 and 3.5 cm), and lateral corrective forces between 10-150 N on various spinal geometry parameters including their optimization. So far, this model was not used to study the impact of lower limb positioning, investigate new surgical positions or to optimize patient positions for different stages of surgeries.

The general objective of this thesis is to use a combination of finite element modelling and experimental testing to study how surgical patient positioning impacts geometry of the spine and how this knowledge can be used in order to improve surgical interventions. The existing MFPF features were studied as well as some novel features requiring the development of surgical frame accessory prototypes.

This thesis is composed of 5 scientific papers and is organized in 7 chapters. The 1st chapter contains a review of literature and relevant knowledge on spinal pathologies, surgical positioning objectives, surgical frames, and biomechanical finite element models. The 2nd chapter presents the objectives and the hypotheses of the project. The 3rd chapter presents individual studies in the form of scientific papers 1 through 4. The 4th chapter presents the optimization study in the form of scientific paper 5. The 5th chapter details the design of the new surgical positioning features developed. The 6th chapter links the previous chapters providing an overall discussion and the final chapter provides the study conclusions and recommendations.

CHAPTER 1 REVIEW OF LITERATURE

This review of literature covers the following topics: (1.1) functional and descriptive anatomy of the spine, thoracic cage, pelvis, and adjacent members, (1.2) spinal pathologies and their associated operations, and (1.3) modelling of the human trunk.

1.1 Functional and descriptive anatomy of the spine, thoracic cage, pelvis, and lower limbs

The human spine (figure 1.1) is composed of vertebrae, discs, ligaments, and muscles. The vertebrae can be thought of as a chain of blocks stacked one on top of the other connected by inter-vertebral discs acting as hinges. Ligaments connect the blocks providing stability. Muscles also provide stability as well as the forces required for movement.

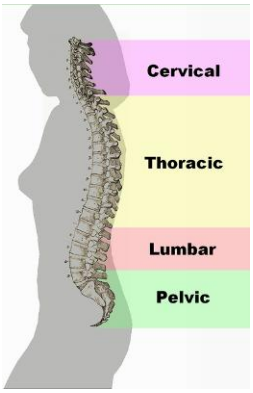

Figure 1.1: Human spine (consulted on October 13th 2010, obtained from http://en.wikipedia.org/wiki/File:Spinal_column_curvature.png)

The spine is composed of 33 vertebrae broken down into 5 categories. There are 7 cervical, 12 thoracic, 5 lumbar, 5 sacral (often fused into one), and 4 coccygeal (often fused into one). Vertebrae categorically vary in size and shape depending on their functionality but share many similar characteristics.

Intervertebral discs (figure 1.2) are the flexible members connecting vertebrae that allow motion and absorb shock. While each individual disc has limited flexibility, their combined effect allows for the back's large range of motion. They represent one fourth of the total spinal column's length and are composed of an annulus fibrosus surrounding a nucleus pulposus.

Ligaments (figure 2) serve as supporting structures and help stabilize the spine while protecting against excessive movement in any one direction. The spinal vertebrae are held together by two types of ligaments, the intrasegmental ligaments hold the individual vertebrae together and the intersegmental ligaments that hold many vertebrae together.

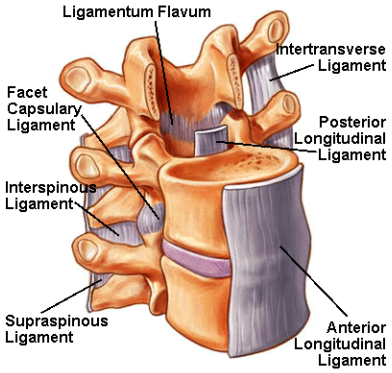

Figure 1.2: Ligaments of the spine (Stewart G. Eidelson. Save Your Aching Back and Neck, A Patient's Guide Second Edition, SYA Press, Inc. 2002)

A motion segment of the human spine is defined as two or more adjacent vertebrae, including the intervertebral disk between them, and the ligaments that bind them together.

Also of note are the costovertebral and zygapophyseal joints. The costovertebral joints are those forming articulations between a given rib and the spine, they include costotransverse joints and joints of rib heads. Costovertebral joints of the head of the rib are the articulations between the head of the ribs and the vertebral bodies. The costotransverse joints are the articulations on each side of the spinal column of a given thoracic rib with the transverse process of its corresponding thoracic vertebra. Zygapophyseal joints (aka facet joints) are the joints that occur between facets of the interior and superior articular processes of adjacent vertebra.

The pelvis (figure 1.3) is composed of three bones: the ilium, ischium, and pubis, which become fused together with age. It is joined to the sacrum by ligaments and provides socket joints for the hips. There are marked differences between the male and female pelvises, with characteristics of the female pelvis being better suited for childbirth. The pelvis plays a protective

role for digestive and reproductive organs and is an important load-bearing part of the skeletal system.

Figure 1.3: The pelvis (Consulted on October 11th 2010, obtained from http://media.photobucket.com/image/pelvis/danielgalvan05/untitled.jpg?o=31)

The hip joint (figure 1.4) is the ball and socket synovial joint between the cup-like acetabulum of the pelvis and the rounded head of the femur. Its primary function is to support the weight of the body in static and dynamic postures. Both surfaces of the joint are covered with a strong lubricated layer of articular hyaline cartilage. A fibrocartilaginous rim called the labrum grips the femoral head and secures it in the acetabulum. A capsule attached proximally to the periphery of the acetabulum covers the femoral head and attaches to the base of the neck and limits the hip range of motion.

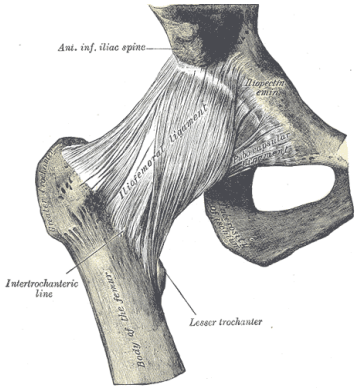

Figure 1.4: The hip joint (*Anatomy of the Human Body* by H. Gray, 1918, Philadelphia: Lea & Febiger. Consulted on October 11th 2010, obtained from http://www.bartleby.com/107/92.html)

Three principle ligaments reinforce the hip joint: the iliofemoral ligament attaches the pelvis to the femur, the pubofemoral ligament attaches across the front of the joint from the pubis to the femur, and the ischiofemoral ligament attaches the ischial part of the acetabular rim to the femur.

There are five muscle groups that allow movement at the hip joint: flexor group (iliopsoas composed of the iliacus and psoas major), extensor group (hamstrings), lateral rotator group, adductor group, and abductor group (figure 1.5). The muscles have origins on the pelvis and insertions on the lower limbs.

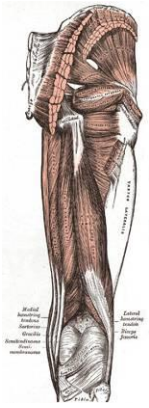

Figure 1.5: The hamstrings (*Anatomy of the Human Body* by H. Gray, 1918, Philadelphia: Lea & Febiger. Consulted on October 11th 2010, obtained from http://www.bartleby.com/107/128.html)

The femur (figure 1.6) is the longest, strongest and most voluminous bone of the human body forming part of the hip and knee. The proximal end of the femur consists of the head which is linked to its body by the neck at an angle of approximately 125^{o} and the greater and lesser trochanter which serve as muscle attachment points. The body of the femur has several attachment points for muscles such as the linea aspera for the biceps femoris and the gluteal tuberosity for the gluteus maximus.

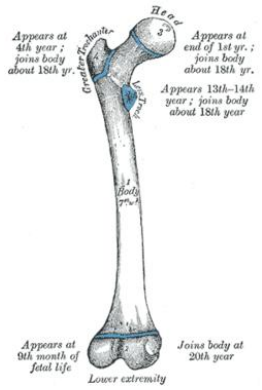

Figure 1.6: The femur (*Anatomy of the Human Body* by H. Gray, 1918, Philadelphia: Lea & Febiger. Consulted on October 11th 2010, obtained from http://www.bartleby.com/107/59.html)

The femur is linked to the tibia and fibula via the knee (figure 1.7), a pivotal hinge joint whose articular bodies are the lateral and medial condyles.

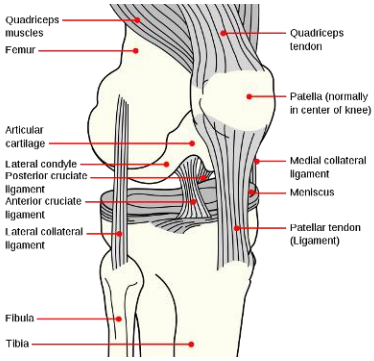

Figure 1.7: The knee joint (obtained on October 11th 2010 from http://commons.wikimedia.org/wiki/File:Knee_diagram.png)

The joint itself is bathed in synovial fluid which is contained inside the synovial membrane called the joint capsule and is surrounded by ligaments which add stability by limiting movement. The tibia and fibula are linked to each other by an interosseous membrane and their proximal portions serve as insertion points for several hip joint muscles including the hamstrings.

A typical ribcage (figure 1.8) consists of 12 pairs of ribs. They are attached posteriorly to the thoracic vertebrae at dedicated facet locations. The first 7 pairs, known as true ribs, are connected anteriorly to the sternum, pairs 8 through 10, known as false ribs, are connected

anteriorly to the cartilaginous portion of the rib above it, and the 11th and 12th pair, known as floating ribs, are not attached anteriorly. Due to their connection to the ribcage, the thoracic vertebrae are limited in their range of motion. The spacing between successive ribs, known as intercostals spacing, contains muscle, nerves, and arteries. The rib cage is elastic, which allows for expansion and contraction during breathing. Its primary function is the protection of the lungs and heart.

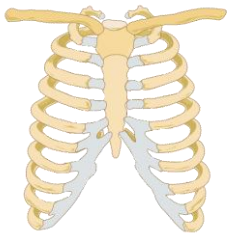

Figure 1.8: The ribcage (obtained on October 11th 2010 from http://commons.wikimedia.org/wiki/File:Rib_cage.gif)

1.1.1 Quantification of spinal geometry

There exist several tools that are used in order to describe the geometry of the spine. The ones presented here will be used in subsequent sections. First a body oriented coordinate system defines planes of interest as well as the orientation of the x, y, and z axes (figure 1.9).

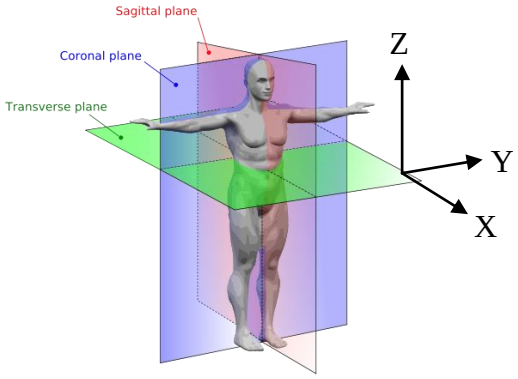

Figure 1.9: Cartesian co-ordinate system oriented with respect to the spine (Obtained on October 11th 2010 from http://en.wikipedia.org/wiki/File:Human_anatomy_planes.svg)

The Cobb angle (figure 1.10) can be used to define the curvature for a specified segment of the spine in the coronal plane.

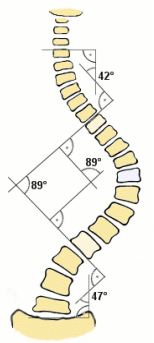

Figure 1.10: Cobb angle (obtained on October 11th 2010 from http://en.wikipedia.org/wiki/File:Scoliosis_cobb.gif)

A line is drawn along the upper endplate of the proximal end vertebra and along the lower endplate of the distal end vertebra of a given segment; the angle of intersection of these two lines is defined as the Cobb angle. The same technique could be used to measure sagittal curves (kyphosis, lordosis).

The spine of a healthy human is generally straight when viewed on the coronal plane (Schultz 1991). In the sagittal plane, there are natural occurring curves as can be seen in figure 1. These curves serve to balance weight, absorb shock, provide protection, and help the body maintain an upright posture. A curve with an anterior facing apex is defined as lodortic, while a curve with a posterior facing apex as kyphotic. The extent to which the spine is curved in the sagittal plane, measured using the Cobb angle, varies among individuals and is age dependent. The thoracic region (top of T1 to bottom of T12) of a mature spine has a mean kyphosis of 38.5° (SD 8.1°) and the lumbar region (top of L1 to bottom of L5) of a mature spine has a mean lordosis of 56.6° (SD 9.1°) (Voutsinas 1986).

Sagittal spinal balance is defined as the vertical alignment of the midpoint of the C7 or T1 body with the posterior superior corner of the sacrum in the sagittal plane (figure 1.11).

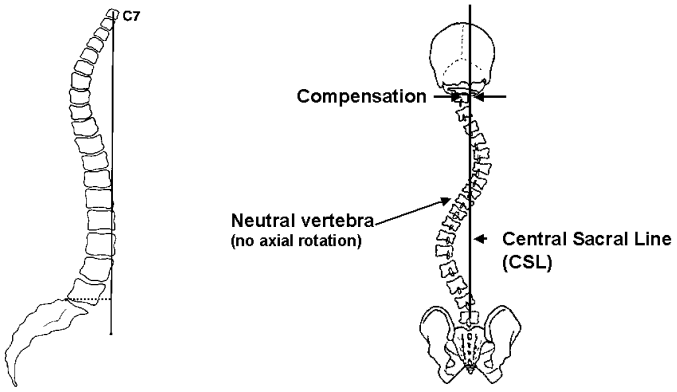

Figure 1.11: Sagittal balance (left) and coronal balance (right) (obtained on October 11th from www.srs.org/professionals/glossary/glossary.php)

Coronal balance is defined as the vertical alignment of the midpoint of the C7 or T1 body with the mid-point of the sacrum in the coronal plane. Spines with a sagittal balance < 40 mm and coronal balance < 25 mm are considered to be normal (Heart 2007) and even a mild imbalance can have detrimental effects (Glassman 2005).

The spine is generally described as having 6 degrees of motion: flexion, extension, left side bending, right side bending, left axial rotation, and right axial rotation. Van Herp et al. (2000) studied the range of motion of the human spine using x-rays and goniometry with the results summarized in Table 1.1.

Table 1.1: Range of motion of the human trunk (Modified from Van Herp 2000)

	Females (n = 50) Age (yr)					Males (n = 50) Age (yr)				
Movement	20–29	30–39	40–49	50–59	60 +	20–29	30–39	40–49	50–59	60 +
Flexion	58.9 ± 10.5	58.2 ± 6.9	57.5 ± 10.2	53.6 ± 11.4	50.8 ± 6.6	56.4 ± 7.1	54.2 ± 9.6	54.2 ± 8.9	58.1 ± 10.6	52.3 ± 8.2
Extension	37.0 ± 10.5	31.2 ± 11.7	29.0 ± 8.5	20.5 ± 6.1	15.1 ± 5.2	22.5 ± 7.8	22.1 ± 9.5	20.0 ± 6.1	17.2 ± 7.2	16.9 ± 5.6
Left side bending	25.1 ± 2.8	25.6 ± 5.6	20.7 ± 3.6	21.9 ± 6.2	19.4 ± 6.1	25.8 ± 7.6	25.6 ± 5.4	19.3 ± 6.2	19.0 ± 5.8	14.4 ± 4.6
Right side bending	26.3 ± 4.3	26.2 ± 7.2	23.4 ± 4.7	23.2 ± 5.7	19.2 ± 5.6	26.2 ± 8.4	25.0 ± 5.0	21.2 ± 7.0	22.4 ± 6.4	15.5 ± 4.3
Left axial rotation	18.6 ± 5.8	18.0 ± 6.2	15.7 ± 4.2	14.7 ± 6.1	14.7 ± 6.5	14.4 ± 5.1	11.9 ± 3.2	11.6 ± 4.9	11.3 ± 3.8	10.9 ± 3.9
Right axial rotation	18.6 ± 4.9	15.6 ± 6.2	13.4 ± 3.8	14.2 ± 6.0	13.0 ± 6.0	12.8 ± 4.1	9.1 ± 4.5	12.7 ± 5.7	11.3 ± 4.3	14.6 ± 6.0

The description of the spine given thus far has been applicable for the normal standing position. There are several factors that can influence spinal geometry including trunk and associated member movement such as left/right lateral as well as anterior/posterior movements of the ribcage (Harrison 1999, 2002), anterior/posterior pelvic tilt (Delisle 1997), leg position (Cho

1995, Hirabayashi 2002), anterior/posterior translation of the head (Penning 1992), and arm position (Stagnara 1982).

Another factor which can influence spinal geometry is body position. As a general rule, it can be said that lumbar lordosis decreased by almost 50% when a patient goes from the standing to sitting position (Lord 1997) which can be attributed to a posterior movement of the pelvis averaging 40° (Schoberth 1962) while the impact of sitting of the thoracic and cervical regions depends largely on seated posture. The influence of going from the standing to the prone and supine positions on spinal geometry will be covered in section 1.2.2.

1.2 Spinal pathologies and their associated surgeries

Scoliosis (figure 1.12) is defined as a deformation of the normally straight spine in the coronal plane. There are several different types of scoliosis for which the causes are known: congenital scoliosis, neuromuscular scoliosis and traumatic scoliosis, however, they only represent the minority of cases. Idiopathic Adolescent Scoliosis (IAS), for which the etiology and pathogenesis remain unknown, represents 80% of all spinal curvatures observed (Steward 2006). Neuromuscular scoliosis is caused by neurological system disorders such as cerebral palsy, spina bifida, muscular dystrophy, polio, spinal muscular atrophy or spinal cord injuries that weaken the stabilizing muscles of the spine.

Figure 1.12: The scoliotic spine (Obtained on October 11th 2010 from http://en.wikipedia.org/wiki/File:Wiki_pre-op.jpg)

There are several different types of scoliotic curves, ranging from single to quadruple, and affecting the cervical, thoracic and/or lumbar vertebrae. Typical patterns have been observed in

AIS; 90% of single thoracic curves are to the right, 80% of thoraco-lumbar curves (curvature apex at T12 or L1) are to the left, more than 70% of single lumbar curves are to the left, and 90% of double major curves are right thoracic and left lumbar (Rinski 1988). Several different curve classification systems have been proposed including the Lenke system (Lenke 2001) which contains 6 different types based on the location of structural curves and a lumbar modifier based on the coronal plane offset of the apical vertebrae.

Although coronal plane Cobb angle is the characteristic deformity associated with scoliosis, it has been recognized as a 3D deformity which includes vertebral rotation, vertebral wedging, loss of sagittal and coronal balance, rib hump, and hypo-kyphosis. Symptoms of scoliosis can include back pain, decreased pulmonary function, psychological and self-image problems, pregnancy complications and early mortality. Curves are potentially progressive and can worsen during growth spurt. Treatment of AIS is varied and depends on the degree of spinal curvatures; generally < 20° by observation, 20° to 40° by bracing and >40°-50° by surgical intervention.

Spinal surgery in AIS can be conducted when a progressive deformity is uncontrolled by brace wear, is too advanced for brace treatment, causes pulmonary dysfunction, or results in undesired cosmetic appearances.

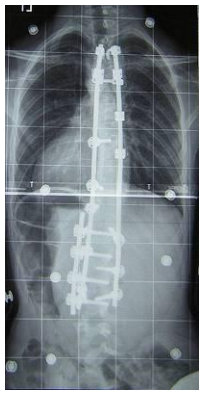

Figure 1.13: Posterior spinal instrumentation (Consulted on October 11th 2010, obtained from http://commons.wikimedia.org/wiki/File:Wiki_post-op.jpg)

Posterior spinal fusion is a process in which two or more vertebrae are fused together with bone grafts. The bone grows between the vertebrae holding them together. During the procedure, the patient is often in the face down (prone) position and an incision is made along the anesthetised patient's back and the back muscles are retracted in order to gain access to the vertebrae. Instrumentation (figure 1.13), consisting of cables, hooks and/or screws which are interconnected by rods. It provides increased stability, facilitates fusion, and allows for the application of corrective forces to the deformity. Modern instrumentation systems include : CD Horizon Legacy which utilizes contoured rods that are rotated to transform the coronal plane deformity 90° to the sagittal plane; in situ rod contouring (Voor et al. 1997) in which the rod is bent in place at various levels and planes to allow for three dimensional manipulation of spinal shape; Vertebral Column Manipulation which allows for direct axial de-rotation of apical vertebrae; the Universal Spine System allows for segmental correction and realignment of the spine through de-rotation and translation of each individual vertebra to pre-contoured rods; and the Moss Miami system involves the use of flexible rods that are and works primarily by distracting and compressing hooks attached to posterior elements of the vertebral bodies. Surgical manoeuvres using spinal instrumentation require the application of sometimes large forces by the surgeons which may be difficult, require additional procedures such as osteotomies and can lead to implant pullout or breakage (Mayo et al. 2010). Compromises must also be made (e.g. more emphasis on adjusting a few spinal geometrical parameters than others) as instrumentation cannot simultaneously adjust the spine in three dimensions. Even with today's advanced instrumentation 100% correction in not achieved and adverse impacts such as flatback syndrome can persist (Xu et al. 2008).

There is a large variability among surgeons with regards to their surgical objectives for the correction of spinal deformities. In one study, 20 surgeons were asked to rank the importance of scoliotic surgical correction parameters; sagittal and coronal balance came out numbers one and two respectively while there was little agreement among the rest (Majdouline 2007). This variability makes providing a universal optimized pre-surgical position difficult and surgeon-specific needs would have to be addressed.

Post-operative surgical results show that even if most patients are satisfied, re-operation is required in approximately 10% of cases (Asher et al. 2010). The average post-operative Cobb angle correction is currently approximately 60% of the spinal deformity (Sobottke et al. 2010, Li et al. 2010).

Spondylolisthesis (figure 1.14) is defined as a translatory movement of two spinal vertebrae relative to each other, generally occurring in the lumbosacral spine. It can be caused by instability between the vertebrae due to degenerative changes of the facet joints, or by congenital or traumatic disruption of the pars interarticularis of the superior vertebrae. Approximately 5-6% of the male population and 2-3% of the female population are afflicted with this pathology (Sadiq et al. 2005).

Figure 1.14: Spondylolisthesis (consulted on October 11th 2010, obtained from http://en.wikipedia.org/wiki/File:SpondylolisthesisL5S1.jpg)

There also exists a degenerative form of spondylolisthesis among the aging population (>50 years old), which can result in the narrowing of the spinal canal (spinal stenosis). Surgical treatment can be required if neurologic involvement exists (e.g. leg weakness) or non-surgical methods (medication, therapy, braces) have failed to relieve symptoms. It will also be considered for children with a progressive forward vertebral slip. The surgery may be performed with either an anterior or posterior approach. It involves fusion of the slipping vertebra to its lower neighbour. Spinal instrumentation, screws placed into the pedicles connected to each other by metal rods, may be used to provide support while spinal fusion occurs. Surgical treatment of spondylolisthesis boasts a high success rate.

Herniated disk (figure 1.15), also referred to as slipped disc, occurs when a portion of the spinal disc pushes outside its normal boundary which can press on the nerves around the spine. They occur primarily in the lumbar spine of middle aged to older men involved in strenuous physical activity. Cervical discs are affected 8% of the time and thoracic discs 1-2% of the time. With age, the intervertebral discs lose some of their strength and cushiness. If the outer part of the disc becomes too weak, it may tear causing part or all of the soft center to push through and press on neighbouring nerves. This results in pain, tingling, numbness, weakness and spasms of the muscles below the affected disk (e.g. legs and lower back). Symptoms are amplified during coughing, laughing, or physical activity.

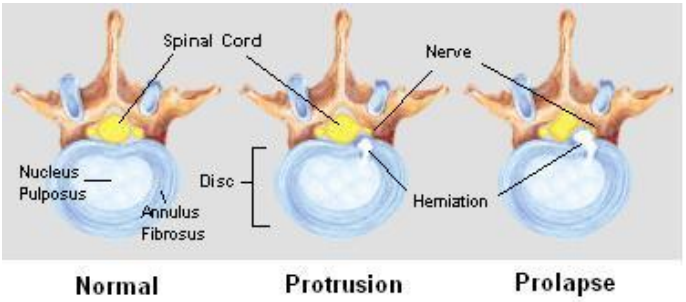

Figure 1.15: Herniated disc (consulted on October 11th 2010, obtained from http://upload.wikimedia.org/wikipedia/en/9/9d/Disc_Herniation.JPG)

Treatments include rest, anti-inflammatory medication and physical therapy. For 90% of patients, this will be sufficient to eliminate the symptoms within a few weeks. If symptoms worsen or do not show signs of improvement a steroid injection or surgery may be required. Surgical options include a diskectomy, removal of the protruding disk and micro-diskectomy, the removal of fragments of nucleated disk through a very small opening, in order to stop the herniated disc from pressing and irritating the nerves. During operation, an incision is made in the skin over the herniated disc and the muscles over the spine are pulled from the bone is order to gain access to the disc. A small amount of bone may also require removal in order to allow the surgeon to see the compressed nerve. The portion of the disc in contact with the nerve is then removed.

Kyphosis (or hyperkyphosis) (figure 1.16) is the curving of the spine that causes a bowing of the back, which leads to a hunchback or slouching posture. Kyphosis can occur at any age resulting from trauma, developmental problems, or degenerative diseases. Symptoms include

back pain, fatigue, spinal stiffness, and respiratory difficulties. A type of kyphosis occurring in adolescents, for which the cause is unknown, is known as Scheuermann's disease. It is the result of several vertebrae wedging together. Scheuermann's disease is often associated with tightening of the hamstrings (Hosman 2003).

Figure 1.16: Lateral radiograph of kyphotic spine (Consulted on October 11th 2010, obtained from http://en.wikipedia.org/wiki/File:RadiografiaRXCifosisScheuermann70Grados.jpg)

Treatment varies depending on the cause of the disorder includes bracing and physical therapy. Surgical treatment can be required if the deformity is progressive beyond a severe angle (e.g., 70 degrees for Scheuermann's kyphosis), sagittal balance is significantly abnormal, neurologic symptoms exist, or persistent pain cannot be alleviated using conservative treatment. Two surgical options are posterior fusion and instrumentation or anterior releasing of tightened ligaments with discectomy of damaged discs.

Spinal injuries, known as spinal trauma, are due to physical forces acting on the spine that result in fractures. The leading cause of spinal trauma at approximately 50% is automobile accidents. This is followed by falls, gunshots, and sports related injuries. Approximately 450 000 people in the United States are currently living with spinal cord injuries with an additional 11 000 every year. Two categories of spinal trauma include low and high energy. The vertebra, discs, ligaments and muscle may all be affected. In the case of bone there are compression fractures (bone collapses upon itself) (figure 1.17), burst fractures (pieces of bone explode into surrounding tissue), and fracture-dislocation (bone breaks and pieces slide away from each other).

Figure 1.17: Compressive fracture (consulted on October 11th 2010, obtained from http://radpod.org/wp-content/uploads/2007/04/colunapartida-3.JPG)

Depending on the degree of injury physical therapy, bracing or surgery may be required. Surgery is required in the event instability, collapse, or nerve damage and aims to relieve nervous pressure and improve spine alignment/instability. It addition to traditional instrumentation techniques, the vertebrae may be strengthened (vertebroplasty) or even un-collapsed (kyphoplasty) by the injection of a cement or balloon into the vertebral body.

Degenerative lumbar disc disease occurs when an intervertebral disc in the lower back is compromised resulting in lower back pain. It can be due to simple wear and tear on the spine or a more serious injury such as lower back torsion. Approximately 30% of the population between the ages of 30-50 are afflicted with this pathology and it is the norm for patients above 60. Symptoms include continuous low-grade pain in the lower back (can radiate to the hips and legs) with occasional flares lasting a few days. A common hypothesis is that pain is caused by inflammation if the proteins in the disc space irritating surrounding nerves and abnormal micro-motion instability caused by the inability of the deteriorated annulus fibrous to absorb spinal stresses. Treatment includes medication to combat the pain and inflammation coupled with physical therapy and exercise. When symptoms are severe or do not show signs of improvement after 6 months, surgery, fusion of the lumbar spine, can be considered. The most common site of disc degeneration and site of fusion is the L5-S1 level. An alternative surgical treatment, still in its relative infancy, is artificial disc replacement.

From the above section, it can be noted that surgical intervention by posterior spinal instrumentation and fusion is commonly required for the treatment of severe cases of spinal

pathologies. One crucial step to spinal surgery is patient positioning. Proper positioning should: facilitate exposure, minimize bleeding, minimize chance of damage to vital structures, allow proper ventilation, avoid post-operative morbidity, and preserve sagittal alignment (Schonauer 2004). In order to achieve this, several operating frames have been developed.

1.2.1 Surgical frames

The first and historical gold-standard operating table for spinal fusion was the Relton-Hall frame (Relton 1967) (figure 1.18). Its design consists of 4 padded supports in two 45° v-shaped pairs mounted on a frame that can be placed on a standard operating table. The Relton-Hall frame seeks to reduce bleeding by having the abdomen pendulous thus relieving pressure on the abdominal wall which is transmitted to the inferior vena cava diverting blood flow into the vertebral venous system (Schonauer 2004).

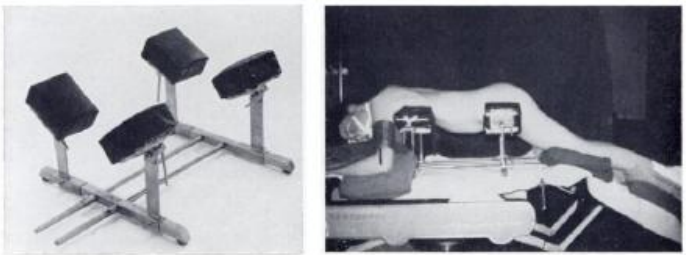

Figure 1.18: The Relton-Hall frame (Relton 1967)

Additional tables that are available for spinal operations are the Jackson, Andrews, Wilson, Axis (Orthopedic Systems, Inc.), and Erothitan frames. As with the Relton-Hall, these frames seek to facilitate surgical exposure and minimize bleeding; they offer the added advantage of being radiolucent and offer some limited patient positioning capabilities. The Jackson surgical table is one of the most frequently used for spinal fusions today. It offers different support cushions, an adjustable leg sling to modify hip flexion and the ability to rotate 360° allowing for both posterior and anterior procedures. The table specifications allow for 10° of Trendelenburg (pelvis higher than the head) / reverse Trendelenburg positioning, and 25° of lateral tilt.

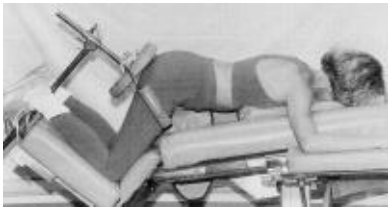

Figure 1.19: Andrews OSI Table (Stephens et al. 1996)

The Andrews table (figure 1.19) allows positioning notably for lumbar spinal surgeries. The degree of hip flexion can be adjusted while the knees are kept flexed 90°. The table specifications allow for 15° of Trendelenburg / reverse Trendelenburg positioning, and 10° of lateral tilt. The Wilson frame attaches to standard orthopedic tables such as the Jackson tables. It consists of two arched cushions that run along the lateral sides of the torso, and is primarily used in laminectomy, decompression, disk surgery and micro-diskectomy procedures. The Erothitan frame can be added to a standard operating table. It allows a large degree of adjustment including: chest pad extension, 20° lateral tilt, head support adjustment, and Trendelenburg / reverse Trendelenburg positions. The Axis Jackson includes a hinged support frame and allows for torsion translation to prevent spine distraction/compression. Its pads can be interchanged to allow for lateral decubitus patient positioning.

1.2.2 Patient positioning and spinal geometry

A factor of great importance during surgical positioning, that has been the subject of many studies as outlined in the subsequent section, is how it impacts the sagittal alignment of the spine. A primary concern is preservation of lumbar lordosis and sagittal balance in order to avoid sagittal imbalance and pseudarthrosis.

The principle factor impacting lumbar lordosis is one's degree of hip flexion. In a comparison of the impact of various surgical tables on lumbar lordosis, Stephen (1996) found a mean lumbar lordosis of 51.7° in the standing position, 52° on the Jackson table, 17° on the Andrews table with hips flexed 90°, and 27.3° on the Andrews table with the hips flexed 60°. A clinical trial performed by Benfanti (1997) on the Wilson frame have shown that 95% of standing lordosis is maintained if the hips are fully flexed, 74% is maintained when the hips were flexed 33° for anesthetized patients, and 86% is maintained for un- anesthetized patients when the hips were flexed 28°; the correlation between degree of hip flexion and percentage of retained lordosis

was poor. Legaye (1998) developed predictive equations for lordosis based on pelvic parameters for both healthy and scoliotic patients. They noted that the higher the scoliotic parameters, the more restricted the capacity to modulate the lordotic curve with pelvic parameter changes. A more extreme flexed hip position, known as the knee-chest position Tarlov (1967) can be advantageous for several common surgeries such as microdiscectomy as it causes the lumbar intervertebral disc space to be widened posteriorly. Thoracic kyphosis, while an important consideration for cases of hypo-kyphotic scoliosis or kyphosis, has received little attention with regards to changes dues to surgical positioning. Jackson (2005) and Marsicano (1998) respectively showed a 7° increase (T4-T12) and an 8° decrease (T5-T12) of thoracic kyphosis on the Jackson frame. A conclusion that can be drawn from these clinical trials is that hip flexion has an important impact on lumbar lordosis however, the correlation between the two is subject to inter-patient variability. Additionally, thoracic kyphosis changes must also be considered. As a general rule, hips should not be flexed greater than 30° in order to maintain sufficient lumbar lordosis to avoid flat back symptoms.

Loss of lumbar lordosis due to hip flexion is a result of associated backwards tilting of the pelvis. Backwards tilting of the pelvis increases posterior ligament tension, posterior muscle activity (if un-anaesthetized), and compression of the spine. The degree of pelvic tilting depends on an individual's range of hip flexion, which in turn is limited by the hamstring muscles when the knees are extended. Several studies have examined the effects of hamstrings on the lumbar spine. Stokes (1980) examined the relationship between hamstring tightness and loss of lumbar lordosis in the seated position showing individuals with tight hamstrings experienced additional loss of lumbar lordosis when knees were straightened to 45° in the seated position. Hosman (2003) examined how hamstring tightness influences lumbar-pelvic ROM, lumbar lordosis and sacral slope in pre and post surgical patients with Scheuermann kyphosis. It was found that patients with tight hamstrings had to compensate the new balance associated with their corrected kyphosis with their lumbar spine as opposed to a combination of pelvic tilt and lumbar spine in patient with normal hamstrings.

It has been shown that prone surgical positioning has an impact on the geometry of the spine in the coronal plane, with several factors such as elongation of the spine due to the

elimination of axially directed gravitational effects, relaxation of the back muscles due to anaesthesia, and stripping of the muscles during surgical exposure contributing to Cobb angle reduction. Delorme (2000) showed a 37% correction in Cobb angle of the scoliotic spine due to surgical positioning and anaesthesia. Similar results were found by Behairy (2000) showing one-third of total coronal spinal deformity correction was obtained prior to instrumentation. Klepps (2001) and Torell (1985) showed that approximately 1/4th of curve correction could be achieved by the supine positioning of un-anesthetised patients. Comparison of the aforementioned results leads to the conclusion that approximately 10% of correction is due to the relaxation effects of anaesthesia. Polly (1998) found that 31% of curve correction was due to patient positioning with an additional 7-17% correction coming as a result of surgical opening. Torell et al 1985 have found that scoliotic deformity reduction due to supine positioning is independent of curve severity. Transverse plane deformities, such as vertebral body rotation which are coupled to Cobb angle, have also been shown to correct during patient positioning (Yazici 2001).

It has been hypothesized that patient positioning can be used to reduce surgical effort and improve post-operative results. Despite this, current surgical frames offer very little patient positioning possibilities and in most procedures the patient remains static. One attempt at intra-operative correction of spinal deformation is the use of halo-traction. In this procedure, the head is lifted with a counter weight apparatus which results in straightening of the spine. However, its use is limited to large and stiff scoliotic deformities and it has not been shown to improve post-operative corrections (Mac-Thiong 2004). Possible explanation for this is the way in which halo-traction elongates the spine through longitudinal forces which cannot be maintained once the patient is erect.

Two recent surgical frame prototypes have been developed which seek to exploit a range of patient positioning possibilities; the dynamic positioning frame (DPF) (figure 1.20) and the multi-functional positioning frame (MFPF) (figure 1.21).

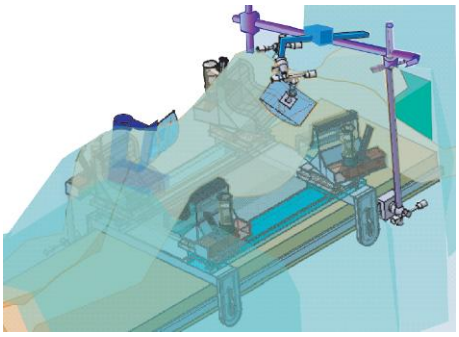

Figure 1.20: CAD drawing of the Dynamic Positioning Frame (DPF)

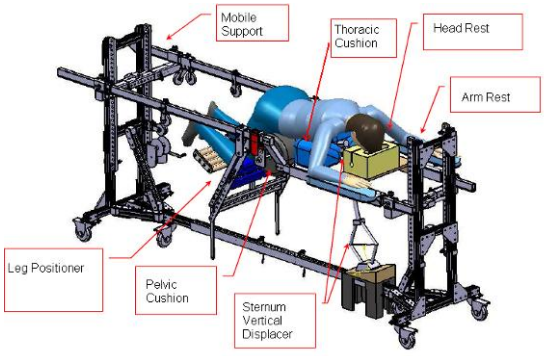

Figure 1.21: CAD drawing of the Multi-functional Positioning Frame (MFPF)

The DPF has 4 support cushions (2 thoracic and 2 pelvic) which can be adjusted intraoperatively longitudinally, laterally, or vertically. Also included are two corrective cushions which can apply forces to the scoliotic deformity; to the curve apex and to the rib hump (Duke 2009) (US Patent 6,941,951). Clinical testing showed that the DPF could provide further deformity reduction relative to the Relton-Hall frame, however, the resultant interface pressure were higher.

The MFPF has 2 thoracic cushions which can be adjusted longitudinally and vertically, a pelvic cushion which can be adjusted vertically, a lower limb positioning which can go from 15° in extension to 50° in flexion, head and arm supports, and a portable sternum vertical displacer which can be placed under the MFPF and lift the patient's torso up off of the thoracic cushions (Canet 2008). The MFPF is the next iteration of the DPF.

1.3 Biomechanical Modelling of the human spine

1.3.1 Types of models

As a general statement, biomechanical modeling is used to simulate and predict the behaviour of a living organism at different levels including: cells, tissue, organs, systems, and overall body. The advantage of biomechanical modeling over *in-vivo* or *in-vitro* experiments is that multiple varied simulations can be performed without constraints on time, cost, ethics, or sample inconsistencies. The biggest challenge, as with any type of modeling, is being able to reproduce reality accurately enough that the simulations performed yield meaningful results.

There exist several different types of spinal models including: physical models, mathematical models, mechanical system simulation models and finite element models. Modeling the human spine has been done for a variety of reasons including: chair design, brace design, surgical planning, pathology study, and trauma impact investigation.

Physical models use a construct of inorganic materials to represent the spine. One such model was developed by Takemura (1999) using synthetic resin vertebrae and silicon discs fixed on a metal frame. It was used to study the development of scoliotic spinal deformity by applying various forces in different orders. The utility of physical models is limited to qualitative studies as they cannot provide accurate data on displacements and forces or be adapted for inter-patient variability. It would also be extremely difficult to construct a physical model that accurately reproduces the biomechanical behaviour of the spine due to the large number of simplifications that must be made during its construction.

Schultz (1970) derived mathematical model of the spine, which was modeled as a mechanical system of deformable and rigid bodies. If the geometric configuration of a given vertebra is specified, the geometric configuration of an adjacent vertebra may be determined using principles of minimum energy and the process repeated until the entire spine has been described. While many simplifications had to be made for the sake of computation, the mathematical model was able to reproduce published data after some manipulation. A model of this type can describe known movements mathematically but has limited usefulness in terms of

predicting the behaviour of the spine for simulations where the results are not known. Powerful software has been developed which limits the need for manual elaboration of mathematical spinal representation.

A system simulation or kinematic model (figure 1.22) uses the fundamental equations of motion in order to derive displacement, acceleration, and reaction forces based on the mass and acceleration of a given body. Various software, such as ADAMS (MSC Software Inc.), allow for the rapid solution of relatively complex mechanical systems. Van Deursen (2000) developed a mechanical system simulations model of the lumbar spine in order to quantify the mechanical spinal response induced by small alternating pelvic rotations in the seated position. The vertebrae were represented by rigid bodies and linked by a spring-damper construct representing the interverterbal discs. Results showed the natural frequencies and maximum torques in the lumbar spine for different frequencies and amplitudes of hip rotation inputs. The main drawback of system simulation models is that geometry is often assumed as rigid and thus no data can be obtained on internal stresses or strains. They are particularly useful when rapid visualization of system behaviour is required such as with surgical simulators (Aubin et al. 2008)

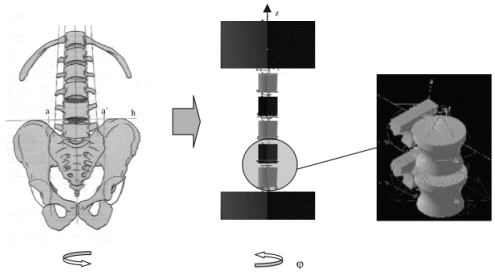

Figure 1.22: System simulation model (van Deursen 2000)

Finite element modeling (FEM) is the most widely used tool in biomechanical modeling of the human spine. It is done using readily available commercialized software such as ANSYS, Abaqus or NASTRAN. They offer of wide range of element types (links, beams, bricks, etc) each with unique properties and which are then attributed material properties (e.g. E and ν). Care must be taken when determining the number of elements and their distribution. As the mesh gets finer, accuracy improves but computational time increases in a non-linear manner. Often a finer global mesh is used which is refined at areas of interest in order to find a compromise between the two.

Once a FEM has been created, its accuracy can be validated by comparing its simulated results against previous or novel experimental testing. There are essentially three types of FEM of the human spine: detailed models, simplified global models, and hybrid models which are a combination of the two.

Detailed or refined models (figure 1.23) are used to study the local behaviour of a specific section of the spine. As a large number of data is required in order to accurately the reproduce the geometry of the spine and computational requirements are relatively high, its application is generally limited to a few motion segments.

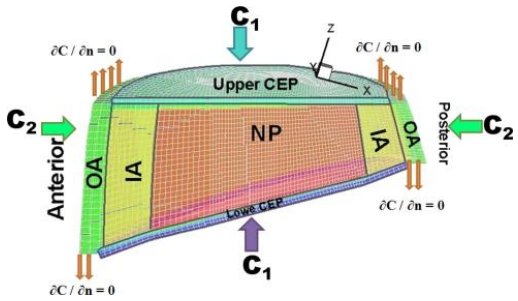

Figure 1.23: Example of a detailed FEM of an intervertebral disc (Mokhbi Soukane et al. 2008)

One of the first detailed FEM of a complete motion segment was developed by Shirazi-Adl (1986). An L2-L3 motion segment was modeled based on *in vivo* measurements. The vertebrae were represented with detail including: the body, transverse process, spinous process, lamina, pedicle, superior and inferior facets. The intervertebral discs included the nucleus pulposus modeled as an incompressible-inviscid fluid and the annulus as a composite of collagenous fibres embedded in a matrix of ground substance. The ligaments are also represented in much detail as a collection of non-linear axial elements. The model contains a total of 715 nodes and was used to study the response of the motion segment to sagittal plane moments including the effects of loss of intradiscal pressure in flexion and removal of the facets in extension. A more recent example of a detailed FEM was developed by Zhang et Song (2006) of the L3-L5 motion segment to investigate the stability and stress distributions resulting from 3 different fusion techniques showing that circumferential fusion provided the best results.

Simplified global models (figure 1.24) are used in order to study the macroscopic behaviour of the spine. Geometry and material properties are represented by enough elements to model the desired behaviour without including any unnecessary detail, thus reducing computational cost. They allow for the inclusion of the complete spine including additional elements such as muscles or the rib cage, however, due to the simplified geometrical representations detailed internal stress/strain distributions are not available.

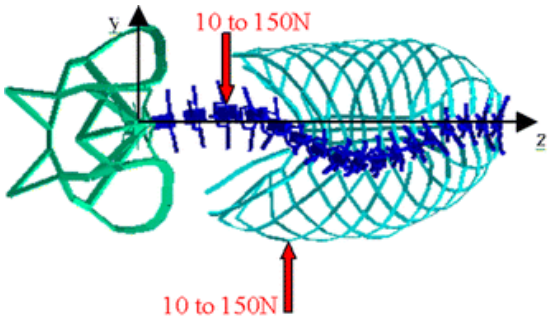

Figure 1.24: Example simplified global FEM of the spine ribcage and pelvis (Duke 2008)

Stokes and Laible (1990) created a simplified global model of the spine which included the lumbar and thoracic vertebrae, ribs, sternum, and intercostals ligaments in order to study how the impact of asymmetric growth of the thorax on the initiation of spinal lateral curvature and axial rotation as seen in scoliosis deformities. Vertebrae were defined by nodes representing the vertebral body center, transverse and spinous processes, and rib head-vertebral articulation where applicable. Ribs were represented by 11 nodes along their center lines, and the sternum and intercostals ligaments requiring an additional 28 nodes for model total of 336. Results showed that asymmetric rib growth did result in some lateral deviation and vertebral rotation as observed in scoliosis, however, the levels of the deformity were smaller than anticipated. Simplified global FEMs which include a large number of details are sometimes referred to as intermediate FEMs.

Hybrid FEMs (figure 1.25) are a combination of global and detailed FEMs. The majority of the geometry is simplified and a particular region which is under study is refined. It offers the ability to include global spinal geometry while still maintaining detailed results.

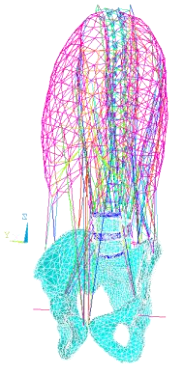

Figure 1.25: Hybrid spine FEM (Gharbi 2008)

Gharbi (2008) developed a hybrid FEM of the spine, ribcage, and pelvis, including back muscles, which was refined in the L4-pelvis region to study the effects of mechanical loading of the development of spondylolisthesis. It was determined that shear and bending mechanisms can both result in spondylolisthesis and that their relative importance depends on spino-pelvic determinants.

1.3.2 FEM geometry

The first and one of the most important steps in creating a FEM is geometrical representation of the object under study. The easiest and most accurate way to do this for the spine, associate members, and soft tissue is by using reconstruction techniques such as CT or MRI scanning. This process is generally not done directly to patients due to the high levels of radiation emitted by CT scanning and the cost and time associated with MRI scanning. Instead, the geometry of human cadavers is reconstructed and adapted to match that of a given patient using their standard pre-surgical x-rays. Radiographs, while exposing the patient to some radiation, are necessary in order to assess spinal geometry.

Delorme (2003) validated a means to reconstruct three-dimensional patient specific geometry of the spine, ribcage, and pelvis based on 3 radiographs (PA, PA angled 20° downwards, and LAT) and a calibration device (figure 1.26). High-resolution images of dry specimens were deformed using a dual kriging technique in which displacement fields calculated to map reference model anatomical control points onto the personalized radiographic geometry

were then applied to the rest of the reference model based on a statistical weighted average dependent of their proximity to the control points. This process has shown an accuracy of 3.3 +/- 3.8 mm. Benameur (2003) developed a similar method of reconstruction which uses 2 radiographs and a statistical priori knowledge of vertebral geometry which has shown a mean error of 1.5 mm. Finally, Novosad (2004) developed a technique for 3D reconstruction of spinal geometry from a single AP radiograph calibrated to match priori 3-D geometric models which has shown a mean reconstruction error of 2.89 mm. Accurate geometry of lower limb geometry has been modeled based on the transverse slices of the Visible human project (Viceconti).

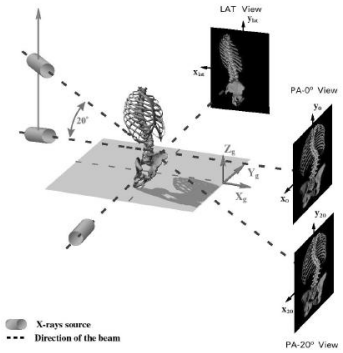

Figure 1.26: 3D Reconstruction Technique (Delorme 2003)

FEM geometrical representation of ligaments and muscles is generally done based on the location of their origins and insertions. Most anatomy books list these origins and insertions which are often recognizable landmarks. Alternatively, scaled mapping of origins and insertions can be performed based on data collected from analysis of cadaver specimens. For example, White (1989) has provided the coordinates of the origins and insertions of all lower limb muscles along with a scaling method based on the location of two bony landmarks for each Cartesian axis in the pelvis, femur, and lower leg. Cross sectional areas of trunk muscles (Chaffin 1990) and lower limb muscles (Horsman 2007) have been catalogued in literature and can be scaled for a given subject.

The next important step in creation of a FEM of the human trunk and associated members is the designation of material properties to the elemental representation of the reconstructed geometry. As an initial step baseline material properties can be obtained from literature and then

adapted to match documented clinical and patient specific tests. Material properties are available from a multitude of sources that do not always agree with each other. They have been experimentally obtained for the vertebrae and inter-vertebral discs (White 1990, Skali 1993, and Goel 1990), ribs, sternum, pelvis, and costal cartilage (Roberts 1970), lower limbs (Papini 2007), lower limb muscles (Kovanen 1984) and spinal ligaments (Goel 1990).

Attempts have been made to group the mechanical contributions of the many spinal anatomical factors into global stiffness properties. Panjabi (1970) derived a 36 coefficient matrix describing the 3D stiffness characteristics of the thoracic spine based on experimental results. A method to incorporate stiffness matrices into models was later proposed by Gardner-Morse et al. (1990). Alternatively, methods have been developed which allow for subject-specific personalization of FEM spine material properties using standard pre-operative spinal flexibility assessment tests such as lateral bending (Petit et al. 2004) (figure 1.27), traction (Lamarre 2009), fulcrum bending, and push prone test. Testing is simulated with the FEMs and then material properties, usually of the intervertebral discs, are optimized in such that the simulations and testing match. This method allows for improvement of model behaviour but is limited by testing reproducibility issues and often data in only one plane is available.

Figure 1.27: Radiograph of a side bending test (Saint-Justine University Hospital database)

One previous finite element model was used to investigate the impact of surgical positioning on the geometry of the spine (Duke 2005, 2008). This simplified global model contained 2974 elements and 1440 nodes. Patient specific 3D Geometry of the spine, pelvis, and ribcage was obtained using a bi-planar reconstruction technique (Delorme 2003). Material

properties were obtained from literature and personalized using side bending radiographs (Petit et al. 2004). Interface with the surgical frame was represented by the application of nodal displacements and forces. Firstly, the model was used to simulate prone positioning on the DPF for two patients. The simulations results showed good correlation with intra-operative x-rays once an anaesthesia factor was included in order to relax the soft tissue, however, this model could not be used in a predictive manner due to the large variation observed with the aesthesia factor. In a second study positioning parameters: pelvic incidence (+/-15°), chest cushion location (under ribs 3-6 or 6-9), chest cushion height (0 and 3.5 cm), and corrective forces between 10-150 N at the rib hump, lateral thorax and lateral lumbar region were adjusted and the resulting geometrical changes to decompensation, balance, main thoracic Cobb, lumbar Cobb, thoracic AVT, lumbar AVT, AVR, kyphosis, lordosis, and rib hump measured. The impact of each positioning parameter on the geometrical indices was evaluated and the positioning configuration which optimized each geometric parameter evaluated. The optimized positions were not experimentally validated but this study showed the potential for modulation of a wide range of spinal geometrical parameters through patient positioning.

CHAPTER 2 OBJECTIVES AND HYPOTHESES

2.1 Objectives

The general objective of this doctoral project was to study how patient positioning for surgeries of the spine impacts spinal geometry and how could it be exploited to improve surgical interventions. To address this main objective, technical development was needed to adapt and further develop a finite element model (FEM) of the spine, thoracic cage, pelvis, and relevant adjacent structures in order to simulate and predict geometric changes to the spine resulting from patient positioning on the MFPF. Also, complementary experimental tests were required to validate FEM behaviour and provide proof of concept for the novel surgical positions developed.

Specific objectives of this project were:

Objective 1: Adapt and develop a FEM of the spine, thoracic cage, pelvis, and adjacent structures that is able to simulate the geometric effects on the spine resulting from:

- going from the standing to prone position; and
- for the adjustment of MFPF positioning parameters.

Objective 2: Experimental testing of prone positioning on the MFPF and the impact of its existing features (hip flexion/extension and sternum raising) for their ability to manipulate spinal geometry. Validate the FEM using the results of these experimental tests.

Objective 3: Exploit the FEM in order to study additional surgical positions allowing modification of spinal geometrical parameters not possible on the original MFPF design. Experimentally assess these new positions using proof of concept features constructed for the MFPF.

Objective 4: Exploit the FEM in order to study the impact of combined MFPF positioning parameters on the geometry of the spine (especially the leg positioning and thoracic components) including developing a method allowing for individual and global optimization of spinal geometrical parameters.

2.2 Hypotheses

Hypothesis 1: A FEM of the human vertebral column, thoracic cage, pelvis, and relevant adjacent

structures can simulate the geometric effects on the spine, resulting from a patient moving from a standing position to a prone position on the MFPF with a coronal and sagittal plane Cobb angle accuracy of 5° for a segmental curve.

Hypothesis 2: Leg positioning has an important impact on the geometry of the spine. Manipulation of a patient's leg position while on the MFPF can:

- modify the lumbar lordosis by +25%, -40% and the thoracic kyphosis by +20%, -10% relative to a neutral prone position; and
- reduce the primary coronal plane deformation Cobb angle of a scoliotic spine by 10% relative to a neutral prone position.

Hypothesis 3: The combined adjustments of various patient positioning parameters while prone on a surgical table has an important impact on the 3D geometrical configuration of the spine which can be utilised to obtain the desired spinal shape for a given surgery. Adjustments made to the support and corrective cushions combined with the manipulation of a patient's leg position while on a MFPF can:

- modify lumbar lordosis by +30%, -60% and thoracic kyphosis by +60%, -30% relative to a neutral prone position; and
- reduce the primary coronal plane deformation Cobb angle of a scoliotic spine by 25% relative to a neutral prone position.

2.3 Organization of the thesis

The objectives of this thesis and the three hypotheses are addressed through the form of 5 scientific papers that were submitted or published in peer-reviewed journals. The relationship between the specific papers and objectives/hypotheses is graphically depicted in figure 2.1. Articles 1-4 are presented in Chapter 3 while article 5 is presented in Chapter 4.

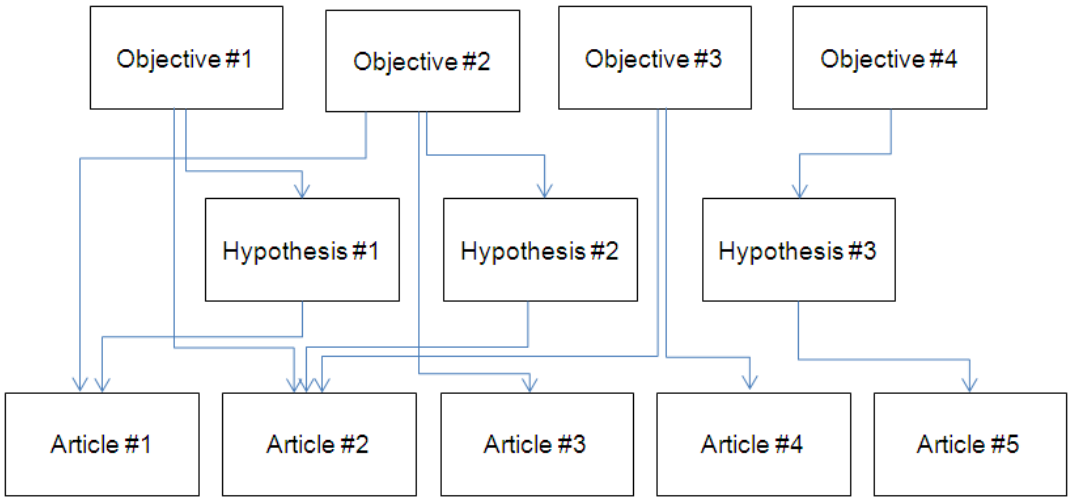

Figure 2.1: Thesis organizational chart

CHAPTER 3 BIOMECHANICAL STUDIES OF PATIENT POSITIONING AND ITS IMPACT ON THE SCOLIOTIC SPINE

The following chapter addresses the objectives 1, 2 and 3 and hypotheses 1 and 2 of this project through the form of 4 scientific papers.

3.1 The impact of prone surgical positioning on the scoliotic spine

The study of prone positioning was a first and important step upon which many other aspects of this project depended. Previous studies have shown that scoliotic deformities are reduced as a result of prone positioning on other surgical frames. This paper aimed to determine what changes in spinal geometry would result from prone positioning on the MFPF. Further, the 3D reconstruction process used to obtain patient-specific geometry used in this project was based upon radiographs acquired in the standing position. In order perform subsequent MFPF patient position simulations, a valid method of placing the FEM in the prone position on the MFPF must first be developed. Finally, the impact of MFPF and patient parameters on prone positioning spinal geometrical changes were studied in order to aid in predicting spinal geometrical changes and to determine what design changes can be made to the MFPF in order to improve the prone positioning process. The realisation of the prone positioning component of objective 2 (experimental testing of prone positioning on the MFPF and validation of FEM prone positioning) and hypothesis 1 are presented in this paper entitled “the impact of prone surgical positioning on the scoliotic spine”, for which the contribution of the first author is considered to be 85%. It was submitted to *Journal of Spinal Disorders and Techniques* on November 11th 2010.

3.1.1 Article 1: Impact of prone surgical positioning on the scoliotic spine

Impact of Prone Surgical Positioning on the Scoliotic Spine

CHRISTOPHER DRISCOLL[1,2] BEng, CARL-ERIC AUBIN[1,2] PhD,
FANNY CANET[1,2] MASc, HUBERT LABELLE[2] MD,
JEAN DANSEREAU[1] PhD

1 – Dept. of Mechanical Engineering,
École Polytechnique de Montréal
P.O. Box 6079, Station Centre-Ville
Montréal, Québec, H3C 3A7, Canada

2 – Sainte-Justine University Hospital Center
3175 Cote-Ste-Catherine Rd.
Montreal, Quebec, H3T 1C5, Canada

Address for notification, correspondence and reprints:

Carl-Eric Aubin, Ph.D., P. Eng.
Full Professor
& Canada Research Chair 'CAD Innovation in Orthopedic Engineering' and 'NSERC / Medtronic Research Chair in Spine Biomechanics'
P.O. Box 6079, Station "Centre-Ville", Montréal (Québec), H3C 3A7 CANADA
E-mail: carl-eric.aubin@polymtl.ca
Phone: 1 (514) 340-4711 ext 4437; Fax: 1 (514) 340-5867

3.1.1.1 ABSTRACT

Objective: To study the impact of patient specific prone positioning on the sagittal and coronal curves of scoliotic spines, including the impact of various patient and surgical frame factors.

Summary of Background Data: Prone operative positioning has been shown to impact the geometry of various individual spinal segments. Its impact on global spinal geometry and influential factors remains unknown.

Methods: Lateral and coronal radiographs were acquired of six scoliotic patients while standing, prone on a dynamically adjustable surgical frame, and intra-operatively on the Relton-Hall frame. Standing lateral bending radiographs were also acquired. Lordosis, kyphosis, and Cobb angles were measured in each position. Personalized FEMs, including the spine, ribcage, pelvis and lower limbs were generated for each patient based on their standing radiographs. The FEM's ability to reproduce prone spinal geometry was evaluated while using different values of intervertebral disc elastic moduli: published, optimized based on lateral bending radiographs and optimized based on prone radiographs. The 6 FEMs were then exploited to study the impact of surgical frame cushion configuration, standing curve magnitudes and patient weight on spinal geometry changes due to prone positioning.

Results: All coronal and sagittal curves decreased in the prone position; averaging 12% in lordosis, 19% in kyphosis, 7%, 14% and 26% respectively for proximal thoracic, main thoracic and thoraco-lumbar/lumbar Cobb angles. FEM prone simulations yielded best results when optimized using the prone position radiographs (delta < 5° for all segmental curves). Lateral bending optimization yielded similar results to using published properties. Surgical frame cushion configuration, standing curve magnitudes and patient weight all had an important impact on spinal geometries with the exception of thoracic cushion longitudinal position. A strong correlation (R=0.986) was found between standing kyphosis and its reduction in the prone position.

Conclusions: Prone positioning results in a reduction of all spinal segmental curves which is dependent on a number of patient and surgical frame factors.

KEY WORDS

prone positioning • spine • scoliosis • surgery • finite element modeling

ACKNOWLEDGEMENTS

Project funded by the Natural Sciences and Engineering Research Council of Canada (Industrial Research Chair with Medtronic of Canada). Special thanks to Dr William Horton from the Emory Spine Center for technical guidance in the positioning device conception and evaluation and Michael Cademartori for taking all the radiographs.

3.1.1.2 INTRODUCTION

Prone surgical positioning has an important impact on the spinal geometry of scoliotic patients. While studies have shown that Cobb angles are reduced by 25 to 33% (Delorme et al. 2000, Behairy et al. 2000, Mac-Thiong et al 2002) due to prone positioning, its impact on sagittal curves remains unclear. Conflicting results have been obtained with regards to whether standing lordosis is maintained in the straight leg prone position or if the hips must be extended. Stephens et al. 1996 and Guanciale et al. 1996 respectively showed slight increases (2% and 6%) in lordosis due to straight leg prone positioning on the Jackson and 4-post type frames. On the other hand, Tan et al. 1994 showed an 18% reduction in standing lordosis using chest rolls and Befanti et al. 1997 a 3% reduction of standing lordosis on the Wilson frame with pillows placed under their subject's legs such that their pelvis started elevating off its surface. Conflicting results have also been obtained as to the impact of prone surgical positioning on thoracic kyphosis. Jackson et al. 2005 and Marsicano et al. 1998 respectively showed a 7^{o} increase (T4-T12) and a 8^{o} decrease (T5-T12) of thoracic kyphosis on the Jackson frame. These previous studies on the impact of prone positioning on spinal geometry have all been limited to the study of a single segment in either the sagittal or coronal planes.

Reductions in sagittal spinal curves below normal physiologic values following scoliotic instrumentation is detrimental and should be avoided. These reductions can have a negative

impact on post-operative spinal balance and fusion efficiency (Vialle et al. 2005), be a contributing factor to flatback syndrome, and even result in long term complications such as adjacent level degeneration (Kumar et al. 2001), especially if a large portion of the spine is going to be instrumented.

The factors which influence changes in spinal geometry during prone positioning are complex. Certainly intervertebral disc flexibility, disc and vertebral wedging and other deformations such as shape of the zygapophyseal joints play a role, however, scoliotic deformity reduction has been shown to be independent of curve severity, at least in the supine position (Torell et al 1985). Additional factors such as surgical frame design (Duke et al. 2008), patient sagittal curves and patient weight may also influence prone changes in spinal geometry.

It is desirable to have knowledge on how the complete spinal geometry of a given patient will be impacted by prone surgical positioning. This would allow for improved surgical planning (e.g. surgeons will have a better idea of what spinal geometries to expect intra-operatively which can't always be visualized with current imaging techniques). This would also allow for improved subsequent patient positioning on surgical frames (e.g. to correct a known loss in lordosis by extension of the hips).

A previous study by Duke et al. 2005 attempted to reproduce changes in the scoliotic deformities of two patients due to prone positioning on the Relton-Hall (RH) frame using a finite element model (FEM) whose intervertebral disc stiffness was personalized based on lateral bending tests. The FEM was able to reproduce coronal plane changes within 10° after the inclusion of a relaxation factor to account for the effects of anesthesia. This study utilized several important concepts such as a method to simulate prone positioning using vertebral segmental weight re-orientation and design of experiment exploitation during the disc personalization process.

The objective of this study was to experimentally validate and exploit a FEM of the spine, ribcage, pelvis and lower limbs in order to study the impact that patient specific prone positioning has on the sagittal and coronal curves of scoliotic spines, in addition to testing which factors influence this impact. It is hypothesized that prone positioning will result in at least a 15% reduction in sagittal curves which, along with Cobb angles, can be influenced by patient weight, standing segmental curve magnitudes, and surgical frame configuration up to an additional 20%. It is also hypothesized that personalized FEMs can reproduce changes to all sagittal and coronal curves due to prone positioning with an accuracy of 5°.

3.1.1.3 METHODS

EXPERIMENTAL TESTING

Experimental testing was performed at Sainte-Justine University Hospital Center in Montreal with approval obtained from the ethics committee. A total of 6 pre-operative adolescent idiopathic scoliosis patients, 5 females and 1 male, participated in the study, as summarized in Table 1. They had received no prior surgical treatment and were scheduled to undergo spinal instrumentation shortly after their participation in the study. Pre-operative standing postero-anterior (PA) radiographs showed an average proximal thoracic (PT) Cobb angle of 25° (3° to 46°; std 17°), average main thoracic (MT) Cobb angle of 57° (33° to 83°; std 17°) and an average thoracolumbar / lumbar (TL/L) Cobb angle of 37° (19° to 44°; std 9°). Pre-operative standing lateral radiographs showed an average T12-S1 lumbar lordosis of 69° (61° to 85°; std 11°) and an average T4-T12 thoracic kyphosis of 33^{o} (4° to 67°; std 23°).

Patients were weighed, their heights and lower limb lengths measured, and then placed in a neutral prone position on a multi-functional positioning frame prototype (MFPF) which included two adjustable thoracic cushions, two adjustable pelvic cushions, arm and head rests,

and a dynamically adjustable leg-positioning feature (Figure 1). Due to surgical frame design, patient's hips and knees were both in slight flexion (averaging 15° and 32° respectively) which was assumed to have a minimal impact on spinal curves based on previous works (Driscoll et al. 2010), but which was nevertheless accounted for during the FEM simulations. PA and lateral 36" (91.4 cm) radiographs were taken of each patient's spine using a mobile radiograph device operated by a trained technician. In addition, standing PA left and right lateral bending radiographs (taken a few days before the surgery), and PA and lateral intra-operative radiographs (prone on RH frame) were acquired. The representative radiographs of patient #1 are shown in Figure 1. All radiographs were digitally analyzed using Synapse imaging software (Fujifilm USA) with lordosis, kyphosis, and scoliotic Cobb angles measured for each case as defined by the measurement manual of the Spinal Deformity Study Group (O'Brien 2005). The 17" (43.2 cm) intra-operative radiographs did not allow for measurement of lumbar lordosis or high thoracic Cobb angles for all cases as they did not capture the entire spine; these measures were not considered in the analyses. Wilcoxon matched pairs tests were performed comparing segmental curve geometry in the standing position and in the prone position in both surgical frames.

FINITE ELEMENT MODELING

A previously developed FEM representing the osseo-ligamentous structures of the spine, ribcage, pelvis, and lower limbs including muscles was adapted for the purposes of this study (Figure 2). Patient-specific trunk geometry was obtained using a biplanar reconstruction technique (Cheriet et al. 2007) based on pre-operative standing postero-anterior (PA) and lateral radiographs in which the patient wore a calibration plate containing radio-opaque markers. Anatomical landmarks were identified and their 3D coordinates obtained using a self-calibration

and optimization algorithm which were then used to transform detailed vertebral geometry using a free form deformation technique (Cheriet et al. 2007, Kadoury et al. 2007). The accuracy of this reconstruction method has been shown to be 3.3 mm (Delorme et al. 2003). Geometry of the lower limbs was obtained by linear interpolation and scaling of Visible Human Project FEM geometry (Viceconti from www.tecno.ior.it/VRLAB) based on direct measurement of femur and tibia lengths. Published material properties were attributed to all elements as described elsewhere by Driscoll et al. 2010 and Duke et al. 2005. In total the FEM contains 1790 nodes and 1247 elements and has been previously used to study the impact of lower limb positioning (hip flexion and extension) on the sagittal curves of the spine including the influence of subject specific lower limb muscle flexibilities (Driscoll et al. 2010).

Introduced were nodes defining the center of mass for transverse body segments representing T1 through L5 sliced at the midpoint of their superior and inferior intervertebral discs according to the work of Pearsall et al. (1996) which were then linked to their respective vertebral body centroids using un-deformable beam elements. These nodes were located anterior to the vertebral body centroids by a distance averaging 30 mm and ranging from 4 to 46 mm.

PRONE POSITIONING SIMULATIONS

The experimental testing was reproduced using the personalized FEMs of each patient reconstructed from their standing pre-operative radiographs and lower limb measurements. Prone positioning on the MFPF was simulated in three phases: two phases in which gravitational forces applied to the FEM were re-oriented representing the FEM going from the standing to prone position and a third phase in which displacements were applied to the FEM to reproduce body position on the MFPF.

In the first phase of gravitational force re-orientation, forces equivalent to trunk transverse body segment weights for each vertebral level, defined as a percentage of body weight by Pearsall et al. 1996 and personalized for each patient, were applied to nodes representing the transverse body segment centers of mass in the vertical or positive longitudinal direction. Forces equivalent to head, shoulder and upper limb weights defined as a percentage of body weight by Winter 1990 were also included. Head weight was applied to the T1 segment center of mass while shoulder and upper limb weight was applied as evenly distributed loads to the thoracic vertebrae segment centers of mass; all in the vertical direction. These forces ranged from 2.3% to 2.6 % of body weight in the lumbar region, from 1.6% to 3.0% of body weight in the thoracic region, and was 9.7% of body weight at T1. A zero displacement constraint (all directions) and a zero rotation constraint in the transverse and coronal planes were applied to the nodes representing the acetabula while the displacement of T1 was constrained in the lateral and AP directions. These constraints allowed the spine freedom to extend over a fixed pelvis which could sagitally rotate along the bi-femoral head axis while ensuring that sagittal and coronal balance was maintained.

In the second phase of gravitational force re-orientation, forces equivalent to transverse body segment weights for each vertebral level, as detailed in phase 1, were applied in the transverse plane PA direction as a combination of point forces and distributed loads: one third to each vertebral body centroid and the remaining two thirds distributed over the nodes representing the thoracic cage contained in the segment. This distribution was based on the analysis of a transverse section of the Visible Human Project (male) thoracic cage in which the surface area of bone, muscle, and adipose tissue within the vertebral region antero-posterior (AP) slice was compared to the area of tissues in the remaining segment while factoring for relative densities. In the lower lumbar region, forces equivalent to the entire segment weight were applied to the

vertebral body centroids. During this phase, the weight of the head, shoulders and upper limbs were not included as they were supported by dedicated cushions on the MFPF. Nodes representing the anterior portion on the thoracic cage and pelvis were constrained for lateral and AP displacements if they were in contact with the surgical frame cushions as visible on the MFPF prone radiographs with an additional zero displacement constraint in the longitudinal direction applied to the pelvis nodes in order to fix the model in space.

In the third phase, some final geometrical adjustments were made to the FEM in order to better represent conditions on the MFPF. The AP positions of the anterior thoracic cage nodes were displaced such that their relative position to the anterior pelvis nodes matched that of their corresponding MFPF cushions. Pelvic tilt was also adjusted to that measured on the radiographs by fixing the superior centroid of S1 and displacing the acetabulum nodes in the AP direction.

Resultant spinal sagittal and coronal plane curves (lordosis, kyphosis, and Cobb angles) were measured using the intercepts of the lines linking the end vertebrae superior and inferior endplate centroids and the values obtained compared to the experimental results.

For each patient, the described prone positioning simulation was performed 5 times each with different values of intervertebral disc elastic moduli; baseline, optimized using the prone position radiographs, optimized using the left bending radiographs, optimized using the right bending radiographs, optimized using both the left and right bending radiographs.

The baseline intervertebral disc elastic modulus was taken from literature (4.2 MPa from Goel & Weinstein 1990). The intervertebral disc elastic moduli optimized using the prone position radiographs was based on the results of a 3 state, 9 factor, 81 run design of experiment. The 9 factors, thoracic and lumbar intervertebral disc moduli grouped in adjacent pairs except for the T12-S1 disc which was alone, were multiplied and divided by 4 times their baseline values. The multiplication factor was chosen based upon a sensitivity study of the FEM for which the

corresponding disc elastic moduli represented the limits of physiological behavior (maximum spinal elongation). The dependant factor to be optimized was the sum of the differences (delta, Δ) between coronal and sagittal plane segmental curves observed on the prone position radiographs and obtained with the FEM simulations:

$$\Phi = \Delta L + \Delta K + \Delta PT + \Delta MT + \Delta TL/L$$

where L = Lordosis, K = kyphosis, PT = proximal thoracic Cobb angle (only the structural curves were considered), MT = main thoracic Cobb angle, and TL/L = thoracolumbar / lumbar Cobb angle.

The intervertebral disc elastic moduli optimization based on the lateral bending radiographs was done using an adaptation of the methods of Petit et al. 2004 and Duke et al. 2005; in this case the lateral bending radiographs were taken in the standing position (as opposed to in the supine one). The lateral bending tests were simulated with the FEM and the intervertebral disc elastic moduli optimized in order to minimize the difference between the simulated and radiographically observed values of coronal plane scoliotic Cobb angle changes. For this the nodes representing the patient's pelvis were fixed in space while the node representing the vertebral body centroid of T1 was displaced such that its position in the coronal plane relative to S1 matched that measured on the bending radiographs. This simulation was repeated while varying the intervertebral disc elastic moduli based on a 3 state, 9 factor, 81 run design of experiment in which the adjacently paired elastic moduli were multiplied and divided by 4 times their baseline values. The dependant factor to be optimized (Φ) was the sum of the differences between coronal plane segmental curves measured on the radiographs and obtained with the FEM simulations for left bending, the right bending, and both the left and right lateral bending tests:

$$\Phi = \Delta \text{ PT left bending} + \Delta \text{ PT right bending} + \Delta \text{ MT left bending}$$
$$+ \Delta \text{ MT right bending} + \Delta \text{ TL/L left bending} + \Delta \text{ TL/L right bending.}$$

STATISTICA V7 software (StatSoft Inc) was used to generate all experimental designs as well as analyze their results; providing the impact of each grouped pair of intervertebral disc elastic moduli on segmental curve changes and their quadratic regression coefficients for Φ. Regression equations were then solved for the minimized case using a MATLAB V7.5 software (MathWorks Inc) pattern search function.

STUDY OF FACTORS WHICH CAN INFLUENCE PRONE POSITIONING

Additional simulations were performed in order to determine the impact that patient weight, degree of sagittal curves, severity of scoliotic curves, and surgical frame configuration have on the spinal geometry changes experienced due to prone surgical positioning. Repeated prone positioning simulations were performed with the FEMs of each patient (disc properties optimized based on prone radiographs) while independently varying the factors under study. Patient weights were varied by ± 50%, sagittal curves (lordosis and kyphosis together) by ± 30%, scoliotic curves (PT, MT, and TL/L together) by ± 30%, and the location of the thoracic cushions (left and right simultaneously) relative to the pelvic ones by ± 10 cm in vertical position and ± 10 cm in longitudinal position. Sagittal and coronal plane curve magnitude variations were performed with the reconstruction software by lateral displacement of the spline apices representing the patient's spine in the appropriate plane. The relative positions of thoracic and pelvic cushions were modified in the longitudinal position by the choice of ribcage nodes constrained in phase two of the prone positioning simulation and in vertical position by AP displacement of the ribcage nodes in phase three of the prone positioning simulation.

3.1.1.4 RESULTS

Experimental prone positioning on the MFPF resulted in an average 8° or 12% (3° to 16°; ±5°) reduction in lordosis ($p = 0.0412$), an 11° or 19% (1° to 29°; ±11°) reduction in kyphosis ($p = 0.0796$), an 8° or 14% (5° to 16°; ±4°) reduction in MT ($p = 0.0277$) and a 9° or 26% (1° to 15°; ±5°) reduction in TL/L ($p = 0.0277$). Both patients with a structural PT had it reduced by 3° or 7%. The detailed results are summarized in Table 2 in the form of absolute angles with inclusion of percentage change relative to the standing position in brackets.

A large range of spinal flexibilities were measured on the bending radiographs. For the left bending case, the MT increase ranged from 4% to 43% while TL/L decrease ranged from 22% to 89%. For the right bending case MT decrease ranged from 0% to 70% while TL/L increase ranged from 13% to 69%. PT values could not be measured in all cases due to invisibility of the upper end vertebrae on the radiographs. Pre-operative lateral bending tests are summarized in Table 3 in the form of absolute Cobb angles and percentage change relative to the standing position for both the left and right lateral bending cases. Spearman correlations between the % changes in spinal geometry during the lateral bending tests and during prone positioning; $\Delta MT_{bending}$ vs. ΔMT_{prone} and $\Delta TL/L_{bending}$ vs. $\Delta TL/L_{prone}$ (considering left hand bending only, right hand bending only, and combined left hand and right hand bending) were weak with the highest being 0.200 between the changes in TL/L Cobb for left bending and prone positioning.

A graphical depiction of the three phases of the prone positioning simulation for patient #1 can be found in figure 2 which shows the forces and boundary conditions prior to their application. Phase 1 resulted in a noticeable elongation of the spine and reduction in all segmental curves as well as a slight anterior rotation of the lower thoracic cage. The only visible impact of

phase 2 was a small compression of the thoracic cage. Finally, phase 3 brought the FEM thoracic cage and pelvis into positions consistent with those visible on the lateral prone radiographs.

Using the baseline intervertebral disc material properties, the model was able to predict the experimental results for reduction of segmental curve angles with an average difference of 5° (±4°) for lordosis, 6° (±6°) for kyphosis, 1° for PT, 14° (±10°) for MT, and 5° (±2°) for TL/L. Optimization of the intervertebral disc properties using the prone position radiographs improved FEM behavior resulting in average difference of 2° (±2°) for lordosis, 4° (±3°) for kyphosis, 1° for PT, 4° (±3°) for MT, and 5° (±3°) for TL/L. When using the personalization method based on lateral bending tests the average differences obtained with the three methods (left bending only, right bending only, and combined left and right bending) were very close to each other with average differences in values of lordosis, kyphosis, PT, MT, and TL/L were respectively 9°, 6°, 2°, 10° and 5°; ranges and further details in Table 2.

Experimental intra-operative prone positioning on the RH resulted in an average 14° or 42% (0° to 25°; ±10°) reduction in kyphosis ($p = 0.04312$), a 20° or 29% (5° to 42°; ±14°) reduction in MT ($p = 0.0277$), and a 14° or 38% (2° to 24°; ±8°) reduction in TL/L ($p = 0.0277$) as compared to the standing position. These values have an average additional 16% decrease in segmental curves relative to experimental results found for prone positioning on the MFPF (22% for kyphosis, 15% for MT, and 12% for TC/LC) which was quite varied from one patient to the next (3% to 32%; ±10%). The detailed results for each patient are summarized in Table 2 along with their percent changes relative to the standing position which are in brackets. It should be noted that patient #2, as opposed to the other patients, underwent surgery several months after the experimental testing and as such their curves had time to progress (39° and 27° increases in MT and TL/L respectively). Thus percent changes for patient #2 are relative to their standing radiographs which were taken again just prior to surgery.

The intervertebral discs (T1-2 through L4-5), whose elastic moduli were found to significantly impact ($p < 0.05$) changes in segmental curves for at least two of the patients during the prone positioning simulations were T7-8 to L4-5 for lordosis, T4-5 to L2-3 for kyphosis, T5-6 to L3-4 for MT Cobb, and T9-10 to L4-5 for TL/L Cobb. During the bending simulations they were T7-8 to L4-5 for MT Cobb and T7-8 to L4-5 for TL/L Cobb. The values of intervertebral disc elastic moduli obtained by the prone position optimization process showed higher values than reported in literature for normal spines averaging 11 MPa (2.9 to 16.8; ±4 MPa) and their distribution showed no patterns between apices or end vertebrae.

The majority of influential factors studied had an important impact on prone spinal geometry. Increasing and decreasing standing sagittal curves resulted in respectively more and less reductions due to prone positioning. Increasing and decreasing standing coronal curves also resulted in respectively more or less reductions due to prone positioning. Changing the standing sagittal curve magnitudes did not impact prone coronal curve reductions and vice versa. Changing the relative vertical position of the thoracic cushions had an important impact on sagittal curves. Raising it by 10 cm resulted in 56% more kyphosis and 26% more lordosis than the normal prone position; lowering it by 10 cm caused 39% less kyphosis and 14% less lordosis. Coronal curves were only very slightly impacted by changes in vertical position of the thoracic cushions. Increasing a patient's weight (thus increasing the amount of equivalent weight forces reoriented) caused additional reduction in segmental curves in the prone position and vice versa; most noticeably with kyphosis and MT Cobb. MFPF thoracic cushion longitudinal position had no impact of prone position spinal geometry. The average results for the 6 patients and their standard deviations are detailed in Table 4.

3.1.1.5 DISCUSSION

The average experimentally measured reductions in sagittal curves due to prone positioning on the MFPF were around the hypothesized value of 15%. Intra-operatively on the RH, reduction in kyphosis was even higher at 29%. These reductions all had p-values < 0.05 with the exception of kyphosis on the MFPF which was 0.0796. The fact that two patients were hypo-kyphotic influenced the statistical analysis. The higher a patient's standing kyphosis, the more it was reduced due to prone positioning. This was shown experimentally with a Spearman correlation of 0.986 between standing kyphosis and its reduction due to prone positioning on the MFPF. This was also shown by the study of FEM influential factors which showed that increasing and decreasing standing kyphosis by 30% resulted in respective 11% more and 12% less losses due to prone positioning. The changes in lordosis due to prone positioning were not dependent on standing values (Spearman = -0.143). This is probably due to the fact that lordotic curves are more pronounced and thus have more potential for reduction.

In order to avoid maintaining sagittal curve losses due to prone positioning post-operatively, corrective measures must be taken prior to final instrumentation and fusion. Spinal instrumentation, such as those which utilize rotation maneuvers or in-situ rod contouring can increase sagittal curves but this is not always the case; incidences of flatback syndrome still persist. Another way of countering prone positioning sagittal curve losses is through surgical frame configuration. As was shown by the study of influential factors, increasing the vertical position of the thoracic cushions relative to the pelvic ones increased both lordosis and kyphosis. A 10 cm difference in vertical position maintained standing lordosis and cut the losses in kyphosis by half. Finally, subsequent patient positioning on the surgical frame can also be used to

increase sagittal curves such as by extending the lower limbs (Driscoll et al. 2010) or raising the sternum (Driscoll et al. 2010).

As with previous studies (Mac-Thiong et al 2002), all Cobb angles were reduced due to prone positioning; both MT and TL/L showed significant reductions on the MFPF and RH. TL/L curves had higher reductions than MT curves 26% vs. 15% on the MFPF and 38% vs. 26% on the RH. This difference can be attributed to the fact that the lumbar spine is more flexible than the thoracic spine due to the presence of the rib cage (Edmondston et al 1999). Coronal plane curve reductions experienced due to prone positioning are beneficial to the surgical intervention by requiring less subsequent correction with surgical instrumentation. Larger Cobb angles resulted in higher losses due to prone positioning, as shown both experimentally and with the FEM study of influential factors; most noticeably with MT Cobb. The Spearman correlation between standing MT Cobb and its reduction due to prone positioning was 0.522 on the MFPF and 0.943 on the RH.

The FEM developed was able to reproduce the experimental results with an average error across all segmental curves of 4° (maximum: 11°, minimum: 0°, and standard deviation: 3°) when optimized based on the prone position radiographs giving confidence in their exploitation, however, accuracy drops to an average error of 7° (maximum: 26°, minimum: 0°, and standard deviation: 7°) when done pre-operatively using lateral bending tests (left and right hand combined). This may be due to the fact that lateral bending tests are not done in a systematic way, are quite variable and have been shown to have poor reproducibility (Cheh et al. 2007). A simple method of assessing patient-specific spinal geometrical changes due to prone positioning would be to take pre-operative radiographs while they are on the surgical frame. If this is not possible (e.g. due to equipment limitations or availability) the FEM can be used, however, it is suggested that an improved method of personalizing spinal flexibility such as calibrated suspension

flexibility testing (Lamarre et al. 2009) be used. The FEM described in this study could be further exploited to study additional patient positions on the MFPF as well as help in the development of novel positions for future surgical frame designs. Simulation of prone positioning was a first and important step in that process.

One of the limits of the FEM utilized in this study is the simplified representation of the intervertebral discs by elastic beam elements when in fact they are complex structures with poro-viscoelastic behavior. This simplified representation was chosen for computation considerations and acceptable since immediate and global geometry was being looked at. Another limit was the method in which spinal stiffness was adjusted by uniquely changing the material properties of the intervertebral discs when other elements such as the anterior longitudinal ligament stiffness, facet capsular ligament stiffness, vertebral wedging, and the pathological shape of zygapophyseal joints may also play a role (Hukins et Meakin 2000). The approach utilized essentially groups the impact of all these factors into the stiffness contributions of the disc. While doing so does not impact the global stiffness of a given functional unit, it may overestimate the intervertebral disc elastic moduli values obtained by the optimization methods.

The additional segmental curve reductions obtained on the RH relative to the MFPF can be attributed to the effects of anesthesia and surgical opening (Mac-Thiong et al. 2003). Its large fluctuation (between 3% and 32%) suggests that these effects are not the same for all patients. Attempting to find a link between additional segmental curve reductions observed intra-operatively and standing geometry, lateral bending test flexibility, or patient weight yielded no strong correlations. However, scoliotic curves which were non-structural (TL/L for patients 5 and 6) showed the most additional reduction. While it is possible that the difference in surgical frame types (MFPF vs. RH) may have also influenced the additional segmental curve losses, the FEM study of influential factors suggests that this would not be the case as long as the relative vertical

position of the thoracic and pelvic cushions was the same (as was the case here). Other possible influential factors not tested by the FEM (e.g. hip flexion) were also similar between the frames.

In the study of influential factors it was shown that increasing or decreasing the FEM weights resulted in respectively more and less segmental curve losses due to prone positioning. This result is due to the fact that the same FEM standing geometry was utilized regardless of their attributed weight. In reality, a heavier patient's spine will be more compressed in the standing position and will experience more elongation (and sagittal curve reduction) due to prone positioning but ultimately result in the same prone position geometry. The prone position spinal geometry was here independent of weight.

3.1.1.6 CONCLUSION

Prone operative positioning has an important impact on both the sagittal and coronal curves of the vertebral column which are all reduced relative to the standing position. While deformity reduction may facilitate the surgical intervention, loss of standing sagittal curves must be addressed by surgical positioning for best post-operative results. The FEM developed can be used to reproduce segmental curve reductions within average segmental curve errors of 5° and exploited to further study prone positioning especially when using intra-operative data for model personalization. Finally, patient and surgical frame factors can have an important impact on prone curve reductions.

3.1.1.7 REFERENCES

Delorme S, Labelle H, Poitras B, Rivard CH, Coillard C, Dansereau J. Pre-, intra-, and postoperative three-dimensional evaluation of adolescent idiopathic scoliosis. J Spinal Disord. 2000 Apr;13(2):93-101.

Behairy YM, Hauser DL, Hill D, Mahood J, Moreau M. Partial correction of Cobb angle prior to posterior spinal instrumentation. Ann Saudi Med. 2000 Sep-Nov;20(5-6):398-401.

Mac-Thiong JM, Labelle H, Petit Y, Aubin CE. The effect of the Relton-Hall operative frame on trunk deformity in adolescent idiopathic scoliosis. Eur Spine J. 2002 Dec;11(6):556-60. Epub 2002 Aug 7

Stephens GC, Yoo JU, Wilbur G. Comparison of lumbar sagittal alignment produced by different operative positions. Spine. 1996 Aug 1;21(15):1802-6; discussion 1807.

Guanciale AF, Dinsay JM, Watkins RG. Lumbar lordosis in spinal fusion. A comparison of intraoperative results of patient positioning on two different operative table frame types. Spine. 1996 Apr 15;21(8):964-9.

Tan SB, Kozak JA, Dickson JH, Nalty TJ. Effect of operative position on sagittal alignment of the lumbar spine. Spine. 1994 Feb 1;19(3):314-8.

Benfanti PL, Geissele AE. The effect of intraoperative hip position on maintenance of lumbar lordosis: a radiographic study of anesthetized patients and unanesthetized volunteers on the Wilson frame. Spine. 1997 Oct 1;22(19):2299-303.

Jackson R, Behee K, McManus A. Sagittal spinopelvic alignments standing and in an intraoperative prone position. Spine J. 2005 Sept; 4(5) : S5.

Marsicano JG, Lenke LG, Bridwell KH, Chapman M, Gupta P, Weston J. The lordotic effect of the OSI frame on operative adolescent idiopathic scoliosis patients. Spine. 1998 Jun 15;23(12):1341-8.

Vialle R, Levassor N, Rillardon L, Templier A, Skalli W, Guigui P. Radiographic analysis of the sagittal alignment and balance of the spine in asymptomatic subjects. J Bone Joint Surg Am. 2005 Feb;87(2):260-7.

Kumar MN, Baklanov A, Chopin D. Correlation between sagittal plane changes and adjacent segment degeneration following lumbar spine fusion. Eur Spine J. 2001 Aug;10(4):314-9.

Torell G, Nachemson A, Haderspeck-Grib K, Schultz A. Standing and supine Cobb measures in girls with idiopathic scoliosis. Spine. 1985 Jun;10(5):425-7.

Duke K, Aubin CE, Dansereau J, Labelle H. Computer simulation for the optimization of patient positioning in spinal deformity instrumentation surgery. Med Biol Eng Comput. 2008 Jan;46(1):33-41.

Duke K, Aubin CE, Dansereau J, Labelle H. Biomechanical simulations of scoliotic spine correction due to prone position and anaesthesia prior to surgical instrumentation. Clin Biomech (Bristol, Avon). 2005 Nov;20(9):923-31.

Driscoll C, Aubin CE, Canet F, Labelle H, Dansereau J. Biomechanical study of the influence of lower limb surgical positioning on spinal geometry. (Submitted to J Spinal Dis Tech October 2010).

O'Brien MF, Kuklo TR, Blanke KM, et al. Spinal Deformity Study Group–Radiographic Measurement Manual. Minneapolis, MN: Medtronic Sofamor Danek, Inc; 2005.

Cheriet F, Laporte C, Kadoury S, Labelle H, Dansereau J. A novel system for the 3-D reconstruction of the human spine and rib cage from biplanar x-ray images. IEEE Trans. Biomed. Eng. 2007; 54:1356-8.

Kadoury S, Cheriet F, Laporte C, Labelle H. A versatile 3D reconstruction system of the spine and pelvis for clinical assessment of spinal deformities. Med. Biol. Eng. Comput. 2007; 45:591-602.

Delorme S, Petit Y, de Guise JA, Labelle H, Aubin CE, Dansereau J. Assessment of the 3-D reconstruction and high-resolution geometrical modeling of the human skeletal trunk from 2-D radiographic images. IEEE Trans Biomed Eng. 2003 Aug;50(8):989-98.

Viceconti M, From: The BEL Repository, "http://www.tecno.ior.it/VRLAB/".

Pearsall DJ, Reid JG, Livingston LA. Segmental inertial parameters of the human trunk as determined from computed tomography. Ann Biomed Eng. 1996 Mar-Apr;24(2):198-210.

Winter D.A., Biomechanics and Motor Control of Human Movement, Second edition. John Wiley & Sons, Inc., Toronto, 1990.

Goel, K., Weinstein J., Biomechanics of the Spine: Clinical and Surgical Perspective, CRC Press, Inc, Boca Raton, Florida, 1990.

Petit Y, Aubin CE, Labelle H. Patient-specific mechanical properties of a flexible multi-body model of the scoliotic spine. Med Biol Eng Comput. 2004 Jan;42(1):55-60.

Driscoll CR, Aubin CE, Canet F, Labelle H, Dansereau J. The Impact of Intra-Operative Sternum Vertical Displacement on the Sagittal Curves of the Spine. Eur Spine J. 2010 Mar;19(3):421-6.

Edmondston SJ, Allison GT, Althorpe BM, McConnell DR, Samuel KK. Comparison of ribcage and posteroanterior thoracic spine stiffness: an investigation of the normal response. Man Ther. 1999 Aug;4(3):157-62.

Cheh G, Lenke LG, Lehman RA Jr, Kim YJ, Nunley R, Bridwell KH. The reliability of preoperative supine radiographs to predict the amount of curve flexibility in adolescent idiopathic scoliosis. Spine. 2007 Nov 15;32(24):2668-72.

Lamarre ME, Parent S, Labelle H, Aubin CE, Joncas J, Cabral A, Petit Y. Assessment of spinal flexibility in adolescent idiopathic scoliosis: suspension versus side-bending radiography. Spine (Phila Pa 1976). 2009 Mar 15;34(6):591-7.

Hukins DWL, Meakin JR. Relationship Between Structure and Mechanical Function of the Tissues of the Intervertebral Joint. American Zoologist. 2000 40(1):42-52.

3.1.1.8 FIGURES AND TABLES

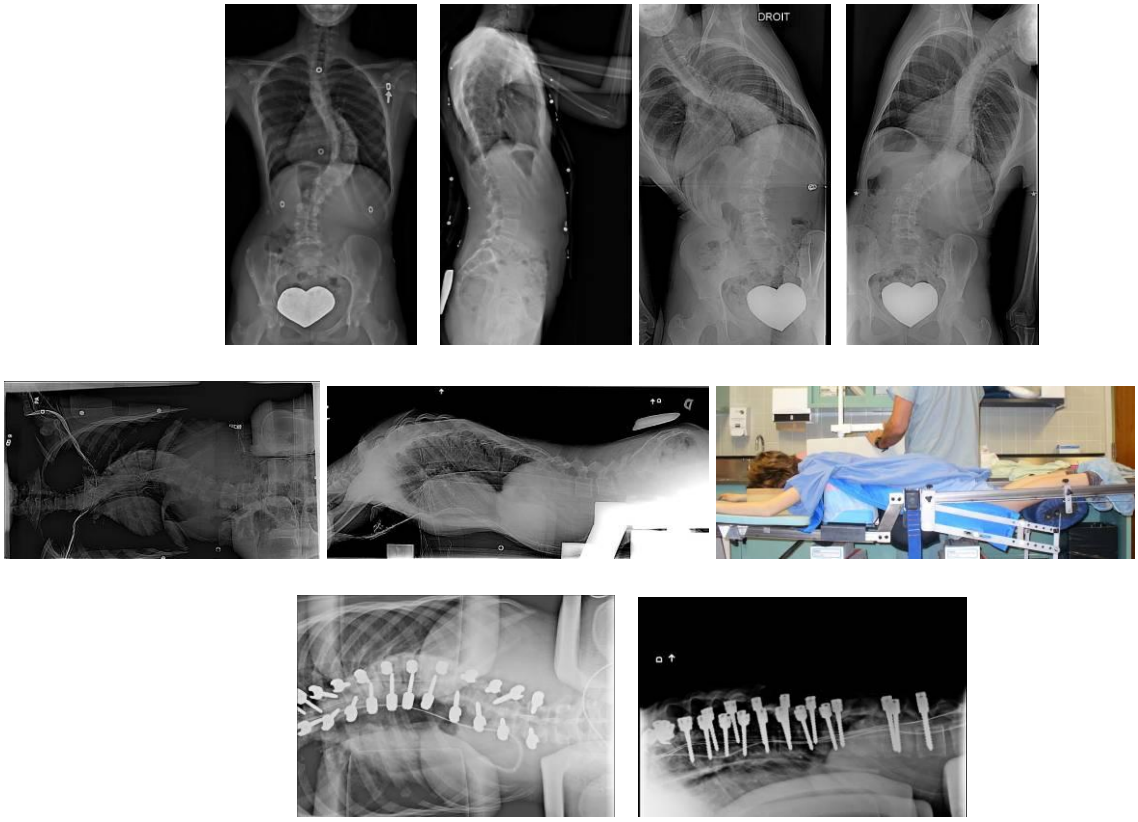

Figure 3.1 (A1F1): Representative radiographs of patient #1 from left to right, top row: PA standing, lateral standing, left and right standing lateral bending; middle row: PA and lateral on MFPF with picture of experimental setup; and bottom row: PA and lateral on Relton-Hall frame

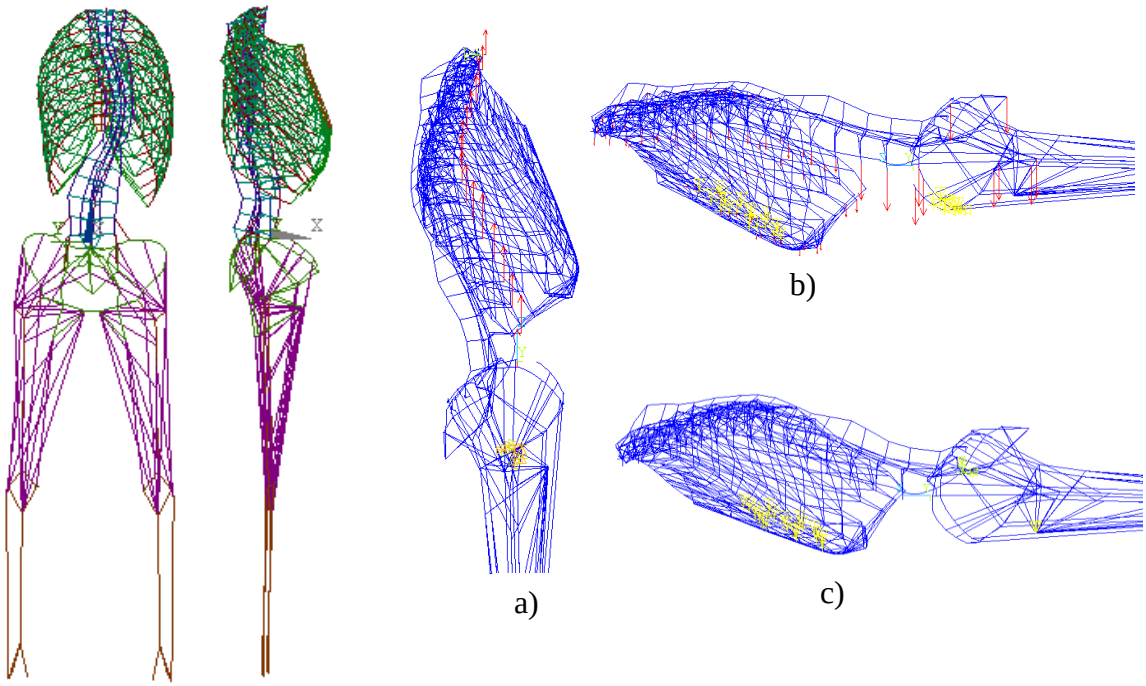

Figure 3.2 (A1F2): PA and Lateral Views of the developed FEM along with the three phases of the prone positioning simulations (patient #1): a) vertical application of forces equivalent to trunk segmental, head, shoulder and upper limb weights; b) AP application of forces equivalent to trunk segment weights; c) pelvic tilt and thoracic vertical position adjustment

Table 3.1 (A1T1): Patient data

Sex	Weight (kg)	Height (cm)	T12 - S1 Lordosis	T4 – T12 Kyphosis	Scoliotic Cobb Angle (end vertebrae)			Lenke
					PT	MT	TL/L	
F	44	161	85°	67°	42° (T1-T7)	68° (T7-L1)	40° (L1-L4)	4A
F	48	161	63°	4°	3° (T1-T6)	33° (T6-T11)	36° (T11-L4)	6C
F	40	159	62°	27°	28° (T1-T6)	83° (T6-T12)	39° (T12-L4)	3A
F	35	142	83°	45°	21° (T1-T3)	55° (T3-T9)	41° (T9-L3)	3C
F	39	170	62°	40°	46° (T2-T8)	53° (T8-L2)	19° (L2-L4)	2A
M	60	179	61°	15°	11° (T1-T3)	49° (T3-T11)	44° (T11-L4)	1B

Table 3.2 (A1T2): Comparison of experimental and simulated results for prone positioning (percentage of change in parentheses)

#	Result Type		T12 - S1 Lordosis	T4 – T12 Kyphosis	Cobb Angle		
					PT	MT	TL/L
1	Exp	MFPF	69° (-19%)	38° (-43%)	39° (-7%)	61° (-10%)	33° (-18%)
		RH	-	46° (-31%)	-	45° (-34%)	22° (-45%)
	Sim	Baseline	71°	37°	39°	47°	32°
		Optimized	72°	40°	40°	56°	34°
		Left Bending	71°	39°	39°	50°	34°
		Right Bending	66°	37°	44°	52°	30°
		Left & Right Bending	63°	36°	39°	48°	29°
2	Exp	MFPF	59° (-6%)	5° (+25%)	-	27° (-18%)	23° (-36%)
		RH	-	2° (-50%)	-	48° (-36%)	47° (-25%)
	Sim	Baseline	56°	3°	-	23°	31°
		Optimized	60°	4°	-	27°	34°
		Left Bending	47°	3°	-	24°	30°
		Right Bending	56°	3°	-	25°	32°
		Left & Right Bending	50°	3°	-	25°	31°
3	Exp	MFPF	55° (-11%)	17° (-37%)	-	67° (-19%)	24° (-38%)
		RH	-	9° (-67%)	-	41° (-51%)	31° (-21%)
	Sim	Baseline	50°	14°	-	42°	28°
		Optimized	55°	18°	-	59°	30°
		Left Bending	48°	18°	-	54°	30°
		Right Bending	47°	14°	-	45°	29°
		Left & Right Bending	48°	17°	-	49°	30°
4	Exp	MFPF	80° (-4%)	29° (-36%)	-	50° (-9%)	40° (-2%)
		RH	-	28° (-38%)	-	48° (-13%)	39° (-5%)
	Sim	Baseline	73°	32°	-	43°	34°
		Optimized	80°	38°	-	46°	36°
		Left Bending	78°	39°	-	44°	34°
		Right Bending	66°	38°	-	48°	32°
		Left & Right Bending	69°	33°	-	42°	34°
5	Exp	MFPF	51° (-18%)	30° (-25%)	43° (-7%)	45° (-15%)	13° (-32%)
		RH	-	15° (-63%)	-	37° (-30%)	5° (-74%)
	Sim	Baseline	50°	13°	44°	36°	16°
		Optimized	55°	23°	43°	45°	18°
		Left Bending	43°	5°	47°	36°	14°
		Right Bending	47°	14°	42°	35°	15°
		Left & Right Bending	45°	9°	44°	35°	13°
6	Exp	MFPF	53° (-13%)	15° (0%)	-	43° (-12%)	32° (-27%)
		RH	-	15° (0%)	-	44° (-10%)	20° (-55%)
	Sim	Baseline	40°	5°	-	16°	27°
		Optimized	49°	9°	-	37°	36°
		Left Bending	36°	14°	-	23°	28°
		Right Bending	38°	3°	-	29°	33°
		Left & Right Bending	27°	16°	-	33°	30°

Table 3.3 (A1T3): Lateral bending Cobb angles and percentage change relative to standing position

#	Left Bending Cobb (% change)			Right Bending Cobb (% change)		
	PT	MT	TL/L	PT	MT	TL/L
1	41° (-2%)	81° (+19%)	26° (-35%)	60° (+43%)	47° (-31%)	45° (+13%)
2	1° (--%)	47° (+42%)	19° (-47%)	-	29° (-12%)	61° (+69%)
3	-	86° (+4%)	30° (-23%)	15° (-46%)	75° (-10%)	46° (+18%)
4	6° (-71%)	73° (+33%)	32° (-22%)	32° (+52%)	55° (0%)	54° (+32%)
5	33° (-28%)	76° (+43%)	3° (-84%)	49° (+7%)	16° (-70%)	23° (+21%)
6	-	56° (+14%)	5° (-89%)	12° (+9%)	37° (-24%)	57° (+30%)

Table 3.4 (A1T4): Average changes in spinal geometry due to prone positioning while varying patient and surgical frame parameters (standard deviations in brackets)

FEM Condition		Lordosis		Kyphosis		PT		MT		TL/L	
Parameter	Change	Deg.	%	deg.	%	deg.	%	deg.	%	deg.	%
Baseline	none	-8 (4)	-11 (6)	-11 (10)	-29 (17)	-3 (1)	-6 (1)	-12 (6)	-20 (6)	-5 (3)	-13 (7)
Weight	+50%	-12 (4)	-17 (6)	-15 (12)	-43 (18)	-5 (3)	-11 (6)	-22 (13)	-37 (17)	-7 (3)	-18 (6)
	-50%	-4 (2)	-6 (3)	-6 (6)	-16 (11)	-1 (1)	-2 (3)	-8 (4)	-13 (6)	-3 (1)	-7 (3)
Sagittal Curves	+30%	-12 (5)	-17 (7)	-14 (15)	-40 (16)	-4 (1)	-9 (3)	-14 (9)	-24 (14)	-5 (2)	-12 (5)
	-30%	-5 (3)	-7 (4)	-6 (5)	-17 (15)	-3 (2)	-6 (4)	-11 (7)	-19 (10)	-5 (3)	-13 (5)
Coronal Curves	+30%	-8 (5)	-12 (6)	-12 (10)	-38 (20)	-4 (1)	-10 (2)	-19 (10)	-32 (15)	-7 (3)	-19 (4)
	-30%	-8 (4)	-12 (5)	-11 (10)	-35 (13)	-3 (3)	-7 (6)	-11 (8)	-19 (11)	-3 (2)	-9 (5)
Thoracic Cushion Height	+ 10 cm	+10 (10)	+15 (16)	+4 (11)	+27 (35)	-3 (2)	-6 (4)	-8 (7)	-15 (14)	-2 (3)	-4 (7)
	- 10 cm	-18 (4)	-24 (4)	-21 (13)	-68 (13)	-4 (3)	-9 (6)	-12 (8)	-23 (15)	-3 (6)	-15 (7)
Thoracic Cushion Longitudinal	+ 10 cm	-1 (1)	-1 (2)	+1 (1)	+2 (1)	0 (0)	0 (0)	0 (0)	0 (0)	0 (0)	0 (0)
	- 10 cm	0 (1)	0 (2)	-1 (1)	-2 (1)	0 (0)	0 (0)	0 (0)	0 (0)	0 (0)	0 (0)

3.2 Biomechanical study of patient positioning during surgery of the spine: influence of lower limb positioning on spinal geometry

The second paper was a detailed study of one of the MFPF's original and most prominent positioning features the lower limb positioner. Two papers were written on the impact of the MFPF's lower limb positioner on spinal geometry; one preliminary uniquely performed with the FEM (Appendix A) and the one presented here which used a combination of experimental testing and FEM simulations. The paper in Appendix A was included as part of this project because of its sensitivity study which showed that lower limb muscle flexibility (initial strain), as opposed to their stiffness (elastic modulus) or size (cross-sectional area), is the most important factor in the transmission of hip flexion/extension to changes in spinal geometry. In addition it showed the importance of the level of knee flexion during hip flexion for modulation of spinal geometry. The paper in this chapter required inclusion of the lower limbs into the previously developed FEM of the spine, ribcage and pelvis. While movement of the lower limbs could have been simulated through pelvic inclination the relationship between lower limb position and pelvic inclination is not known. Lower limb positioning is a feature available on other surgical frames. As such, the current article investigated not only the impact of the MFPF lower limb positioner but also the impact of moving a patient's lower limbs throughout their entire range of motion. The realisation of objective 1 (FEM adaptation to allow for the study of patient positioning on the MFPF) and hip/flexion extension components of objectives 2 and 3 of the thesis (study of hip flexion/extension on the MFPF and study of additional hip flexion/extension positions not possible on the MFPF) are presented in this paper entitled "biomechanical study of patient positioning during surgery of the spine: influence of lower limb positioning on spinal geometry", for which the contribution of the first author is considered to be 85%. It was accepted for publication in *Journal of Spinal Disorders and Techniques* in December 2010.

3.2.1 Article 2: Biomechanical study of patient positioning: influence of lower limb positioning on spinal geometry

Biomechanical Study of Patient Positioning: Influence of Lower Limb Positioning on Spinal Geometry

CHRISTOPHER DRISCOLL[1,2], CARL-ERIC AUBIN[1,2], FANNY CANET[1,2], HUBERT LABELLE[2], WILLIAM HORTON[3], JEAN DANSEREAU[1]

1 – Dept. of Mechanical Engineering,
École Polytechnique de Montréal
P.O. Box 6079, Station Centre-Ville
Montréal, Québec, H3C 3A7, Canada

2 – Sainte-Justine University Hospital Center
3175 Cote-Ste-Catherine Rd.
Montreal, Quebec, H3T 1C5, Canada

3 – The Emory Spine Center
59 Executive Park Dr NE
Atlanta, GA 30329

Address for notification, correspondence and reprints:

Carl-Eric Aubin, Ph.D., P. Eng.
Full Professor
& Canada Research Chair 'CAD Innovation in Orthopedic Engineering' and 'NSERC / Medtronic Research Chair in Spine Biomechanics'
P.O. Box 6079, Station "Centre-Ville", Montreal (Quebec), H3C 3A7 CANADA
E-mail: carl-eric.aubin@polymtl.ca
Phone: 1 (514) 340-4711 ext 4437; Fax: 1 (514) 340-5867

3.2.1.1 ABSTRACT

Objective: The objective of this study was to use finite element model (FEM) simulations and experimental testing in order to study the relationship between lower limb positioning for surgeries of the spine and changes in sagittal curves.

Methods: Four volunteers underwent lower limb flexibility and range of motion testing before being placed prone on a new surgical frame where lateral radiographs of their spines were taken in positions of hip flexion (average 48°) and extension (average 13°). Personalized FEMs were created representing each volunteer's spine, rib cage, pelvis, and lower limbs. Optimization of model behaviour was performed by adjustment of lower limb muscle initial strains. The FEMs were exploited to examine the impact of more extreme and intermediate lower limb positions; 30° of hip extension to 90° of flexion at intervals of 20°.

Results: With increased hip flexion, lordosis and kyphosis decreased an average of 52% (35°) and 16% (6°). Personalization of the 4 FEMs allowed reproduction of the experimental results within 5° and their subsequent exploitation showed the linear changes in lordosis and kyphosis between extreme positions decreasing an average of 84% (59°) and 34% (13°) with increased hip flexion. A strong correlation was found between experimental change in lordosis and individual hamstring flexibilities (R=-1) which allowed for the development of a predictive equation for lordosis in terms of hip flexion which factors straight leg raise test results.

Conclusion: Knowledge gained through this study can be used to improve intra-operative control of sagittal curves through lower limb positioning.

KEY WORDS

surgical positioning • lower limbs • spine • biomechanics • finite element modeling

3.2.1.2 INTRODUCTION

The role of patient positioning during spinal surgical procedures has evolved in both its objectives and importance. Traditional 4-post designs, which aimed at maintaining the patient while minimizing bleeding, have been adapted to allow greater flexibility such as lower limb movement and thoracic pad adjustment. Attention has been turned to exploiting patient positioning in order to obtain an improved intra-operative geometry of the spine, which could not only facilitate surgical procedures, but also improve post-operative results (Duke et al., 2008).

One important desired outcome of many adult spine reconstructions and adolescent idiopathic scoliosis (AIS) surgeries is preservation or restoration of sagittal balance (Majdouline et al., 2007). It has been shown that preservation of physiological sagittal curves can improve long-term fusion results (Edwards and Levine, 1989) and functional outcomes in adult deformity (Glassman et al., 2005).

Surgical positioning of the lower limbs has a significant impact on the sagittal curves of a patient's spine. The relationship between hip flexion and lumbar lordosis has been studied by Stephens et al. (1996) on the Andrews frame and Befanti and Geissele (1997) on the Wilson frame for 10 asymptomatic volunteers and 13 intra-operative patients respectively. It was concluded that hip flexion results in a loss of lumbar lordosis and that the correlation between the two is subject to inter-subject variability. These studies are limited in that they only investigate a few lower limb positions and as such spine behavior throughout the frames' lower limb range of motion is not known. Another important factor contributing to the sagittal balance of the spine is thoracic kyphosis (Knight et al.). Despite this, its relationship with lower limb positioning has not been studied. The relationship between hip extension and spinal sagittal curves also remains unstudied.

A Multi-Functional Positioning Frame (MFPF), has been developed (Figure 1), whose two principal positioning features include a lower limb positioner and a sternum vertical displacer. The impact of 10 cm of vertical displacement of the sternum has been shown to significantly increase spinal sagittal curves and thoracic intervertebral disc space (Driscoll et al. 2009). The impact of its lower limb positioner, which allows movement from approximately 15° in extension to 50° in flexion, on spinal geometry has not yet been studied. Due to the previously shown inter-patient variability in the relationship between lower limb positioning and changes in lordosis (Stephens et al 1996, Befanti & Geissele 1997), it is desirable to know how the MFPF's lower limb positioner will impact a given patient. Further, it has been questioned if the MFPF's lower limb positioner's range of motion should be increased because it would possibly allow for additional sagittal curve manipulation.

The factors that contribute to spinal geometry modulation during surgical positioning of the lower limbs are not known. Stokes et al. (1980) have shown that the degree of lordosis loss in the seated position is related to a given patient's hamstring flexibility. If patient-specific predictions are to be made about the MFPF leg positioner, then similar relationships must be developed for lower limb positioning.

Finite element models (FEMs) have previously been used to study the impact of patient positioning on the geometry of the vertebral column. One such study by Duke et al. (2008) used a FEM of the spine, ribcage, and pelvis with the impact of lower limb positioning simulated through the modulation of pelvic inclination by 15^{o} in each direction. It was found that pelvic inclination has a significant impact on lordosis, kyphosis, apical vertebral rotation, apical vertebral translation, and main thoracic Cobb angle. FEMs allow the impact of multiple positioning simulations on spinal geometry to be studied without the need to expose subjects to unnecessary doses of radiation.

The objective of this study is to develop a subject-specific FEM which is able to simulate the impact of lower limb positioning on the geometry of the spine and exploit it to study the relationship between positioning on the current and possible future MFPF lower limb positioner and changes in sagittal curve geometry. It is hypothesized that lower limb positioning, that could be obtained with a system like the MFPF, can importantly modulate lumbar lordosis and thoracic kyphosis and that the primary factor impacting the degree of spinal geometry modulation is the flexibility of the hamstring and quadriceps muscles.

3.2.1.3 METHODS

EXPERIMENTAL TESTING

Experimental testing was performed on 4 healthy adult volunteers at Sainte-Justine University Hospital with approval obtained from the ethics committee. Flexibility and range of motion of the subject's lower limbs were evaluated. Hip flexion was measured with the subject in the supine position on a floor mat. One leg remained flat against the floor while the other was maintained in a position of maximum flexion with the aid of the arm on the side of the flexed hip. Hip extension was measured with the subject in the prone position on a floor mat. One leg remained flat against the floor while the other was put in a position of maximum extension with the aid of a research staff. Hamstring flexibility was measured using a standardized leg raise test with the subjects in the supine position on a floor mat. One leg remained flat against the floor while the other was maintained in a position of maximum hip flexion with the knee extended with the aid of a belt passing under the sole of the foot. Finally anterior thigh muscle flexibility was measured with the subject standing back against a wall end. With a straight back, the stance leg was maintained fully extended while the other was held knee flexed, with the aid of the hand on the side of the flexion, and then the hip maximally rotated posteriorly. In all cases, measurements

were taken for both legs and the angle of flexion or extension was measured by the intercepts of the lines established by linking the greater trochanter and femoral lateral condyle as measured with a goniometer. Assistance was provided to ensure the opposite leg contact with the floor/wall and to prevent unwanted pelvic rotation. Subject morphological measurements were also recorded including: thigh cross-sectional area, femur and tibia lengths, and hip and thoracic cages widths. A summary of the subject data can be found in Table 1.

Subjects were then placed on the MFPF. 36" (91.4 cm) lateral radiographs were taken of each subject's spine in both the extreme flexion and extreme extension positions (Figure 1) using a mobile radiograph device operated by a radiographic technician. Subjects were not under anaesthesia but in a relaxed state (no voluntary muscle contractions). Lower limb position at the time of radiograph acquisition, as well as movement between positions, was recorded using a 3D optoelectronic system (Polaris Northern Digital Inc) with 3 markers placed on the subject's right leg: (1) lateral to the femoral head (2) lateral to the articular joint of the knee, and (3) lateral to the lateral malleolus. Markers were positioned based on a combination of palpation and observation of joint motion center of rotation. Hip flexion and extension were defined as the angle between markers 1-2 and the horizontal. Knee flexion was defined as the supplementary of the angle between markers 1-2 and markers 1-3.

Lordosis and kyphosis were measured on digitized radiographs using Synapse image analysis software (Fujifilm Medical Systems USA) from the limit endplates of L1-L5 and T4-T12 respectively. All measurements were repeated by two separate study members yielding an average difference of 3° (standard deviation 2°); average values were used.

FINITE ELEMENT MODELING

A previously developed FEM of the spine, rib cage and pelvis which uses a biplanar reconstruction technique (Delorme et al., 2003) from standing lateral and PA radiographs to obtain subject specific geometry was adapted for the purposes of this study. This FEM, which has been described elsewhere (Duke et al., 2005), has been validated and exploited for a number of applications including surgical positioning and the influence of brace design on AIS deformity correction (Clin et al., 2007). Two FEMs were generated for each experimental subject; one based on their flexed position radiograph and one based on their extended position radiograph on the MFPF. Since standing radiographs were not available for the subjects of this study (ethical exposure limitation), spine/ribcage/pelvis geometry was obtained by free-form deformation (Delorme et al., 2003) and interpolation of the reconstructed FEM of a healthy subject from the Saint-Justine University Hospital database. In the sagittal plane control points for the free-form deformation process were the coordinates of the T4 to L5 superior and inferior vertebral endplate centroids, spinous processes, and acetabulums measured on the radiographs, relative to the centroid of the superior endplate of S1. The displacement fields required to map the nodes of the reference model corresponding to the control points of a given radiograph were applied to all the spine and pelvis nodes of the reference model based on a statistical weighted average dependent of their proximity to the control points. Computations were performed using specialized software VESPER V1.6 (Whelan et al., 2001). For the thoracic cage longitudinal displacement of each rib node was set to that of its corresponding vertebrae centroid node and in the anterior-posterior direction a linear scaling was performed based on the relative ribcage thicknesses. In addition, the thickness of each vertebra and intervertebral disc was measured on the radiographs and used to define their respective model element cross-sectional areas. Scaling of radiographic measurements to account for the perspective projection was done based on the thickness of an oblique radio-opaque beam of the surgical frame. In the coronal plane, the spine was assumed to

be perfectly straight. The vertebral cross-sectional areas, hip width, and thoracic cage width of each subject was used to linearly scale the lateral position of the reference model nodes representing the vertebral posterior elements, pelvis, and thoracic cage respectively. When comparing the sagittal segmental curves of the subject models generated through this process to their respective radiographs they were within 2^{o} of each other which was deemed acceptable for the purposes of the current study.

Lower limbs were introduced into the FEMs. Detailed geometry of the femur, tibia, and fibula, was obtained from the Visible Human Project's (VHP) lower limbs (Viceconti) and linearly scaled for a given subject based on direct measurement of distances from the greater trochanter to the femoral lateral condyle and from tibial medial condyle to the tibial medial malleolus. Relative positions of knees and lateral malleolus to the hip joint were set to match the positions recorded with the optoelectronic sensors. Bone material properties were attributed a published value (Papini et al., 2007) ($E = 9100$ N/mm^2 and $\nu = 0.3$). Hip joints were modeled using universal joints and the knees by uniaxial joints in the sagittal plane. A rotational stiffness was applied to the hip and knee joints representing passive effects. Hip rotational stiffness (8 Nm/rad) was obtained from the works of Tafazzoli and Lamontagne (1996) for the straight leg condition, and knee rotational stiffness (36 Nm/rad) was obtained from the works of Zhang et al. (1998). Hip joint range of motions in flexion and extension was personalized for each subject based on their experimentally measured values

A total of 31 muscles per leg were modeled including the hamstrings, gluteals, anterior thigh muscles, and adductors. Muscle origins and insertions were obtained by mapping the coordinates defined by White et al. (1989) for a 1.77m, 65 kg male to the FEM. Linear scaling, based on the locations of two bony landmarks for each Cartesian axis, was performed for local coordinate systems in the pelvis, femur, and lower leg. Baseline lower limb muscle cross-

sectional areas were obtained from Horsman et al. (2007), who established the average physiological cross-sectional areas by dividing muscular volume measured on a cadaver by optimal fiber length. The cross-sectional areas were linearly scaled such that their total cross-sectional area at mid thigh level corresponded to the values measured for a given subject with the contribution of the adipose tissue, skin, and bone considered to be 30% based on image analysis of a VHP (male) transverse section through the thigh #2035. An elastic modulus of 14.2 N/mm^2, based on the experimental trials of Kovanen et al. (1984) on rodent musculus rectus femoris (linear region of the stress-strain curve), was uniformly applied to all lower limb muscles along with a Poisson's ratio of 0.49. Only passive muscular properties were considered since the MFPF's mechanically controlled lower limb movement is slow and constant without inducing voluntary or involuntary muscular contractions. For the straight leg condition, lower limb hamstring muscle initial strains, representing laxity, were uniformly set at 4% based on previously described simulations reproducing published results for the loss of lumbar lordosis due to hip flexion (Driscoll et al., 2008) and the remaining lower limb muscle initial strains were attributed a nominal value of 0.1%. These strains were then adjusted to reflect the relative displacements of their respective origins and insertions in the positions of radiograph acquisition.

Finally, tibial-fibular ligaments (anterior and posterior superior ligaments, anterior and posterior inferior ligaments, inferior transverse ligaments, and interosseous ligaments) and femoral-fibular ligaments (lateral collateral ligament) were modeled as un-deformable elements based on the assumption that the relative displacements between the lower members were negligible for the range of motions simulated. Ligaments spanning the knee and hip joints were not represented due to the fact that relative translational motion at the joints was constrained. In all, the model (Figure 2) contains 1790 nodes and 1247 elements.

MODEL EVALUATION

Simulations were performed to reproduce the experimental testing with the subject FEMs to assess their accuracy so that they could be exploited to study additional lower limb positions. For each subject two types of simulations were performed resulting in a total of 8 tests. First the FEMs reconstructed based on the flexed position radiographs underwent hip extension simulations such that the final lower limb position matched that in which the extension radiograph was taken. Then the FEMs reconstructed based on the extended position radiographs underwent hip flexion simulations such that the final lower limb position matched that in which the flexion radiograph was taken. For all simulations, rotational constraints were applied directly to the hip and knee joints. A zero displacement constraint (all directions) and zero rotation constrain (transverse and coronal planes) was applied to a node point midway between the patient's acetabulums, linked with a rigid element, to constrain the model in space and represent pelvic cushion contact. An additional zero displacement constraint in the transverse and anterior-posterior directions was applied to a node in the middle of the anterior-lateral segment of each 3rd and 4th rib in order to represent thoracic cushion contact. The remaining nodes remained unconstrained.

The flexion and extension simulations were performed twice; once with baseline lower limb muscle initial strains and once with personalized hamstrings and anterior thigh muscle initial strains obtained from an optimization process, as they have been found to contribute to pelvic rotation during hip flexion and extension manoeuvres (Driscoll et al. 2008). In each case values of lordosis and kyphosis, measured by the angle between the intercepts of the lines linking the nodes representing the end vertebrae superior and inferior endplate centroids, were compared to those measured on the radiographs.

Lower limb initial strain personalisation was done using a 2 factor 10 run central-composite experimental design. Experimental testing simulations were repeated while independent values of straight leg hamstring and anterior thigh muscle initial strains were increased and decreased by 4% of their baseline values with the dependent value Φ being the sum of the absolute differences between the experimentally measured and numerically predicted sagittal curves: Φ = Δ lordosis flexion + Δ kyphosis flexion + Δ lordosis extension + Δ kyphosis extension. STATISTICA V7 software (StatSoft Inc) was used to both generate and analyze the experimental design. The resulting quadratic regression coefficient based equations were run through a MATLAB V7 (MathWorks Inc) search pattern optimization algorithm which provided values of hamstring and anterior thigh muscle initial strains for which Φ was minimized.

FEM EXPLOITATION

The personalized FEM of each subject was exploited to study the impact of lower limb positioning over an even larger range of motion than possible on the MFPF and that could be encountered during surgical positioning. Specifically the impact of intermittent MFPF positions and more extreme MFPF positions to see if the relationship between lower limb positioning and sagittal curve modulation is a constant over this range and if additional changes can be obtained relative to the current leg positioner design. While maintaining the knees flexed at 30°, hip positioning was varied between 30° in extension to 90° in flexion at intervals of 20°. The sagittal curves in each position were recorded.

3.2.1.4 RESULTS

A comparison of the simulated and experimentally measured sagittal curves for both the flexed and extended positions (Figure 3) is summarized in Table 2. For each subject the lower

limb position during radiograph acquisition is detailed along with the values of thoracic kyphosis and lumbar lordosis, both measured on the radiographs and predicted with the model. The simulated values in brackets are the values obtained with the personalized lower limb muscle initial strains. Passing from an extended hip position (avg. 13^{o}) to a flexed hip position (avg. 48^{o}) on the surgical frame caused a respective reduction in lordosis of 36° (47%), 27° (42%), 31° (54%), and 46° (65%) for the 4 subjects accompanied by a 6° (8%), 6° (15%), 3° (13%), and 7° (18%) reduction in kyphosis.

With the baseline material properties, the FEM was able to predict sagittal curve changes between the two positions (flexing the extended reconstructions and extending the flexed reconstructions) of lordosis within 5^{o} only for 4 out of 8 tests and kyphosis within 5^{o} for 7 out of 8 tests; with an average difference of 6^{o}. With personalized initial strains, the FEM was able to predict sagittal curves within 6^{o} and had an average difference of 3^{o}. The main difference between experimental and simulated results found when using the baseline muscle properties was with the underestimation of lordosis changes for subjects 1 and 4 who had low hamstring flexibilities whose initial strains were both increased by the optimization process. Physically their muscles were tighter in the neutral straight-leg position and had less potential to stretch thus limiting movement. The Spearman correlation between change in lordosis observed between the two experimental positions and femur length, thigh cross-sectional area, and thigh flexibility was poor with respective values of 0.40, -0.63, and 0.40. The correlation between change in lordosis and hamstring flexibility was high with a value of -1.

The results of the FEM exploitation are depicted graphically in Figure 4. Flexing and extending the subject lower limbs beyond the values seen in the experimental testing allowed for additional modulation of sagittal spinal curves. On average passing the hips from a 30^{o} extended position to a 90^{o} flexed position caused a respective reduction in lordosis of 69° (87%), 53°

(78%), 51° (80%), and 63° (90%) for the 4 subjects accompanied by a 10° (27%), 7° (16%), 14° (47%), and 21° (48%) reduction in kyphosis.. The decreases in both indices with respect to increase in hip flexion were found to be relatively linear with a tendency to level off at around the neutral hip position where muscles would not be strained. The overall slopes were slightly steeper for patients with less flexible hamstrings.

3.2.1.5 DISCUSSION

The results of this study show that a subject's lordosis and kyphosis can both be importantly changed due to lower limb positioning on the MFPF which could be exploited intra-operatively to facilitate surgical intervention of spinal pathologies such as by increasing intervertebral disc angles for screw placement or decompression procedures. Results also show how sagittal curves, which tend to decrease while in the prone position (Tan et al., 1994; Marsicano et al., 1998), can be increased by hip extension thus allowing for restoration of standing values which would be desirable for final instrumentation and fusion. Although modern instrumentation allows for sagittal curve adjustment during de-rotation maneuvers or in-situ rod contouring, instances of post-operative flatback persist (Mazel 2005). Positioning of the lower limbs allows manipulation of sagittal curves throughout the entire course of an operation (right up until set screw fixation) and can be used in conjunction with instrumentation.

FEM exploitation allowed for the quantification of the relation between the amount of hip flexion/extension on the MFPF and the impact on both sagittal spine curves through the entire range of possible lower limb surgical positions as opposed to only lordosis data in just one or two positions as has been presented in previous studies. This additional data revealed the linear relationship between hip flexion and lordosis decrease and how kyphosis is also impacted. The FEM also has the advantage of no variability in spinal geometrical measurements. It could be

further exploited in order to test the impact of lower limb positioning on other spinal geometrical parameters, such as scoliotic curves, as well as to study the effect of combined positions possible on the MFPF such as lower limb and thoracic cage displacement.

The high correlation found between hamstring flexibility and change of lordosis between positions is in agreement with the hypothesis that it is the primary factors contributing to lordosis modulation during lower limb surgical positioning. This is consistent with the results of a previously performed sensitivity study of the FEM (Driscoll et al., 2008) which has also shown that the influence of hamstring flexibility can be further enhanced by knee extension in combination with hip movement as extension of the knee pulls the tibia and fibula muscle insertions further away from their origins resulting in increased tension.

The Spearman correlation coefficient relating experimentally measured lower limb muscle flexibilities and the corresponding FEM initial strains obtained with the optimization process was very high for the hamstring muscles (R = -1) and moderate for the anterior thigh muscles (R = -0.40). With additional testing to verify these relationships, flexibility testing could be used to directly calibrate patient FEMs without the need for the optimization process. These FEMs could then be utilized to predict sagittal curve changes due to lower limb positioning for a given patient to aid in determining operative positioning on the MFPF. Additionally, it could be used as a visualization tool to supplement the often limited intra-operative spinal views.

An alternate predictive method would be to exploit the linearity of the relationship between hip flexion and lordosis using regression equations to approximate the data in Figure 4 a). The equation relating hip rotation to lordosis takes the form Lf = Li – HR x PF where Lf = final lordosis (in degrees), Li = initial lordosis (in degrees) in the straight leg condition, HR = hip rotation (in degrees - positive for flexion and negative for extension), and PF = patient factor (dictating the slope). Since it was found that hamstring flexibility is the most influential factor

determining the degree of lordosis loss, PF can be approximated by correlating it to the amount of hip rotation measured in the straight leg raise (SLR) test. This was done for the 4 study subjects to yield PF = 0.79 – 0.0033 x SLR. Putting it together Lf = Li – HR x (0.79 – 0.0033 x SLR). For example if a patient with an initial lordosis of 50° who obtained 80° in the straight leg raise test and had their hips flexed 20° the resultant lordosis would be Lf = 50° - 20° x (0.79 – 0.0033 x 80°) = 40°.

Validation of global FEM behaviour has previously been performed (Duke et al., 2005) and was not the intention of this study. We recognize that hip flexion contractures could influence this data, and the model could be enhanced by representation of the ligaments and capsules of the hip and knee. The experimental changes in sagittal curves were accurately reproducible with the FEM after adjustment of its lower limb initial strains based on subject flexibility testing and that was deemed sufficient for further FEM exploitation. Structures such as the ribcage, which relied on some geometrical assumptions, were present to ensure proper boundary conditions and we have verified that their accuracy does not influence the results of the current study.

The present study was performed on healthy volunteers in an experimental setting as part of a feasibility study. It is possible that the presence of a spinal pathology and the effects of anaesthesia would impact the degree to which sagittal curves are impacted by lower limb positioning although based on previous studies (Benfanti and Geissele, 1997; Legaye et al., 1998) it is believed that this difference would be small.

3.2.1.6 CONCLUSION

A FEM has been developed which allows for study of the impact of subject-specific lower limb positioning on lumbar lordosis and thoracic kyphosis both of which can be importantly modulated on the MFPF. The relationship between lower limb positioning on the MFPF and

changes in sagittal curves is linear and additional modulation can be achieved by increasing the leg positioner's range of motion. The primary factor influencing sagittal curve changes due to lower limb positioning is hamstring flexibility.

3.2.1.7 REFERENCES

Duke K, Aubin CE, Dansereau J, Labelle H. Computer simulation for the optimization of patient positioning in spinal deformity instrumentation surgery. Med Biol Eng Comput. 2008 Jan;46(1):33-41.

Majdouline Y, Aubin CE, Robitaille M, Sarwark JF, Labelle H. Scoliosis correction objectives in adolescent idiopathic scoliosis. J Pediatr Orthop. 2007 Oct-Nov;27(7):775-81.

Edwards CC, Levine AM. Complications associated with posterior instrumentation in the treatment of thoracic and lumbar injuries. In: Garfin SR, ed. Complications of Spine Surgery. Baltimore: Williams and Wilkins, 1989:164-99.

Glassman S, Bridwell K, Berven S, Horton W, Schwab F. The Impact of Positive Sagittal Balance in Adult Deformity. Spine 2005 Vol. 30 (18): 682-688.

Stephens GC, Yoo JU, Wilbur G. Comparison of lumbar sagittal alignment produced by different operative positions. Spine. 1996 Aug 1;21(15):1802-6; discussion 1807.

Benfanti PL, Geissele AE. The effect of intraoperative hip position on maintenance of lumbar lordosis: a radiographic study of anesthetized patients and unanesthetized volunteers on the Wilson frame. Spine. 1997 Oct 1;22(19):2299-303.

Knight RQ, Jackson RP, Killian JT, Stanley EA. White paper on sagittal plane alignment. Scoliosis Research Society.

Driscoll CR, Aubin CE, Canet F, Dansereau J, Labelle H. The impact of intra-operative sternum vertical displacement on the sagittal curves of the spine. Eur Spine J. 2009 Nov 10.

Stokes IA, Abery JM. Influence of the hamstring muscles on lumbar spine curvature in sitting. Spine. 1980 Nov-Dec;5(6):525-8.

Delorme S, Petit Y, de Guise JA, Labelle H, Aubin CE, Dansereau J. Assessment of the 3-D reconstruction and high-resolution geometrical modeling of the human skeletal trunk from 2-D radiographic images. IEEE Trans Biomed Eng. 2003 Aug;50(8):989-98.

Duke K, Aubin CE, Dansereau J, Labelle H. Biomechanical simulations of scoliotic spine correction due to prone position and anaesthesia prior to surgical instrumentation. Clin Biomech (Bristol, Avon). 2005 Nov;20(9):923-31.

Clin J, Aubin CE, Labelle H., Virtual prototyping of a brace design for the correction of scoliotic deformities. Med Biol Eng Comput. 2007 May;45(5):467-73.

Whelan, B.M., McBratney, A.B., and Minasny, B., 2001. Vesper – Spatial prediction software for precison agriculture. In: ECPA 2001. Third European Conference on Precision Agriculture. (G. Grenier, S. Blackmore Eds.) pp. 139-144. Agro Montpellier, Ecole Nationale Agronomique de Montpellier.

Viceconti M, From: The BEL Repository, "http://www.tecno.ior.it/VRLAB/".

Papini M, Zdero R, Schemitsch EH, Zalzal P. The biomechanics of human femurs in axial and torsional loading: comparison of finite element analysis, human cadaveric femurs, and synthetic femurs. J Biomech Eng. 2007 Feb;129(1):12-9.

Tafazzoli F, Lamontagne M. Mechanical behaviour of hamstring muscles in low-back pain patients and control subjects. Clin Biomech (Bristol, Avon). 1996 Jan;11(1):16-24.

Zhang LQ, Nuber G, Butler J, Bowen M, Rymer WZ. In vivo human knee joint dynamic properties as functions of muscle contraction and joint position. J Biomech. 1998 Jan;31(1):71-6.

White SC, Yack HJ, Winter DA. A three-dimensional musculoskeletal model for gait analysis. Anatomical variability estimates. J Biomech. 1989;22(8-9):885-93.

Horsman K, Koopman HF, van der Helm FC, Prosé LP, Veeger HE. Morphological muscle and joint parameters for musculoskeletal modelling of the lower extremity. Clin Biomech (Bristol, Avon). 2007 Feb;22(2):239-47.

Kovanen V, Suominen H, Heikkinen E. Collagen of slow twitch and fast twitch muscle fibres in different types of rat skeletal muscle. Eur J Appl Physiol Occup Physiol. 1984;52(2):235-42.
Tan SB, Kozak JA, Dickson JH, Nalty TJ. Effect of operative position on sagittal alignment of the lumbar spine. Spine. 1994 Feb 1;19(3):314-8.

Driscoll C, Aubin CE, Labelle H, Dansereau J. The relationship between hip flexion/extension and the sagittal curves of the spine. Stud Health Technol Inform. 2008;140:90-5.

Marsicano JG, Lenke LG, Bridwell KH, Chapman M, Gupta P, Weston J. The lordotic effect of the OSI frame on operative adolescent idiopathic scoliosis patients. Spine. 1998 Jun 15;23(12):1341-8.

Mazel C, Zrig M, Antonietti P, de Thomasson E. [Impaction posterior wedge osteotomy for the treatment of postsurgical flatback: 22 cases]. Rev Chir Orthop Reparatrice Appar Mot. 2005 Oct;91(6):530-41.

Legaye J, Duval-Beaupere G, Hecquet J, et al. Pelvic incidence: a fundamental pelvic parameter for three-dimensional regulation of spinal sagittal curves. Eur Spine J 1998; 7: 99–103.

3.2.1.8 FIGURES AND TABLES

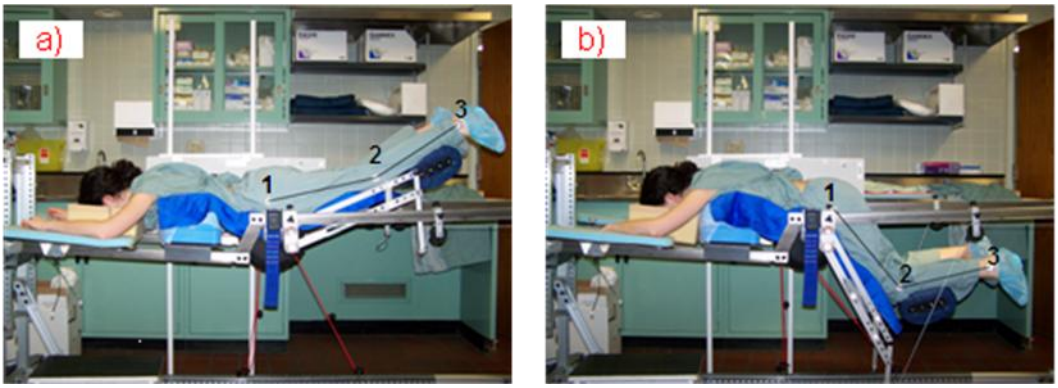

Figure 3.3 (A2F1): MFPF Leg Positioner; Extended (A) and flexed (B) positions

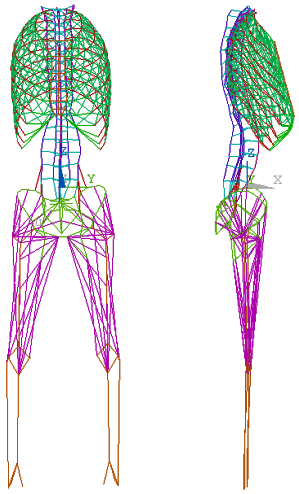

Figure 3.4 (A2F2): Coronal and sagittal views of the developed FEM

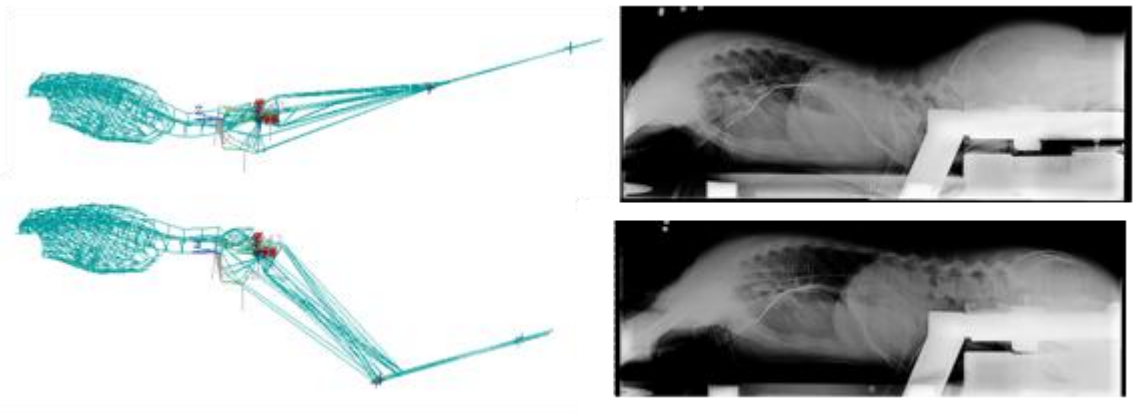

Figure 3.5 (A3F3): Comparison of simulations and experimentally measured results

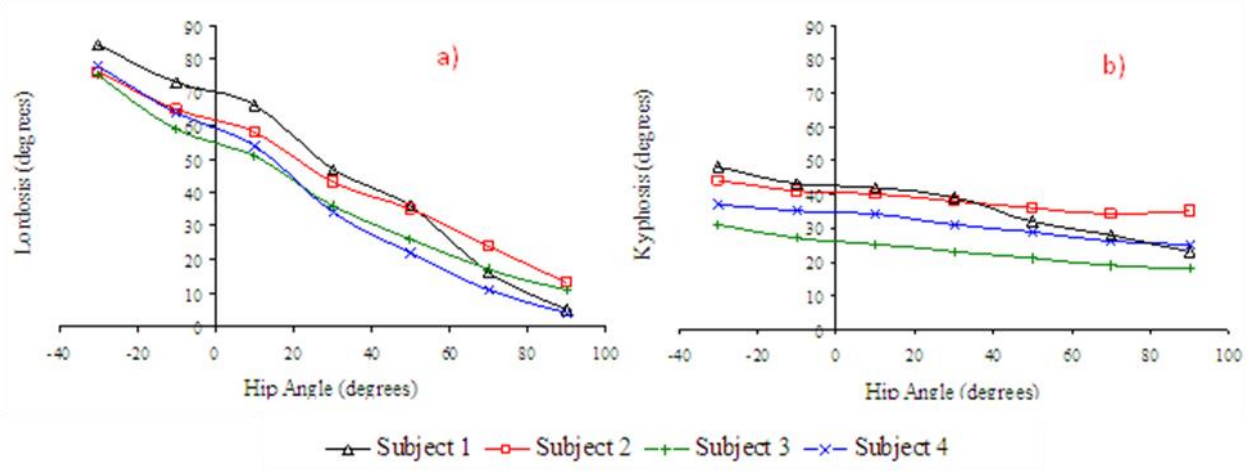

Figure 3.6 (A2F4): Simulation of change in lordosis (a) and kyphosis (b) due to hip angle modulation

Table 3.5 (A2T1): Subject Data

#	Sex	Age (yrs)	Thigh CSA (cm^2)	Length of femur (cm)	Length of tibia (cm)	Max Hip Flexion (degrees)	Max Hip Extension (degrees)	Hamstring Flexibility (degrees)	Thigh Flexibility (degrees)
1	M	30	147	46	47	133	35	73	8
2	M	28	147	39	38	137	38	101	0
3	F	27	103	43	43	144	44	96	25
4	F	25	92	41	41	131	43	67	14

Table 3.6 (A2T2): Comparison of simulations and experimentally measured results (all values in degrees). Values in parenthesis are those obtained after initial strain optimization

Subject	Hip Flexion	Knee Flexion	Radiograph Lordosis	Simulation Lordosis	Radiograph Kyphosis	Simulation Kyphosis
	Flexed Position					
1	46	52	40	46 (41)	28	30 (29)
2	49	56	37	33 (37)	33	37 (38)
3	51	64	26	27 (27)	20	22 (22)
4	46	58	25	43 (29)	31	37 (33)
	Extended Position					
1	11	15	76	66 (73)	34	32 (35)
2	15	9	64	68 (67)	39	43 (42)
3	13	21	57	61 (60)	23	27 (27)
4	14	28	71	55 (66)	38	42 (44)

3.3 The impact of intra-operative sternum vertical displacement on the sagittal curves of the spine

The third paper was a detailed study of another of the MFPF original and most prominent positioning features: the sternum vertical displacer. The sternum vertical displacer is a novel positioning device which allows the torso to be lifted off the MFPF by the vertical displacement of a cushion which interfaces with the sternum. Although only experimental testing is presented in the article, results were utilized to validate the FEM's ability to reproduce positioning using this MFPF feature. This was required for the final paper which utilizes the FEM to study the impact of combined MFPF feature use. The main concern with the vertical displacer was possible increases in interface pressures once the torso was lifted off the MFPF. As such interface pressure measurement was included in the experimental testing. The realisation of the sternum raising component of objective 2 (experimental testing of sternum raising on the MFPF) is presented in this paper entitled "the impact of intra-operative sternum vertical displacement on the sagittal curves of the spine", for which the contribution of the first author is considered to be 85%. It was published in European Spine Journal in February 2009.

3.3.1 Article 3: The impact of intra-operative sternum vertical displacement on the sagittal curves of the spine

The Impact of Intra-Operative Sternum Vertical Displacement on the Sagittal Curves of the Spine

CHRISTOPHER DRISCOLL[1,2], CARL-ERIC AUBIN[1,2], FANNY CANET[1,2], JEAN DANSEREAU[1] , HUBERT LABELLE[2]

1 – Dept. of Mechanical Engineering,
École Polytechnique de Montréal
P.O. Box 6079, Station Centre-Ville
Montréal, Québec, H3C 3A7, Canada

2 – Sainte-Justine University Hospital Center
3175 Cote-Ste-Catherine Rd.
Montreal, Quebec, H3T 1C5, Canada

Address for notification, correspondence and reprints:

Carl-Eric Aubin, Ph.D., P. Eng.
Full Professor
& Canada Research Chair 'CAD Innovation in Orthopedic Engineering' and 'NSERC / Medtronic Industrial Research Chair in Spine Biomechanics'
P.O. Box 6079, Station "Centre-Ville", Montréal (Québec),
H3C 3A7 CANADA
E-mail: carl-eric.aubin@polymtl.ca
Phone: 1 (514) 340-4711 ext 2836; Fax: 1 (514) 340-5867

3.3.1.1 ABSTRACT

Patient positioning is an important step in spinal surgeries. Many surgical frames allow for lumbar lordosis modulation due to lower limb displacement, however, they do not include a feature which can modulate thoracic kyphosis. A Sternum Vertical Displacer (SVD) prototype has been developed which can increase a subject's thoracic kyphosis relative to the neutral prone position on a surgical frame. The kyphosis increase is obtained by lifting the subject's torso off the thoracic cushions with a dedicated sternum cushion that can be displaced vertically. The objective of this study was to evaluate the impact of SVD utilization on the sagittal curves of the spine. Experimental testing was performed on 6 healthy volunteers. Lateral radiographs were taken in the neutral and sternum raised positions and then analyzed in order to compare the values of sagittal curves. The displacement of volunteers and surgical frame components between positions was recorded using an optoelectronic device. Finally, interface pressures between the volunteers and surgical frame cushions were recorded using a force sensing array. Average results show that passing from the neutral to sternum raised positions caused an increase of 53% in thoracic kyphosis and 24% in lumbar lordosis; both statistically significant. Sensors showed that the sternum was raised a total of 8 cm and that interface pressures were considerably higher in the raised position. The SVD provides a novel way of increasing a patient's thoracic kyphosis intra-operatively which can be used to improve access to posterior vertebral elements and improve sagittal balance. It is recommended that its use should be limited in time due to the increase in interface pressures observed.

Keywords

spine • surgical positioning • kyphosis • surgical frame

3.3.1.2 INTRODUCTION

In recent years, positioning objectives for spinal surgeries have evolved to include intra-operative modulation of the patient's vertebral column geometry[1,2]. Thus far, the primary focus has been on the modulation of lumbar lordosis due to positioning of the lower limbs[3,4,5] and as a consequence many surgical frames now allow flexion or extension of patients' hips. While some studies have attempted to quantify the impact of prone positioning on thoracic kyphosis[6,7,8], no devices have been introduced which allow modulation of thoracic kyphosis intra-operatively.

A new Multi-Functional Positioning Frame (MFPF) has been developed. The MFPF holds patients in the prone position with two thoracic cushions, two pelvic cushions, and a lower limb positioning feature. It also includes a sternum vertical displacer (SVD) feature, still in the prototype phase, which is a portable device that can be placed under the MFPF, or other similarly designed surgical frames, and lifts the patient's torso up off of the thoracic cushions. Its Y-shaped cushion, made of memory foam material, is meant to interface with the patient anterior to the thoracic cushions just below the sterno-clavical joint and should not surpass the sternum distally to avoid pressure on the abdomen. Displacement, offset by 15 degrees posteriorly relative to the vertical, is obtained with an electronically operated jack.

The objective of this study is to evaluate the impact of the SVD device on the sagittal curves of the spine for subjects on the MFPF. It is hypothesized that use of the SVD can significantly and safely increase thoracic kyphosis relative to the neutral prone position.

3.3.1.3 METHODS

Experimental testing was performed on 6 asymptomatic young adult volunteers, 3 males and 3 females aged 20 to 28 (Table-1), at Sainte-Justine University Hospital Center in Montreal

with approval obtained from the ethics committee. Subjects were weighed and their heights recorded. They were then placed in the prone position on the MFPF where two 36 inches (91.4 cm) lateral radiographs were acquired; one in the neutral position and one with the SVD lifted approximately 15 cm. Each radiograph was analysed using Synapse image analysis software (Fujifilm Medical Systems USA) and the following indices were measured: T4-T12 thoracic kyphosis, apical thoracic segment (from T4 to T8) intervertebral disc angles and space (defined here as the distance between the posterior tips of vertebral body endplates interfacing a given disc), L1-L5 lumbar lordosis, T4-S1 sagittal plane decompensation (vertical distance between T4 and S1 vertebral body centroids), and ribcage width at the T5 level (anterior edge of ribcage to posterior edge of T5 perpendicular to horizontal reference). Scaling of radiographic measurements to account for the perspective projection of the radiographic image was done based on the thickness of an oblique radio-opaque beam of the surgical frame that was used as a calibration object. The change in kyphosis and lordosis between positions was statistically analyzed using a Wilcoxon matched pairs tests performed with STATISTICA V8 software (StatSoft Inc).

Motion between radiographic positions of both the subjects and SVD was recorded using a 3D optoelectronic system (Polaris Northern Digital Inc) with reflective markers placed on the SVD jack and subjects' head (posterior to the ear), lateral-posterior portion of the ribcage at the T5 level, and hip joint.

Subject thoracic mobility was evaluated two different ways; actively and passively. In the first test, subjects were asked to laterally bend their torso to the left and right in the standing position while maintaining their feet shoulder width apart; as is done for pre-operative scoliosis patients. The maximum lateral displacement of T1 relative to S1 in each case was recorded using a plumb line, ruler and level. In the second test, subjects were placed in the lateral left and right

decubitus positions with a 10 inch diameter cylindrical rigid support (fulcrum) placed under the mid portion of their ribcage. The angle made between points T1, the apical vertebrae over support, and S1, all identified via palpitation, was measured with a goniometer.

Finally the interface pressure between the subjects and MFPF cushions in each radiographic position was recorded using a force sensing array (FSA - Vista Medical, Winnipeg) composed of 225 sensors with a capacity of up to 300 mmHg and analyzed by accompanying software (FSA4). The complete experimental setup can be seen in Figure-1.

3.3.1.4 RESULTS

A summary of spinal geometries in the neutral and sternum lifted positions, as well as the flexibility data, can be found in Table-1 and can be visualized with the radiographs of all cases in Figure-2. Going from the neutral to sternum raised position caused a statistically significant ($p=0.0277$) increase in kyphosis which averaged 14˚ (± 5˚) or 53%. It also caused a statistically significant ($p=0.0277$) increase in lordosis averaging 10˚ (± 4˚) or 24%, an increase in decompensation averaging 81 mm (± 15 mm), and a ribcage compression ranging between 10 and 30 mm. The Spearman's correlation between the change in kyphosis between positions and flexibility measurements was respectively 0.26 for lateral bending and 0.58 for fulcrum bending.

As can be observed on the radiographs, the apex of the increase in kyphosis is inline with the SVD line of action at about the T5 or T6 level. Within the apical thoracic segment the average intervertebral disc angle increased from 1.7° (± 0.6°) to 4.5° (± 0.8°) and the average intervertebral disc space increased from 3.2 mm (± 0.3) to 4.2 mm (± 0.5). The values for individual discs are summarized in Table-2.

The results for the motion capture are represented graphically in Figure-3 for the representative case of subject #4. Both the SVD jack and ribcage marker were displaced at 15˚

from the vertical; while the jack moved a total of 15 cm, the ribcage moved only 8 cm. It can also be noted that the subject's hip remained relatively fixed (less than 3 cm of distal translation) and there was a 6 cm distal-posterior displacement of the head which included approximately 3 cm of vertical lifting.

The average and peak interface pressures for the sternum cushion in the raised position were respectively 4 and 6 times higher than for the thoracic cushions in the neutral position with the FSA maximum reading of 300 mmHg being reached for the sternum cushion in the raised position. A zero pressure reading was obtained for the thoracic cushions in the sternum raised position, confirming that the subjects were completely lifted up off of them. The pelvic cushion interface pressures were not impacted by the raising of the sternum. The results of the average interface pressure measurements for all subjects are summarized in Table-3 with the minimum and maximum values for each case in brackets.

3.3.1.5 DISCUSSION

The SVD significantly increased kyphosis, as was desired, and had the consequent effect of increasing lordosis although this increase was relatively less. Examination of the radiographs shows that it was the anterior-posterior displacement of the kyphotic apex which led to the increase in kyphosis and not a global displacement of the torso. It is believed that simply raising the thoracic cushions would lead to the anterior-posterior displacement of the entire thoracic cage and have less of an impact on kyphosis. Further, if the anterior displacement was at the proximal level of the thoracic cage resulting in a back hyper-extended position, as seen with the Bohler[9] fraction reduction and Scaglietti[10] spondylolisthesis reduction techniques, the resultant would actually be a reduction of kyphosis.

The subjects in this study were free of any pathology that would impact spinal flexibility such as scoliosis and hyper-kyphosis. Although no strong correlation was found between the flexibility measurements taken on the test subjects and their increase in kyphosis in the SVD raised position, it is possible that stiff spines would experience less kyphosis increase with the SVD. The current study is a proof of concept showing that thoracic intervertebral disc space and kyphosis can indeed be increased by operative positioning. The next steps remain to validate the SVD for patients with spinal pathologies and utilize it in an operative setting.

The utility of a device such as the SVD is in its ability to increase intervertebral disc space in the thoracic region thus allowing better access to the discs and posterior vertebral elements. This can be beneficial for decompression maneuvers such as in diskectomy, laminectomy, corpectomy, osteophyte removal, and foraminectomy procedures. This concept can also be exploited in order to reduce hypo-kyphosing effects that are seen in instrumentation procedures[11] or to restore a more natural sagittal balance to patients with a hypo-kyphotic scoliosis[12]. The SVD could be used to slightly raise the sternum off the thoracic cushions during final instrumentation and fusion of thoracic vertebrae in order to ensure that the desired degree of kyphosis is obtained. The exact amount of sternum elevation would be left up to the surgeon's discretion depending on the amount of kyphosis that they wish to induce for that particular patient and procedure. The maximum elevation obtainable on the current SVD prototype is 20 cm.

The difference found in the vertical displacement of the SVD and ribcage was due to two factors: cushion compression and ribcage compression. While the majority of the difference was due to cushion compression, a small ribcage compression was also observed. While it is possible that ribcage compression decreased lung capacity, none of the subjects experienced difficulty breathing when in the raised position for a period of approximately 5 minutes.

The MFPF included a head cushion that could slide along its longitudinal position. This avoided straining the subjects' necks while in the sternum raised position due to the observed 6 cm distal displacement of the head. It is suggested that anytime a SVD type device is used, the patient's head be allowed to move, either by surgical frame design or repositioning by the surgical staff. There were no special considerations to be taken for the positioning of the arms or lower extremities as they experienced minimal movement.

The increase in interface pressures found in the sternum raised position can be explained by the decrease in cushion contact area (the thoracic cushion contact area of 249 cm^2 being completely transferred to the sternum cushion contact area of 195 cm^2) and by the difference soft tissue covering the sternum relative to the pectoral region. While it is possible to increase the area of the SVD cushion, doing so will reduce the effect of apical thoracic segment posterior translation. Supplemental testing in which an 84 kg male was kept in the raised position for 30 minutes resulted in no respiratory difficulties and minor reddening of the skin primarily where the lateral edges of the cushion interfaced with the pectoral muscles. As such, a general recommendation is that SVD use be limited to 30 minutes. If a longer use is required, then the patient could be intermittently lowered back onto the thoracic cushions and inspected.

3.3.1.6 CONCLUSION

Raising the sternum using a SVD type device allows for the significant increase of thoracic kyphosis intra-operatively. Its use should only be limited to a short period of time due to its increase in interface pressures and possible decrease in lung capacity.

3.3.1.7 REFERENCES

1. Schonauer C, Bocchetti A, Barbagallo G, Albanese V, Moraci A (2004) Positioning on surgical table. Eur Spine J 13 Suppl 1:S50-5

2. Duke K, Aubin CE, Dansereau J, Koller A, Labelle H (2008) Dynamic positioning of scoliotic patients during spine instrumentation surgery. J Spinal Disord Tech 22(3):190-6

3. Stephens GC, Yoo JU, Wilbur G (1996) Comparison of lumbar sagittal alignment produced by different operative positions. Spine 21 15:1802-7

4. Benfanti PL, Geissele AE (1997) The effect of intraoperative hip position on maintenance of lumbar lordosis: a radiographic study of anesthetized patients and unanesthetized volunteers on the Wilson frame. Spine 22(19):2299-303

5. Driscoll CR, Aubin CE, Canet F, Labelle H, Dansereau J (2009) Biomedical Study of the Influence of Lower Limb Surgical Positioning on Spinal Geometry. J Orthop Res (submitted March)

6. Duke K, Aubin CE, Dansereau J, Labelle H (2005) Biomechanical simulations of scoliotic spine correction due to prone position and anaesthesia prior to surgical instrumentation. Clin Biomech 20(9):923-31

7. Jackson R, Behee K, McManus A (2005) Sagittal spinopelvic alignments standing and in an intraoperative prone position. Spine J 4(5):S5

8. Marsicano JG, Lenke LG, Bridwell KH, Chapman M, Gupta P, Weston J (1998) The lordotic effect of the OSI frame on operative adolescent idiopathic scoliosis patients. Spine 23(12):1341-8

9. Böhler L (1972) [Conservative treatment of fractures of the thoracic and lumbar spine]. Z Unfallmed Berufskr 65(2):100-4.

10. Scaglietti O, Frontino G, Bartolozzi (1976) Technique of anatomical reduction of lumbar pondylolisthesis and its surgical stabilization. Clin Orthop Relat Res (117):165-75.

11. de Jonge T, Dubousset JF, Illés T (2002) Sagittal plane correction in idiopathic scoliosis. Spine 27(7):754-60

12. Sucato DJ, Agrawal S, O'Brien MF, Lowe TG, Richards SB, Lenke L (2008) Restoration of thoracic kyphosis after operative treatment of adolescent idiopathic scoliosis: a multicenter comparison of three surgical approaches. Spine 33(24):2630-6

3.3.1.8 FIGURES AND TABLES

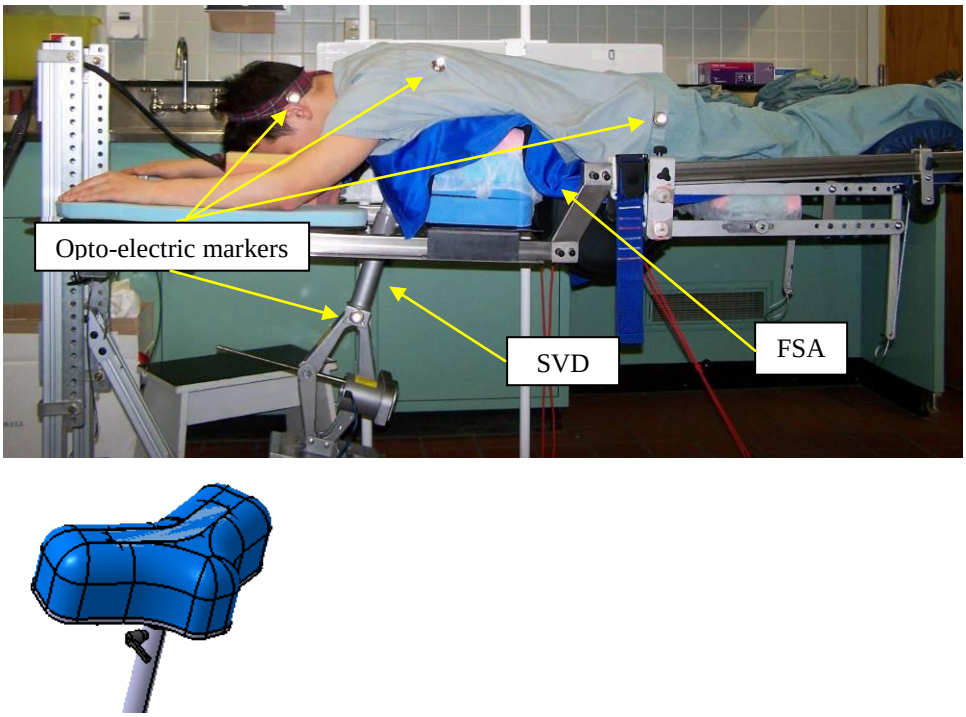

Figure 3.7 (A3F1): a) Experimental setup with a patient in the raised position; b) Details of the SVD cushion

Table 3.7 (A3T1): Subject data and spinal geometries in the neutral and sternum lifted positions

#	Sex	Weight (kg)	Height (cm)	Average Lateral Bending (cm)	Average Fulcrum Bending	Thoracic Kyphosis		Lumbar Lordosis		Decompensation (mm)	
						Neutral	Raised (% change)	Neutral	Raised (% change)	Neutral	Raised
1	F	47	155	17	167°	21°	33° (+57%)	46°	57° (+24%)	19	97
2	M	65	176	38	146°	25°	36° (+44%)	29°	34° (+17%)	18	113
3	M	52	169	25	169°	32°	48° (+50%)	49°	60° (+22%)	50	104
4	F	54	161	21	157°	34°	41° (+21%)	42°	53° (+26%)	38	120
5	F	68	158	22	169°	44°	61° (+39%)	40°	56° (+40%)	57	135
6	M	86	185	35	162°	19°	40° (+111%)	38°	44° (+16%)	35	131

Table 3.8 (A3T2): Apical spinal geometries in the neutral (N) and lifted (L) sternum positions

#	Apical Thoracic Disc Angle (degrees)								Apical Thoracic Intervertebral Disc Space (mm)							
	T4-T5		T5-T6		T6-T7		T7-T8		T4-T5		T5-T6		T6-T7		T7-T8	
	N	L	N	L	N	L	N	L	N	L	N	L	N	L	N	L
1	2.2	5.1	2.0	4.8	2.8	4.7	1.8	4.3	3.3	4.0	3.2	4.5	3.0	3.9	3.3	3.8
2	1.2	4.4	1.4	5.5	1.9	4.9	1.7	4.3	2.9	3.6	2.9	3.7	3.1	3.7	2.6	3.5
3	2.8	4.2	1.3	4.7	1.4	4.5	1.1	3.9	2.8	3.8	3.0	4.4	3.0	4.6	3.2	4.8
4	0.6	5.8	0.9	4.6	2.2	4.6	0.8	3.3	2.8	3.9	2.7	3.5	3.1	3.8	3.3	4.3
5	2.3	4.4	1.4	4.5	1.4	4.5	2.4	6.5	3.2	3.8	3.4	5.0	3.4	4.5	3.4	4.8
6	2.1	4.8	1.7	3.1	1.8	3.1	1.1	3.8	3.5	4.8	3.7	4.6	3.9	5.2	3.2	5.1

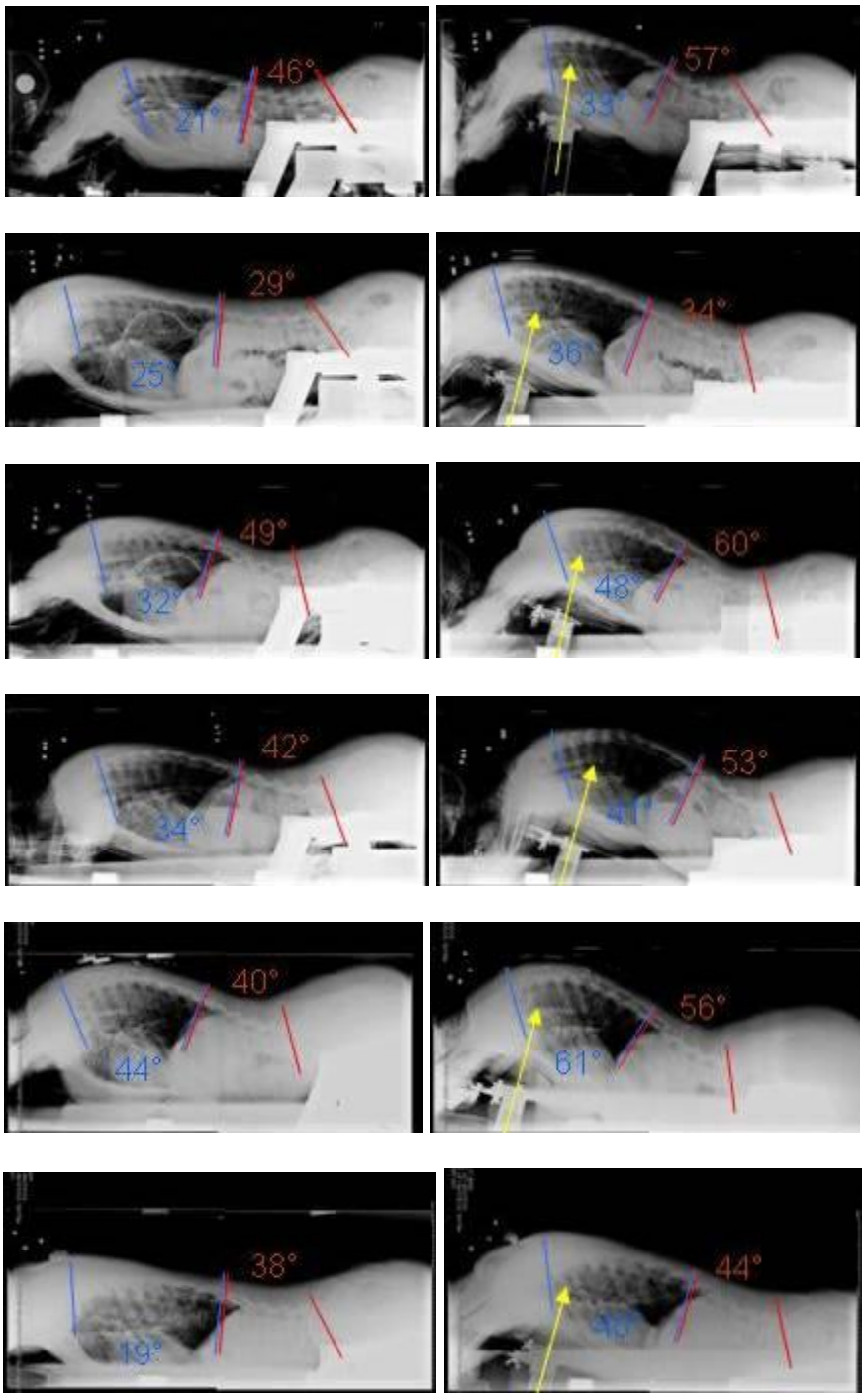

a) b)

Figure 3.8 (A3F2): Radiographs of subjects 1 to 6 in the a) neutral b) raised positions

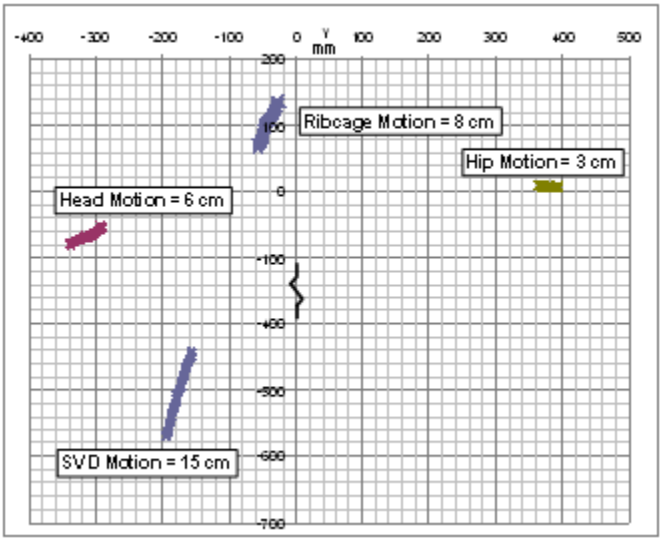

Figure 3.9 (A3F3): Vertical and horizontal displacement of opto-electric sensors between radiographic positions for subject #4

Table 3.9 (A3T3): Average (min-max) interface pressure measurements for all subjects in the neutral and raised positions

Position	Sternum Cushion Interface Pressure (mmHg)		Thoracic Cushions Interface Pressure (mmHg)		Pelvic Cushions Interface Pressure (mmHg)	
	Average	Peak	Average	Peak	Average	Peak
Neutral	absent	absent	26 (23-31)	52 (41-75)	36 (30-45)	129 (73-167)
Raised	111 (44-200)	300*	not in contact	not in contact	34 (26-47)	113 (47-164)

* limit reading of FSA

3.4 Assessment of two novel surgical positions for the reduction of scoliotic deformities

The fourth paper was the study of two novel surgical positions: lateral leg displacement and hip torsion. The MFPF was originally conceived without these two features in mind. While the original MFPF designed proved to be effective at manipulating sagittal curves it was lacking in its ability to manipulate coronal curves which is one of the main objectives of scoliotic surgeries for which the MFPF was to be used. The two features were conceived after exploiting the FEM to determine ways to reduce scoliotic deformities through surgical positioning. After FEM simulations of lateral leg displacement and pelvic torsion proved to be effective at reducing scoliotic Cobb angles and apical vertebral rotations, prototype features (proof of concept) were constructed and experimentally tested on pre-operative scoliotic patients. The results of the experimental testing are presented in this paper. The realisation of the experimental assessment component of objective 3 of the thesis (additional surgical positions allowing modification of spinal geometrical parameters not possible on the original MFPF design) is presented in this paper entitled “assessment of two novel surgical positions for the reduction of scoliotic deformities”, for which the contribution of the first author is considered to be 85%. The FEM study of objective 3 (to come up with novel surgical positions) is not presented however it was performed in order to come up with the lateral leg rotation and pelvic torsion positions presented in this paper in addition to the lateral thorax displacement position described in the fifth paper. It was submitted to *European Spine Journal* on July 7th 2010.

3.4.1 Article 4: Assessment of two novel surgical positions for the reduction of scoliotic deformities: lateral leg displacement and hip torsion

Assessment of Two Novel Surgical Positions for the Reduction of Scoliotic Deformities: Lateral Leg Displacement and Hip Torsion

CHRISTOPHER DRISCOLL[1,2], CARL-ERIC AUBIN[1,2],
HUBERT LABELLE[2], JEAN DANSEREAU[1]

1 – Dept. of Mechanical Engineering,
École Polytechnique de Montréal
P.O. Box 6079, Station Centre-Ville
Montréal, Québec, H3C 3A7, Canada

2 – Sainte-Justine University Hospital Center
3175 Cote-Ste-Catherine Rd.
Montreal, Quebec, H3T 1C5, Canada

Address for notification, correspondence and reprints:

Carl-Eric Aubin, Ph.D., P. Eng.
Full Professor
& Canada Research Chair 'CAD Innovation in Orthopedic Engineering' and 'NSERC / Medtronic Industrial Research Chair in Spine Biomechanics'
P.O. Box 6079, Station "Centre-Ville", Montréal (Québec),
H3C 3A7 CANADA
E-mail: carl-eric.aubin@polymtl.ca
Phone: 1 (514) 340-4711 ext 2836; Fax: 1 (514) 340-5867

3.4.1.1 ABSTRACT

Cobb angles and apical vertebral rotations (AVR) are two of the main scoliosis deformity parameters which spinal instrumentation and fusion techniques aim to reduce. Despite this importance, current surgical positioning techniques do not allow the reduction of these parameters. Two new surgical frame accessories prototypes have been developed: 1) a lateral leg displacer (LLD) allows lateral bending of a patient's legs up to 60° in either direction; and 2) a pelvic torsion device (PTD) which allows transverse plane twisting of a patient's pelvis at 30° in either direction while raising the thoracic cushion, opposite to the raised side of the pelvis, by 5 cm. The objective of this study was to evaluate the ability of the LLD and PTD to reduce Cobb angles and AVR. Experimental testing was performed pre-operatively on 12 surgical scoliosis patients prone on an experimental surgical frame. Postero-anterior radiographs of their spines were taken in the neutral prone position on a surgical frame, and then again for 6 with their legs bent towards the convexity of their lowest structural curve, 4 with their pelvis raised on the convex side of their lowest structural curve and 1 each in opposite LLD and PTD intended use. Use of the LLD allowed for an average supplementary reduction of 16° (39%) for Cobb angle and 9° (33%) for AVR in the lowest structural curve. Use of the PTD allowed for an average supplementary reduction of 9° (19%) for Cobb angle and 17° (48%) for AVR in the lowest structural curve. Both devices were most efficient on thoraco-lumbar/lumbar curves. Opposite of LLD and PTD intended use resulted in an increase in both Cobb angle and AVR. The LLD and PTD provide interesting novel methods to reduce Cobb angles and AVR through surgical positioning which can be used to facilitate instrumentation procedures by offering an improved intra-operative geometry of the spine.

KEY WORDS

spine • surgical positioning • scoliosis • Cobb • vertebral rotation

ACKNOWLEDGEMENTS

Project funded by the Natural Sciences and Engineering Research Council of Canada (Industrial Research Chair with Medtronic of Canada).

3.4.1.2 INTRODUCTION

Patient positioning is a required and important step of spinal instrumentation procedures. Among other things, it has an impact on spinal geometry which can be exploited to reduce pathologic deformities such as scoliosis. Studies[1,2,3] have shown that Cobb angles are reduced on average between 25-37% due to prone positioning, anaesthesia, and surgical opening. While one of the primary objectives of scoliosis instrumentation procedures is reduction of the coronal plane deformation, and more recently on the transverse plane rotation[4], current spinal operating frames such as the Jackson, Relton-Hall, Wilson or Andrews do not allow any additional 3D corrections to be made.

One method to obtain additional correction of the coronal curves, which is sometimes used for patients with severe and rigid deformities, is pre and intra operative traction[5]. It allows for a safe and effective longitudinal elongation of the spine but requires a dedicated device, must be done several weeks before the procedure and has an uncertain impact on post-operative results[6]. An alternate method to achieve further Cobb reduction through patient positioning has been proposed by Duke et al.[7] and involves the application of lateral forces (up to 150 N) to the trunk at the curve apex using adjustable thoracic cushions. Experimental evaluation of this method on 12 patients showed significant increases in spine height and decreases in both rib and trunk torsional deformity. A drawback of this method was increased patient-cushion interface pressures.

A Multi-Functional Positioning Frame (MFPF) has been developed which holds patients in the prone position with two thoracic cushions, two pelvic cushions, and a lower limb support which can all be adjusted in order to manipulate spinal geometry intra-operatively[8]. Two novel accessories, proof of concept prototypes, were added to the frame to allow specific manipulation

of scoliotic deformities: a Lateral Leg Displacer (LLD) and the Pelvic Torsion Device (PTD) (Figure-1).

The LLD installed over the MFPF lower limb support allows the patient's leg to be laterally pulled and maintained either direction up to an angle of 75° via a harness placed over the patient's ankles. Also included is a lateral support cushion, whose longitudinal position on the frame is adjustable and which can prevent lateral movement of the pelvis or thorax. The LLD provides a similar position to the lateral bending test frequently used to evaluate spinal flexibility and known to reduce Cobb angles.

The PTD installed at the level of the pelvis consists of a support cushion that is slanted 30° and is reversible such that either side can be raised. When the PTD is installed, the thoracic cushion on the opposite side of the raised portion of the pelvis is raised by 5 cm using a spacer.

The objective of this study is to experimentally evaluate the ability of the LLD and PTD to modulate scoliotic Cobb angles and apical vertebral rotation (AVR). It is hypothesized that relative to the neutral prone position on the MFPF, these systems can be used to significantly reduce the structural curves and the AVR.

3.4.1.3 METHODS

Experimental testing was performed pre-operatively on 12 surgical adolescent idiopathic or neuromuscular scoliotic patients, 5 males and 7 females aged 11 to 18, at Sainte-Justine University Hospital Center in Montreal with approval obtained from the ethics committee (Table-1). Standard standing postero-anterior (PA) and lateral radiographs, in combination with standing left and right side bending radiographs were acquired and utilized to identify curve types and structurality according to the Lenke method[9]. Subjects were weighed, their heights recorded, and then placed in the neutral prone position on the MFPF where a 36 inches (91.4 cm) PA

radiograph of their spine was acquired. At this point, subjects were placed and maintained in one of two possible positions where a second PA radiograph of their spines was acquired. Patients #1 to #6 had their lower limbs pulled towards the convexity of their lowest structural curve. Subjects #7 to #10 had their pelvis raised on the concave side of their lowest structural curve and opposite thoracic cushion spacer inserted. Two additional patients were tested in positions opposite of the LLD and PTD design intentions: #11 had his lower limbs pulled towards the concavity of his lowest structural curve, and #12 had her pelvis raised on the convex side of her lowest structural curve.

Here and throughout the lowest structural curve refers to the most caudal coronal plane scoliotic curve (MT or TL/L) which is determined to be structural using the Lenke method[9]. It is the curve whose deformity the LLD and PTD directly aim to reduce. The secondary curve refers to the other scoliotic curves: a non-structural TL/L or a MT which can either be structural or non-structural.

Patients #1 to #6 and #11 had their lower limbs laterally bent an angle of between 50° and 60° based on a position that was considered at least mildly comfortable. While laterally displacing the legs, their thoracic cage was observed to ensure that it was maintained in place by the MFPF thoracic cushions. A consistent transverse plane pelvic torsion of 30° was obtained for subjects #7 to #10 and #12 by ensuring that both anterior portions of their iliac crests were in contact with the PTD cushion.

Patients were verbally questioned about their level of comfort in the second position of radiograph acquisition and asked to choose one of four levels; comfortable, mildly comfortable, mildly uncomfortable or uncomfortable. In addition, the time taken to switch between positions was recorded.

Each radiograph was analyzed using Synapse image analysis software (Fujifilm Medical Systems USA) and the following indices were measured. For all patients, scoliotic Cobb angles and AVR using the Nash-Moe method[10]. For patients #1 to #6 and #11, pelvic obliquity, or coronal plane rotation, defined as the angle between the bi-tangent line linking the two proximal apices of the iliac crest and a reference horizontal taken as positive when the left crest is proximal relative to the right one. Vertebral rotations inferior to 10° were not considered in average results due to accuracy issues for small rotations[11].

A radio-opaque beam of the surgical frame was used as a reference horizontal as well as to scale the radiographic distance measurements to account for perspective projection. Changes in spinal geometrical parameters between positions were statistically analyzed using Wilcoxon matched pair tests performed with STATISTICA V7 software (StatSoft Inc). Correlations between Cobb angle reductions obtained with the lateral bending tests and LLD/PTD positioning as well as the correlations between Cobb and AVR changes were tested using the Spearman method. Proximal thoracic curves were not analyzed as part of this study as they were not always visible on the radiographs and the LLD and PTD are not designed to impact them. No patient in the study had structural proximal thoracic curves.

3.4.1.4 RESULTS

Patients experienced a decrease in Cobb angles and AVR while going from the standing to neutral prone position on the MFPF for the 12 patients averaging 10° (1° to 26°; ±8°) or 19% for MT Cobb, 10° (2° to 21°; ±7°) or 21% for TL/L Cobb, 3° (5° to 7°; ±4°) or 4% for MT AVR, and 5° (+3 to 19°; ±8°) or 12% for TL/L AVR (Tables 2 and 3).

Lateral displacement of patients' legs from the neutral prone position towards the convexity of their lowest structural curve (2 MT cases and 4 TL/L cases) resulted in a 16° (9° to

23°; ±6°) or 39% supplementary reduction in Cobb and 9° (3° to 17°; std: 5°) or 33% supplementary reduction in AVR. Statistical analysis showed that both these reductions were significant with respective p values of 0.0277 and 0.0277. When considering only TL/L structural curves average Cobb reduction was 19° or 51%. The impact of lateral leg displacement on the secondary curves depended on their location. The MT secondary curves (n=4) decreased 6° (4° to 9°; ±2°) or 29%. The TL/L secondary curves (n=2) increased 9° and 10°. Secondary curve AVRs were small and minimally impacted. Pelvic obliquity in the laterally displaced position averaged 19° ±4° (14° to 24°). The detailed results for each patient are outlined in Table-2 and can be observed on the radiographs in Figure-2.

The correlation between the lowest structural curve percentage Cobb angle reduction experienced during the lateral bending tests and with the LLD was 0.89 with similar respective average values 40% and 39%. The correlation between reduction in Cobb and AVR in the lowest structural curves was poor at 0.54.

Placing the pelvis in torsion by raising it on the side of the concavity of the lowest structural curve (2 MT cases and 2 TL/L cases) resulted in a 9° (3° to 14°; ±5°) or 19% supplementary reduction in Cobb angle and 17° (4° to 30°; ±12°) or 48% supplementary reduction in AVR. When considering only TL/L structural curves AVR reduction was the most effective with values of 25° (74%) and 30° (79%) achieved. The impact of pelvic torsion on the secondary curves also depended on their location. The MT secondary curves (n=2) decreased 1° and 5°. The TL/L secondary curves (n=2) increased 2° and 3°. It also resulted in an increase in secondary TL/L AVR going from (<10°) to 13° and 17°. The detailed results for each patient are outlined in Table-3 and can be observed on the radiographs in Figure-3.

The correlation between the percentage reduction in Cobb angles experienced during the lateral bending tests and raising the pelvis on the side of the concavity for the lowest structural curves was 1 with the losses experienced due to lateral bending much larger; 50% as compared to 19%. The correlation between reduction in Cobb and AVR in the lowest structural curves was fair at 0.80.

Positioning patient #11 opposite to the LLD design intent resulted a 10° or 24% increase in TL/L Cobb with negligible impact on AVR. Positioning patient #12 opposite to the PTD design intent resulted in a 5° or 17% increase in MT AVR, increased a nil TL/L AVR to 16°, and had negligible impact on Cobb angles.

None of the patients experienced discomfort in the second position of radiograph acquisition; 7 said that they were comfortable (4 on the LLD and 3 on the PTD), 4 that they were mildly comfortable (2 on the LLD and 2 on the PTD), and 1 could not provide reliable input due to an intellectual impairment.

The time taken between LLD positions was approximately 1 minute and consisted of putting the patient's ankle into the harness, pulling their legs to one side via the cable, and fixing the cable to the frame. The thorax remained stable during this process. The time taken between PTD was approximately 3 minutes and consisted of having the patient get off the MFPF, switching the existing pelvic support for the PTD, inserting the thoracic cushion spacer, and placing the patient back on the MFPF.

3.4.1.5 DISCUSSION

This study is considered a proof of concept of two novel surgical positions which allow for the effective reduction of Cobb angles and AVR in the lowest structural curves. Both devices worked best on TL/L curves but can also be effective on MT curves. The supplementary

reduction achieved of the scoliotic deformities was significant. While not tested in the present study is it possible, with some design changes discussed below, to combine their use with the potential for even greater reduction of the scoliotic deformities.

The patient position resulting from LLD use is one known to reduce scoliotic deformities and similar effect is currently exploited during lateral bending spinal flexibility tests and with the Charleston bending brace[12]. Instead of laterally displacing the torso, the LLD moves the lower limbs. A surgical frame which allows lateral displacement of the thoracic cushions could further reproduce the lateral bending position by displacing the torso in the same direction as the lower limbs. Despite only moving the lower limbs, the Cobb angle reductions were comparable to those of the lateral bending tests.

The two tested positioning systems were only functional prototypes; improvements need to be made to their current design in order for them to be practical in a surgical setting. The PTD can be made to incrementally slant thus permitting multiple levels of pelvic torsion, including the level position, and negating the need to switch between pelvic cushions. The LLD can be replaced by a leg harness (slightly wider than the lower limbs) which would have the ability to swivel to either side and be locked in place. This would negate the need for cable pulling / tying and allow more room for the surgical staff to maneuver around the table. Alternatively since pelvic coronal plane rotation is the mechanism of transfer for the reductions seen with the LLD, it could be achieved directly with a pelvic cushion and harness while maintaining the legs relatively straight. A pelvic cushion and harness which could both slant and tilt would allow for simultaneous pelvic rotation and torsion.

The LLD and PTD have many potential intra-operative applications. They could be used to improve vertebral alignment in order to facilitate pedicle screw insertion. They could be used to manipulate coronal curves in order to facilitate rod insertion and allow more flexibility with

regards to the shape of initial rod contouring thus requiring less subsequent in-situ adjustment. For older instrumentation techniques, they could be used in conjunction with distraction maneuvers in order to achieve more Cobb reduction and allow for rotational corrections which would otherwise not be possible. Finally, the LLD could be used in order to correct pelvic obliquity often associated with neuromuscular scoliosis as opposed to using unilateral halo-femoral traction[13]. Patients would be returned to the neutral prone position prior to setscrew/hook tightening and fusion to ensure a level and straight pelvis. In the event that a double curve is present, it is believed that the devices could be used in a two stage approach; 1st to facilitate primary curve instrumentation then altering the direction of pelvic rotation / torsion in order to address the secondary curves. While the LLD and PTD cannot replace the corrective forces applied by modern instrumentation techniques, they can be used in conjunction with them to facilitate the maneuvers.

The pelvic coronal and transverse plane rotation principles investigated in this study can also be applied to minimally invasive surgeries (e.g. vertebral stapling, tether, etc.) whose instrumentation does not allow for large corrective forces to be applied. This could be achieved in the lateral decubitus position by raising and lowering a patient's legs with a lower limb positioner type device[8] to achieve pelvic tilt and by tilting their pelvis to the left and right with a V-shaped pelvic support in order to achieve pelvic torsion.

Since none of the patients experienced discomfort in the laterally displaced legs or pelvic twisted positions, it is believed that additional movement could be induced intra-operatively to provide even more correction of Cobb angles and AVR than presented in this study.

The support cushion aimed at preventing lateral pelvis movement during LLD positioning was not required during this study since the existing pelvic cushions sufficiently held the patient in place. It is possible that more extreme LLD positioning would necessitate use of the support

cushion; if the case then it should be placed at the level of the superior iliac crest on the side toward which the legs are being pulled.

The relatively high correlation and similar values found between lowest structural curve Cobb angle reductions obtained with the LLD and lateral bending tests suggest that the standard pre-operative lateral bending tests could be used in order to identify good candidates for LLD use.

The main difference between the devices presented in this study and halo traction devices is in the manner in which they reduce Cobb angles. Halo traction correction is primarily due to a longitudinal elongation of the spine (increasing disc height), LLD and PTC correction is due to coronal and transverse plane vertebrae alignment (disc angles and rotation). While disc height increase may be hard to maintain post-operatively[5] due to gravitational forces, the changes in disc angles and rotations will be maintained by the instrumentation.

The amount of AVR correction obtained for primary structural curves in the MT region are likely higher than those measured on the radiographs. Since the thoracic cushion on the convex side of the MT deformity is raised this globally rotates the thorax towards the curve concavity which would translate to the spine and appear to increase AVR on coronal plane radiographs. Knowing the differences in height and lateral position between the two superior surface centroids of the thoracic cushions, the global thorax rotation can be estimated at 10°. This thorax twisting is necessary in order to maximize global spinal de-rotation, simply torsioning the pelvis would be less efficient.

The current study is limited by the number of patients especially with regards to the opposite of intended use testing which was only done for one case for each device. While most results were statistically significant, power would increase with additional patients. This was a proof of concept study. Before the LLD and PTD can be used in an operative setting, additional

testing has to be done after incorporation of the proposed design changes. One factor which was not considered in this study was the impact of anesthesia and surgical opening. Traditionally these factors increased spinal flexibility which would lead to additional corrective ability for both devices. Finally intra-operative testing needs to be performed to see if the benefits of the LLD and PTD warrant the additional complexity of patient positioning they would require.

3.4.1.6 CONCLUSION

The LLD allows for a significant reduction of Cobb angle and AVR in the lowest structural curve by lateral bending of the lower limbs towards the scoliotic spine convexity. The PTD allows a significant reduction in Cobb angles and important reductions in AVR by raising the pelvis on the concave side of their lowest structural curve and opposite thoracic cushion. Greatest improvements are obtained with lumbar curves. These proof of concept devices offer two novel ways to facilitate surgical intervention of scoliosis by allowing intra-operative manipulation of the spine.

ACKNOWLEDGEMENTS

Project funded by the Natural Sciences and Engineering Research Council of Canada (Industrial Research Chair with Medtronic of Canada).

3.4.1.7 REFERENCES

1. Delorme S, Labelle H, Poitras B, Rivard CH, Coillard C, Dansereau J. Pre-, intra-, and postoperative three-dimensional evaluation of adolescent idiopathic scoliosis. *J Spinal Disord*. 2000 Apr;13(2):93-101.

2. Behairy YM, Hauser DL, Hill D, Mahood J, Moreau M. Partial correction of Cobb angle prior to posterior spinal instrumentation. *Ann Saudi Med*. 2000 Sep-Nov;20(5-6):398-401.

3. Driscoll CR, Aubin CE, Canet F, Labelle H, Dansereau J. Biomechanical Study of the Impact of Prone Surgical Positioning on the Scoliotic Spine. (Submitted to Clinical Biomechanics June 2010).

4. Lee SM, Suk SI, Chung ER. Direct vertebral rotation: A new technique of three-dimensional deformity correction with segmental pedicle screw fixation in adolescent idiopathic scoliosis. Spine (Phila Pa 1976) 2004;29:343-9.

5. Rinella A, Lenke L, Whitaker C, Kim Y, Park SS, Peelle M, Edwards C 2nd, Bridwell K. Perioperative halo-gravity traction in the treatment of severe scoliosis and kyphosis. Spine (Phila Pa 1976). 2005 Feb 15;30(4):475-82.

6. Mac-Thiong JM, Labelle H, Poitras B, Rivard CH, Joncas J. The effect of intraoperative traction during posterior spinal instrumentation and fusion for adolescent idiopathic scoliosis. *Spine.* 2004 Jul 15;29(14):1549-54.

7. Duke K, Aubin CE, Dansereau J, Koller A, Labelle H. Dynamic positioning of scoliotic patients during spine instrumentation surgery. J Spinal Disord Tech. 2009 May;22(3):190-6.

8. Driscoll C, Aubin CE, Canet F, Labelle H, Dansereau J. Biomechanical study of the influence of lower limb surgical positioning on spinal geometry. (Submitted to J Spinal Dis Tech June 2010).

9. Lenke LG, Betz RR, Harms J, Bridwell KH, Clements DH, Lowe TG, Blanke K. Adolescent idiopathic scoliosis: a new classification to determine extent of spinal arthrodesis. J Bone Joint Surg Am. 2001 Aug;83-A(8):1169-81.

10. Nash CL Jr, Moe JH. A study of vertebral rotation. J Bone Joint Surg Am. 1969 Mar;51(2):223-9.

11. Ho EK, Upadhyay SS, Chan FL, Hsu LC, Leong JC. New methods of measuring vertebral rotation from computed tomographic scans. An intraobserver and interobserver study on girls with scoliosis. Spine (Phila Pa 1976). 1993 Jul;18(9):1173-7

12. Price CT, Scott DS, Reed FE Jr, Riddick MF. Nighttime bracing for adolescent idiopathic scoliosis with the Charleston bending brace. Preliminary report. *Spine*. 1990 Dec;15(12):1294-9.

13. Jhaveri SN, Zeller R, Miller S, Lewis SJ. The effect of intra-operative skeletal (skull femoral) traction on apical vertebral rotation. Eur Spine J. 2009 Mar;18(3):352-6.

3.4.1.8 FIGURES AND TABLES

a)

b)

c)

Figure 3.10 (A4F1): a) Lateral Leg Displacer (LLD) with subject; b-c) Pelvic Torsion Device (PTD) with and without subject.

Table 3.10 (A4T1): Patient and lateral bending data

Subject #	1	2	3	4	5	6	7	8	9	10	11	12
Sex M/F	F	M	M	F	F	F	F	M	M	F	M	F
Weight (kg)	64	45	48	39	46	36	64	58	32	41	50	33
Height (cm)	165	163	166	152	152	155	157	175	147	160	171	154
T12–L5 Lordosis	45°	42°	53°	47°	58°	18°	62°	38°	42°	56°	53°	40°
T4–T12 Kyphosis	32°	24°	52°	14°	40°	14°	33°	23°	58°	46°	32°	10°
Lenke Type	5C	3B	1B	5C	1B	5C	5C	1B	1A	6C	5C	1A
Scoliosis Type	AIS	AIS	Neuro	AIS	Neuro	AIS	AIS	AIS	AIS	AIS	AIS	Neuro
MT Cobb	22° T5-T10	69° T6-T12	90° T6-L2	30° T1-T9	79° T7-L2	15° T1-T9	31° T5-T11	62° T7-L2	70° T5-L3	34° T6-T10	29° T6-T11	79° T5-T12
MT AVR	<10°	32°	48°	<10°	34°	<10°	<10°	33°	42°	13°	<10°	36°
TL/L Cobb	44° T10-L2	52° T12-L4	30° L2-L5	44° T9-L2	46° L2-L5	49° T9-L2	56° T11-L4	22° L2-L5	19° L3-L5	58° T10-L4	57° T11-L4	32° T12-L5
TL/L AVR	28°	24°	<10°	34°	<10°	27°	53°	<10°	<10°	34°	43°	<10°
Left Bend MT	34° +55%	78° +13%	105° +17%	12° -60%	83° +5%	31° +107%	37° +19%	70° +13%	97° +39%	40° +18%	32° +10%	80° +1%
Left Bend TL/L	7° -84%	25° -52%	3° -90%	63° +43%	19° -59%	38° -22%	23° -59%	2° -91%	11° -42%	25° -57%	22° -61%	5° -84%
Right Bend MT	4° -82%	27° -61%	71° -21%	33° +10%	69° -13%	4° -73%	16° -48%	31° -50%	46° -34%	38° +12%	9° -69%	39° -51%
Right Bend TL/L	50° +14%	58° +12%	40° +33%	24° -45%	39° -15%	65° +33%	66° +18%	30° +36%	37° +95%	75° +29%	62° +9%	38° +19%

Table 3.11 (A4T2): Impact of lateral leg displacement (CV = convexity and CC = concavity)

#	Neutral Prone on MFPF					Laterally Displaced Legs					
	MT		TL/L		Pelvic	Direction	MT		TL/L		Pelvic
	Cobb	AVR	Cobb	AVR	Obliquity	of leg pull	Cobb	AVR	Cobb	AVR	Tilt
1	21°	<10°	35°	30°	-1°	CV TL/L	12° (-43%)	<10°	14° (-60%)	19° (-37%)	21°
2	56°	28°	33°	17°	1°	CV TL/L	52° (-7%)	36° (+29%)	10° (-70%)	9° (-47%)	20°
3	74°	41°	25°	<10°	3°	CV MT	65° (-12%)	38° (-7%)	34° (+36%)	<10°	15°
4	23°	<10°	38°	30°	2°	CV TL/L	19° (-17%)	<10°	23° (-39%)	26° (-13%)	14°
5	63°	29°	25°	<10°	-1	CV MT	54° (-14%)	20° (-31%)	35° (+40%)	<10°	24°
6	10°	<10°	47°	27°	0°	CV TL/L	5° (-50%)	<10°	30° (-36%)	10° (-63%)	22°
11	23°	<10°	42°	33°	-4°	CC TL/L	24° (+4%)	<10°	52° (+24%)	33° (±0%)	-17°

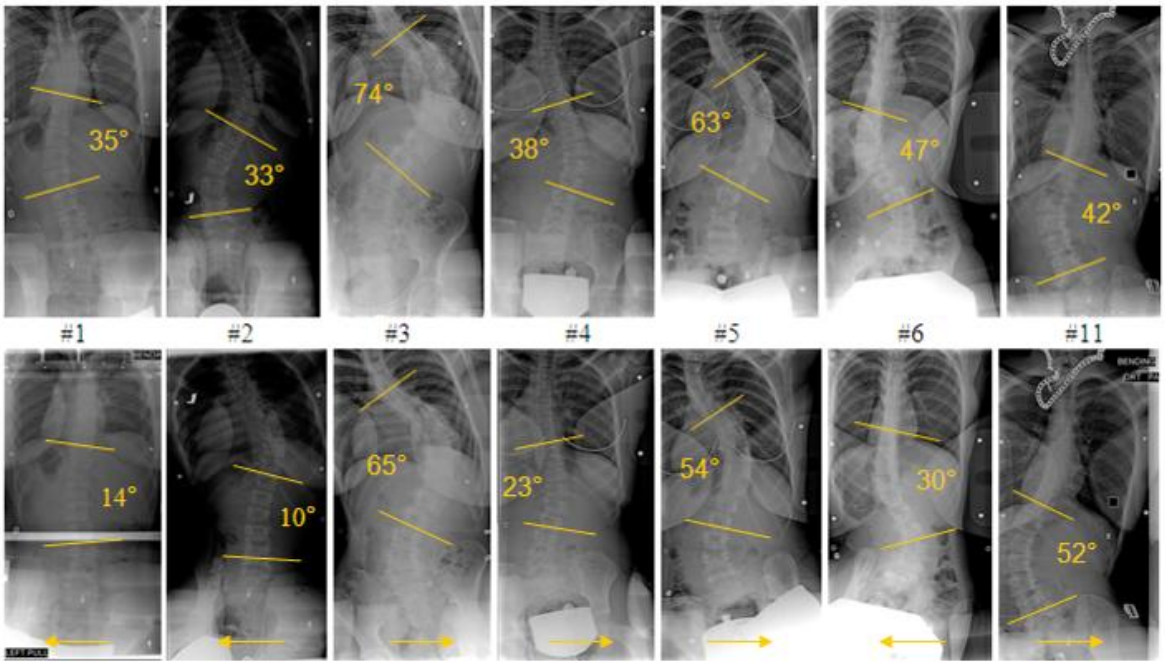

Figure 3.11 (A4F2): Radiographs of patients 1 to 6 and 11 in the neutral prone (top row) and laterally bent leg (bottom row) positions; arrow indicated direction of lower limb displacement

Table 3.12 (A4T3): Impact of pelvic torsion

#	Neutral Prone on MFPF				Twisted Pelvis				
	MT		TL/L		Side Raised	MT		TL/L	
	Cobb	AVR	Cobb	AVR		Cobb	AVR	Cobb	AVR
7	30°	<10°	48°	34°	CC TL/L	29° (-3%)	<10°	34° (-29%)	9° (-74%)
8	52°	32°	14°	<10°	CC MT	44° (-15%)	23° (-28%)	17° (+21%)	17°
9	44°	40°	21°	<10°	CC MT	41° (-7%)	35° (-13%)	23° (+10%)	13°
10	31°	18°	38°	37°	CC TL/L	26° (-16%)	<10°	29° (-24%)	8° (-78%)
12	59°	30°	26°	<10°	CV MT	61° (+3%)	35° (+17%)	28° (+8%)	16°

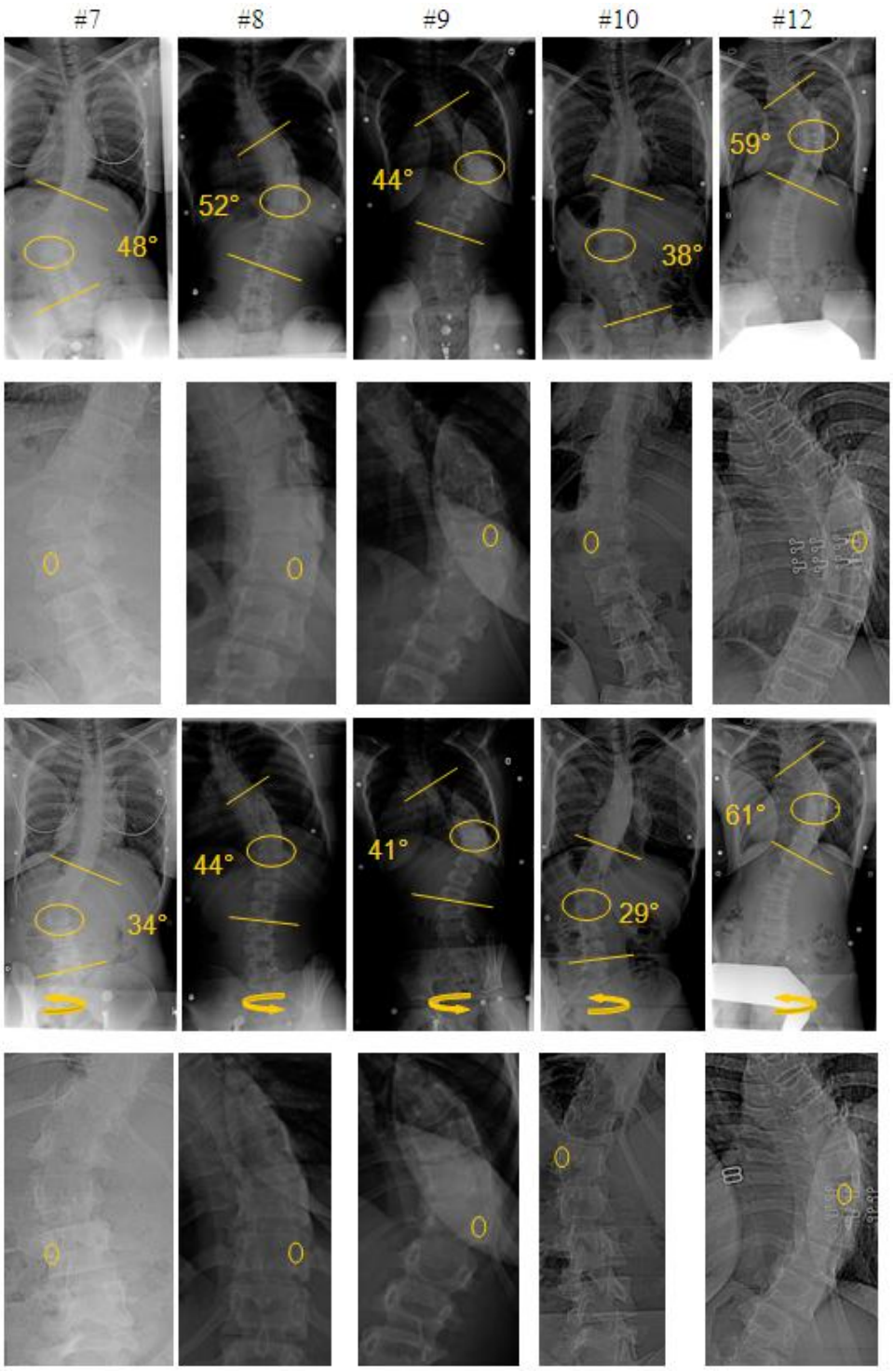

Figure 3.12 (A4T3): Radiographs of patients 7 to 10 and 12 in the neutral prone (1st and second row) and twisted pelvis positions (3rd and fourth row); arrow indicates direction of pelvic torsion

CHAPTER 4 OPTIMIZATION OF SPINAL GEOMETRY FOR SURGERIES OF THE SPINE BY PATIENT POSITIONING

The final paper is a culmination of all the other studies contained in this project. While individual MFPF positioning features were previously studied, it was important to understand their combined impact. Equally important was the need to develop a method for individual surgeons to make use of the MFPF's many positioning features. All previous validation of the FEM's ability to reproduce the impact of individual positioning parameters was needed. The final article is one uniquely of FEM simulations. Since it was uncertain if different curve types would have different optimized positions on the MFPF, 3 distinct curve types were included in this study. This study also includes an additional positioning feature not previously discussed, the lateral thoracic displacer. As with the lateral leg displacer and pelvic torsioner, a prototype features (proof of concept) was constructed. This feature was experimentally tested on a scoliotic patient combined with lower limb displacement the results of which are briefly discussed in Chapter 5. The realisation of objective 4 of the thesis (study and optimization of combined MFPF positioning parameters) is presented in this paper entitled "optimization of spinal geometry for surgeries of the spine by patient positioning", for which the contribution of the first author is considered to be 85%. It was submitted to *Spine* on November 11th 2010.

4.1 Article 5: optimization of intra-operative positioning for scoliosis surgeries

Optimization of Intra-Operative Positioning for Scoliosis Surgeries

CHRISTOPHER DRISCOLL[1,2], CARL-ERIC AUBIN[1,2], HUBERT LABELLE[2], JEAN DANSEREAU[1]

1 – Dept. of Mechanical Engineering, École Polytechnique de Montréal
P.O. Box 6079, Station Centre-Ville
Montréal, Québec, H3C 3A7, Canada

2 – Sainte-Justine University Hospital Center
3175 Cote-Ste-Catherine Rd.
Montreal, Quebec, H3T 1C5, Canada

Address for notification, correspondence and reprints:

Carl-Eric Aubin, Ph.D., P. Eng.
Full Professor
& Canada Research Chair 'CAD Innovation in Orthopedic Engineering' and 'NSERC / Medtronic Industrial Research Chair in Spine Biomechanics'
P.O. Box 6079, Station "Centre-Ville", Montréal (Québec), H3C 3A7 CANADA
E-mail: carl-eric.aubin@polymtl.ca
Phone: 1 (514) 340-4711 ext 2836; Fax: 1 (514) 340-5867

4.1.1 ABSTRACT

Summary of background data: New generation frames for spinal surgeries allow for increased and varied patient positioning capabilities through the introduction of novel positioning features which can be used independently of each other. This increase in patient positioning capability facilitates procedures such as scoliosis instrumentation by allowing intra-operative manipulation of spinal geometry and may improve post-operative results. The impact of the combined use of multiple surgical frame positioning features on spinal geometry remains unknown.

Objective: The objective of this study is to investigate the impact of the combined use of multiple surgical frame positioning features on spinal geometry and develop a method for their optimization.

Methods: Finite element models (FEM) representing the osseo-ligamentous structures of the spine, ribcage, pelvis and lower limbs, including muscles, were created for three different curve types (main thoracic, double major, and triple major) using a radiographic bi-planar reconstruction technique. Each FEM was subjected to an experimental design in which hip flexion and extension, thorax vertical displacement, lateral leg displacement, pelvic torsion and thorax lateral displacement were independently and simultaneously varied and the resultant changes in spinal geometry measured. Regression coefficients describing sagittal and coronal curves, vertebral rotation, balance, and disc space in terms of patient positioning were developed. They were then exploited to study optimization of individual spinal geometrical parameters and global spinal geometry factoring for surgeon-specific desired values and relative importance.

Results: The combined use of multiple surgical frame positioning features allows for a wider range of possible intra-operative spinal geometries than their individual use providing an average 70% improvement in 11 spinal geometrical parameters. Each spinal geometrical parameter was significantly impacted by on average 3 different surgical frame positioning features. The optimized combination of surgical frame positioning features varied between curve types, however, some patterns emerged.

Conclusions: The combined use of multiple surgical frame positioning features allows for increased manipulation of intra-operative spinal geometry and optimization is required to maximize the benefit of their combined use.

KEY WORDS

surgical positioning • scoliosis • optimization • biomechanics • finite element modeling

ACKNOWLEDGEMENTS

Project funded by the Natural Sciences and Engineering Research Council of Canada (Industrial Research Chair with Medtronic of Canada).

4.1.2 INTRODUCTION

The most severe cases of spinal deformity, such as scoliosis, require surgical intervention in order to treat symptoms and re-align the spine. During surgical procedures, patients are typically kept in the prone position on a frame while instrumentation is utilized to manipulate and fix spinal geometry. The role of patient positioning was historically limited to facilitating exposure, minimizing bleeding and the chance of damage to vital structures, allowing proper ventilation, avoiding post-operative morbidity, and preserving sagittal alignment which was accomplished by fixed four post frames such as the Relton-Hall[1]. More modern frames such as the Jackson, Wilson and Andrews (Orthopedic Systems, Inc.) introduced a limited amount of patient positioning features to facilitate surgical interventions such as hip flexion and torso raising. Next generation frames for spinal surgeries allow for increased and varied patient positioning capabilities through the introduction of novel positioning features which can be used independently of each other. One other system is the Multi-Functional Positioning Frame (MFPF) for scoliosis surgeries (Figure 1), a prototype which allows for hip flexion and extension, thorax vertical displacement, lateral leg displacement, pelvic torsion and thorax lateral displacement. This increase in patient positioning capability facilitates procedures such as scoliotic instrumentation by allowing intra-operative manipulation of spinal geometry and may improve post-operative results[2].

Previous studies have examined the impact of individual frame positioning features or movements on specific spinal geometrical parameters such as the impact of hip flexion and extension on sagittal curves[3], the impact of thorax vertical displacement on sagittal curves[4], the impact of lateral leg displacement on coronal curves and vertebral rotation[5], the impact of pelvic torsion on coronal curves and vertebral rotation[5], and the impact of lateral thoracic cage displacement on coronal and transverse plane vertebral rotations[6]. In these studies, each of these positioning features or movements has been shown to have secondary impacts on other spinal geometrical parameters. The combined impact of these multiple surgical positions on spinal geometry is not known.

Although the relation between the ideal post-operative spine shape and proper intra-operative positioning is not well known, the relative importance of various spinal geometrical parameters can change throughout the stages of the operation. Increasing access to posterior vertebral elements and intervertebral discs may be important during pedicle screw/wire/hook insertion or decompression procedures (laminectomy, discectomy, etc.). Decreasing translational and rotational deformities may be important for rod/staple insertion and distraction/reduction maneuvers. Restoration of standing sagittal curves and balance may be important for setscrew/hook tightening and fusion.

A method of optimizing spinal geometrical parameters due to patient positioning on a dynamic frame using a Finite Element Model (FEM) has been proposed by Duke et al. [2]. It was applied to a double thoracic curve and showed that each positioning / force application feature of the frame had a significant impact on multiple spinal geometrical parameters, in particular, lateral thoracic forces on Cobb angles, apical vertebral translation and apical vertebral rotation. The objective of this study is to extend this original study and investigate the impact of the combined use of multiple traditional and novel positioning features on the geometry of different scoliotic

curve types. A secondary objective is to develop a method allowing for the optimization of both individual spinal geometrical parameters and global spinal geometry. It is hypothesized that the combined use of hip flexion and extension, thorax vertical displacement, lateral leg displacement, pelvic torsion and thorax lateral displacement allows for a significant (20%) increase in possible manipulation of spinal sagittal curves, coronal curves, vertebral rotation, balance, and disc space relative to their individual use. It is also hypothesized that combined use of these operative positions can be optimized based on the needs of individual surgeons.

4.1.3 METHODS

This study was performed using a biomechanical FEM which has been previously validated for the study of surgical positioning[2,3], and which is summarized in the next section. Use of this biomechanical model allows numerous surgical positioning simulations to be performed and detailed spinal geometrical changes to be computed.

Finite Element Model

A FEM was created for three different patients with different scoliotic curve types: a single main thoracic (MT), a double major (DM) and a triple major (TM) (Figure 2). The osseo-ligamentous structures of the spine, ribcage, and pelvis were obtained using a biplanar reconstruction technique[7] based on pre-operative standing postero-anterior and lateral radiographs in which the patient wore a calibration plate containing radio-opaque markers. Anatomical landmarks were identified and their 3D coordinates obtained using a self-calibration and optimization algorithm which were then used to transform detailed vertebral geometry using a free form deformation technique[8,9]. Lower limb geometry of the femur, tibia and fibula, including joints, ligaments and muscles, was obtained from interpolation and scaling of Visible Human

Project[10] geometry based on anthropological relationships[11]. Elastic beam elements were used to model the vertebrae (bodies, pedicles, transverse and spinous processes, superior and inferior articular processes), intervertebral discs, rib cage (true, false and floating ribs, sternum and cartilage), pelvis (iliac crest, pubis, sacrum, acetabulum and iliac-lumbar ligaments), and lower limbs (femur, tibia, fibula and associated ligaments). Link elements were used to model the lower limb muscles (linking pelvis to lower limbs), intra and inter vertebral ligaments, and intercostals ligaments. Non-linear links were used to model the costo-verteral and costo-transverse joints. Non-linear contact elements were used to model the zygapophyseal joints.

Radiographs utilized in the reconstruction process were of paediatric patients treated at Saint-Justine University Hospital Center with ethics approval obtained for their utilization.

Material properties were attributed published experimental values, which are described elsewhere along with a more detailed description of the FEM[3].

Prone Positioning Modeling

Each FEM was subjected to an initial and previously described standing to prone positioning process simulation[12]. In summary, forces equivalent to trunk transverse body segment weights for each vertebral level, defined as a percentage of body weight by Pearsall et al.[13], applied to nodes representing the transverse body segment centers of mass were transferred from the longitudinal to transverse planes. Boundary conditions were applied to the nodes of the thorax, pelvis and lower limbs in order to represent contact with the surgical frame's thoracic and pelvic cushions. FEM changes in spinal geometry presented in this study are all relative to this baseline position: prone before any additional positioning.

Optimization of Individual Spinal Geometrical Parameters

Each of FEM was subjected to a 3 phase / 5 factor / 81 run design of experiment (DOE) (Statistica V7) in which surgical positions were independently and simultaneously varied between their limit positions. The factors manipulated and their phases with respect to the baseline prone position were: thorax vertical displacement (TVD: 0, 5 and 10 cm), thorax lateral displacement (TLD: 10 cm left, 0 cm, 10 cm right) (left denoted as negative), hip flexion / extension (HFE: 15° and 50° flexion, 20° extension) (extension denoted as negative), coronal plane lateral leg displacement (LLD: 60° left, 0°, 60° right) (left denoted as negative), and pelvic transverse plane torsion (PT: 30° left, 0°, 30° right) (pelvis raised on left denoted as negative). For each simulation, boundary conditions (BCs) were applied in order to represent the displacements of the surgical positions and the constraints imposed by the support cushions. Thoracic cushion BCs (TVD and TLD displacements) were applied to the anterior-lateral nodes of the 3rd and 4th rib. PT was applied to a node midway between the acetabulums. Lower limb BCs (HFE and LLD rotations) were applied to the hip joints. The two limit phases for each of the five positioning factors are presented in Figure 3.

After each run, the changes in the following spinal geometrical parameters were measured: L1-S1 lumbar lordosis, T4-T12 thoracic kyphosis, proximal thoracic (PT), main thoracic (MT) and thoraco-lumbar/lumbar (TL/L) Cobb angles, sagittal and coronal balance (T1 relative to S1), height of all intervertebral discs, and apical vertebral rotation (AVR) of the PT, MT and TL/L segments. Vertebral angles were measured using the intercepts of the lines linking the end vertebrae superior and inferior endplate centroids. Balance was measured as the lateral distance between nodes representing the T1 and S1 vertebral body centroids in the sagittal and coronal planes. Intervertebral disc height was measured as the distance between the superior and

inferior vertebral body endplate centroids. AVRs were measured as the arctangent of the relative anterior-posterior and lateral positions of pedicles nodes in the transverse plane.

In order to allow optimization of individual spinal geometrical parameters, regression coefficients obtained from statistical analysis of the DOE results, were combined into quadratic predictive equations for each spinal geometrical parameter in terms of the studied surgical positions. In addition, the standardized effects measuring each surgical position's ability to manipulate the spinal geometrical parameters were calculated using ANOVA.

The predictive equations developed were run through a pattern search solver (MATLAB V7.5, MathWorks inc.) to determine which configuration of MFPF features resulted in: minimum Cobb angles (PT, MT, and TL/L), minimum AVR (PT, MT, and TL/L), maximum average disc height (T4 toT8, T9 toT12, and L1 to S1 segments), minimum unbalance (sagittal and coronal), and maximum physiological sagittal curves taken to be 37.5° for kyphosis and 56.1° for lordosis (Voutsinas and MacEwen 1986).

Values of each optimized individual spinal geometrical parameter were calculated and compared to their neutral prone values as well as their values if only the single most influential surgical position was used. Secondary (non-structural) curves and AVR < 10° were not considered in the study.

Optimization of Global Spinal Geometry

The predictive equations for each individual spinal geometrical parameter were combined into two different weighted and normalized cost functions.

The first cost function used the following format:

$$\Phi_1 = \sum w_i \times |(GP_i - GD_i) / (GI_i)|$$

Where w_i are weights attributed to each spinal geometrical parameter having a value ranging from 1 to 5, GP_i represents the predictive equations developed for each spinal geometrical parameter, GD_i represents the desired value of each spinal geometrical parameter, and GI_i represents the initial values of each spinal geometrical parameter in the neutral prone position.

The second cost function used the following format:

$$\Phi_2 = \sum r_i \times w_i \times |(GP_i - GD_i)|$$

Where r_i, a relative scaling factor, replaces the normalization by GI_i. This second cost function attempted to address issues resulting from comparison of different geometrical measure types (Cobb angles in degrees, disc height in mm, vertebral rotation in degrees, etc.) while not relying on GI_i for normalization which can greatly impact the relative importance of each parameter in the cost function for example having an initial unbalance of 100 mm or 10 mm. The values of r_i, 1 for Cobb angles, 1.25 for AVR, 0.2 for balance, and 10 for disc heights were selected in order to allow equivalent units of comparison between the different geometrical parameters (i.e. 10° improvement in Cobb angle would be comparable to an 8° improvement in AVR, a 50 mm improvement in balance, and a 1 mm improvement in disc height). Values of r_i were attributed based on the previous experimental measures of the studied surgical positions to manipulate these parameters.

A validity check was performed on the two global optimization equations for three different stages of a hypothetical scoliosis instrumentation procedure: 1) pedicle screw insertion in the lower thoracic region, 2) rod insertion and rotation, and 3) set-screw tightening and fusion. The desired values attributed for these maneuvers are to provide specific examples of achieving global positioning and may vary between one user and the next. The emphasis here is on the method of global optimization and not the specific resultant patient position.

In the first case, weightings and desired values were attributed based on the need to facilitate access to posterior vertebral elements and reduce vertebral rotation in the lower thoracic region (e.g. an elongated spine with reduced lordosis and increased kyphosis). The disc space (disc height) was considered very important and attributed a desired increase of 30%. AVR, lordosis and kyphosis were also considered very important and attributed respective desired values of 0, 0, and an increase in 30% relative to physiological. Cobb angles were considered moderately important and also attributed a desired value of 0.

In the second case, weightings and desired values were attributed based on the need to decrease translational and rotational deformities in both the thoracic and lumbar regions while having physiological sagittal curves. Cobb angles and AVR were considered very important and attributed desired values of 0. Sagittal curves were considered moderately important and attributed desired physiological values.

In the third case, weightings were taken directly from the Majdouline et al.[15] study based on the relative importance of post-operative geometrical measures. Desired values were selected based on having a normal spine (e.g. no deformities and physiological sagittal curves); disc space was not considered.

The w_i and GD_i values selected for each of the three global optimization cases studied are detailed in Table 3.

4.1.4 RESULTS

Spinal geometrical parameters were all improved as part of the individual optimization process when using multiple combined surgical positions. On average across the three different curve types: +30% in lordosis (within 0° of the desired 56°), +86% in kyphosis (within 2° of the desired 38°), -66% PT Cobb, -49% MT Cobb, -65% TL/L Cobb, restoration of sagittal and

coronal balance (0 mm of unbalance), +29% average disc height between T4 and T8, +18% average disc height between T9 and T12, + 18% average disc height between L1 and S1, and -71% in MT AVR. Taking all the individual spinal geometrical parameters into account, an average 70% improvement of the MFPF prone values was achieved relative to their desired values.

When using only the single most influential surgical position (identified in Table 2 with †) the spinal geometrical parameters were also improved but to a lesser extent. On average across the three different curve types: +27% in lordosis (within 1° of the desired 56°), +49% in kyphosis within (within 9° of the desired 38°), -19% PT Cobb, -29% MT Cobb, -27% TL/L Cobb, perfect sagittal and coronal balance, +5% average disc height between T4 and T8, +9% average disc height between T9 and T12, + 8% in average disc height between L1 and S1, and -59% in MT AVR. Taking all the individual spinal geometrical parameters into account, an average 49% improvement of prone values was achieved relative to their desired values. The detailed results of the individual spinal geometrical parameter optimization process, including the most influential surgical position, are in Table 1.

Optimization of individual geometrical parameters was obtained in different combined surgical positions for each curve type although some patterns emerged. In order to increase the sagittal curves of the studied patients which had relatively flat backs, a combination of thorax raising and hip extension was used. Minimum Cobb angles and AVR with the lower limbs displaced towards the given curve convexity and pelvis raised on the side of the given curve concavity. TL/L Cobb was reduced with the thorax displaced towards its convexity. Disc space was generally increased by using surgical positions which reduced Cobb angles and by flexing the hips. Observed differences in optimized positions between curve types included: lateral thorax position to decrease MT Cobb, vertical thorax position to decrease TL/L Cobb, and thorax, pelvic

tilt and lateral leg position to increase disc space. The detailed surgical positions for the optimization of each individual spinal geometrical parameter are in Table 2.

Each spinal geometrical parameter was on average significantly impacted by 3 different surgical positions ranging from 1 for TM L1-S1 disc space to 5 for DM and TM lordosis. The surgical position which significantly impacted the most spinal geometrical parameters was the TLD with a total of 24 out of the 36 studied over the three curve types; 12 of those for which it was the most influential positioning feature. The surgical position which significantly impacted the least spinal geometrical parameters was the HFE with a total of 10 out of the 36 studied over the three curve types; 3 of those for which it was the most influential positioning feature. In general, the surgical position's impact significance on spinal geometrical parameters was consistent such as TVP being the most influential on kyphosis across the three different curve types. There were, however, differences including the impact significance of TLP on T9-T12 disc space. The impact significance of the different surgical positions on the spinal geometrical parameters is detailed in Table 2.

The two different optimization cost functions each resulted in global minimum spinal geometries for the three different operative conditions (represented by their respective W and GD inputs). When comparing them, the second cost function which included the relative scaling factor, had individual spinal geometrical parameters closer to their desired values (GD) a total of 15 out of 33 times over the three operative conditions. There were also 8 out of 33 times in which the spinal geometrical parameters were equally close to their desired values using both cost functions. Individual spinal geometrical parameters were further from their GD values using global optimization as compared to individual optimization using multiple surgical positions. However, individual spinal geometrical parameters were closer to their GD values using global

optimization as compared to individual optimization when using only the single most influential surgical position.

The optimized surgical positions across the three example operative stages were different from each other. Again, the important point is to demonstrate the impact of different GD and W inputs and not the specific positions which may be different for each user. For pedicle screw insertion in the lower thoracic region the optimized position was thorax raised, flexing the hips, lateral displacing the thorax towards the MT convexity, laterally displacing the lower limbs towards the MT convexity and raising the pelvis on the side of the MT concavity. For rod insertion and rotation the optimized position was raising the thorax, lateral displacement of the thorax towards the MT convexity, laterally displacing the lower limbs towards the MT convexity, extending the hips and keeping the pelvis level. For set-screw tightening and fusion the optimized position was thorax lowered, slight displacement of the thorax towards the MT concavity, extending the hips, laterally displacing the lower limbs towards the MT convexity and slightly raising the pelvis on the side of the MT concavity. The detailed results of the two global optimization cost functions can be found in Table 3.

4.1.5 DISCUSSION

Methods were presented which allow for the optimization of both individual spinal geometrical parameters and global spinal geometry exploiting positioning features. In this study, we used an existing prototype of a positioning device allowing to individually adjust multiple positioning features. Both the individual and global optimized positions required the combined use of multiple positioning features. This was shown two ways: each spinal geometrical parameter was, on average, significantly impacted by three surgical frame positioning features and their optimized geometries were improved when using multiple positioning features relative

to only using the single most influential one (average 22% additional improvement of parameters relative to desired values). For example the TL/L curve of the TM case was significantly impacted by TLD, LLD and PTT. With only using LLD, its initial value of 32° was reduced to 22°; when using all multiple combined surgical positions it was further reduced to 3°.

The strength of the global optimization process presented in this study is the ability of a given surgeon to input his desired value and relative importance for each spinal geometrical parameter. It is expected that these values will vary amongst surgeons because of the known inter-surgeon variability in desirable post-operative spinal geometry[15]. For this reason the optimized positioning configurations for the three surgical hypothetical objectives presented in this study may be different for a surgeon who has a different opinion on the desired value and relative importance of spinal geometrical parameters. The r_i values of the second cost function provide a way for direct comparison of different spinal geometrical parameter units (e.g. mm and degrees) which would otherwise skew the results. It is this r_i that allowed the second global optimization function to yield better results than the first one which relied on normalization based on initial geometrical parameter values.

The operative positions presented in this study such as TVD, TLD, LLD and PTT, which could be achieved using our MFPF prototype, are novel as well as their combined use. The current MFPF was designed for individual use of each of its five positioning features. While the TVP and TLP can easily be combined with one of the lower body positions (HFE, LLP, or PTT), design changes need to be made in order to allow for combined lower body positions as previously suggested[5]. This study shows that it would be worthwhile to bring about those design changes to allow combine the lower limb positioning. It also suggests that these positioning features should be made available on any future surgical frames that may be developed.

It is proposed that the global optimization process developed be used as part of the surgical planning process when exploiting positioning features. This would include patient specific FEM reconstruction because, as was shown, different curve types had different optimized positions for individual spinal geometrical parameters. Further it is proposed that the w_i and GD_i inputs be considered for each stage of the intervention and patient position be manipulated intra-operatively because, as was shown, the optimized positions for the different surgical stages were different.

One of the limitations of this study is that the FEM developed was attributed material properties taken from literature, as a general investigation of different curve types was performed. The results presented may not be the same for patients with different spinal flexibilities. A sensitivity study which attributed increased stiffness to various regions of the spine revealed that although individual spinal geometrical parameters had different optimized values, they were generally achieved in the same positioning configurations. Material property personalization, through methods such as calibrated suspension flexibility testing[16] or lateral bending flexibility testing[17] should be performed when optimizing for these geometrical parameters in a patient-specific manner. The cost functions developed could also be improved by the inclusion of additional geometrical parameters relevant for scoliosis cosmesis such as rib hump and shoulder obliquity.

The next step of this study is experimental validation of the optimization process presented in which spinal radiographs of the optimized positions are compared to FEM predicted geometries.

4.1.6 CONCLUSION

A method has been developed which allows for the combined use of multiple surgical positioning features for the optimization of both specific spinal geometrical parameters and global spinal geometry. The combined use of multiple surgical positioning features offers a wider range of possible intra-operative spinal geometrical manipulation as compared to their individual use.

4.1.7 REFERENCES

1. Relton JE, Hall JE. An operation frame for spinal fusion. A new apparatus designed to reduce haemorrhage during operation. J Bone Joint Surg Br. 1967 May;49(2):327-32

2. Duke K, Aubin CE, Dansereau J, Labelle H. Computer simulation for the optimization of patient positioning in spinal deformity instrumentation surgery. Med Biol Eng Comput. 2008 Jan;46(1):33-41.

3. Driscoll C, Aubin CE, Labelle H, Horton W, Dansereau J. Biomechanical Study of Patient Positioning: Influence of Lower Limb Positioning on Spinal Geometry. J Spinal Disord Tech. (Accepted December 2010).

4. Driscoll CR, Aubin CE, Canet F, Dansereau J, Labelle H. The impact of intra-operative sternum vertical displacement on the sagittal curves of the spine. Eur Spine J. 2009 Nov 10.

5. Driscoll C, Aubin CE, Labelle H, Dansereau J. Assessment of Two Novel Surgical Positions for the Reduction of Scoliotic Deformities: Lateral Leg Displacement and Hip Torsion. Eur Spine J. (Submitted June 2010).

6. Harrison DE, Cailliet R, Harrison DD, Janik TJ, Troyanovich SJ, Coleman RR. Lumbar coupling during lateral translations of the thoracic cage relative to a fixed pelvis. Clin Biomech (Bristol, Avon). 1999 Dec;14(10):704-9.

7. Cheriet F, Laporte C, Kadoury S, Labelle H, Dansereau J. A novel system for the 3-D reconstruction of the human spine and rib cage from biplanar x-ray images. IEEE Trans. Biomed. Eng. 2007; 54:1356-8.

8. Delorme S, Petit Y, de Guise JA, Labelle H, Aubin CE, Dansereau J. Assessment of the 3-d reconstruction and high-resolution geometrical modeling of the human skeletal trunk from 2-D radiographic images. IEEE Trans Biomed Eng. 2003 Aug;50(8):989-98.

9. Kadoury S, Cheriet F, Laporte C, Labelle H. A versatile 3D reconstruction system of the spine and pelvis for clinical assessment of spinal deformities. Med. Biol. Eng. Comput. 2007; 45:591-602.

10. Viceconti, M, International Congress on Computational Bioengineering, M. Doblaré, et al, Eds., Zaragoza, Sept. 24-26,(2003) and: http://www.tecno.ior.it/VRLAB/researchers/repository/BEL_repository.html

11. Klein Horsman MD, Koopman HF, van der Helm FC, Prosé LP, Veeger HE. Morphological muscle and joint parameters for musculoskeletal modelling of the lower extremity. Clin Biomech (Bristol, Avon). 2007 Feb;22(2):239-47.

12. Driscoll CR, Aubin CE, Canet F, Labelle H, Dansereau J. Biomechanical Study of the Impact of Prone Surgical Positioning on the Scoliotic Spine. J Spinal Disord Tech. (submitted November 2010).

13. Pearsall DJ, Reid JG, Livingston LA. Segmental inertial parameters of the human trunk as determined from computed tomography. Ann Biomed Eng. 1996 Mar-Apr;24(2):198-210.

14. Voutsinas SA, MacEwen GD. Sagittal profiles of the spine. Clin Orthop Relat Res. 1986 Sep;(210):235-42.

15. Majdouline Y, Aubin CE, Robitaille M, Sarwark JF, Labelle H. Scoliosis correction objectives in adolescent idiopathic scoliosis. J Pediatr Orthop. 2007 Oct-Nov;27(7):775-81.

16. Lamarre ME, Parent S, Labelle H, Aubin CE, Joncas J, Cabral A, Petit Y. Assessment of spinal flexibility in adolescent idiopathic scoliosis: suspension versus side-bending radiography. Spine (Phila Pa 1976). 2009 Mar 15;34(6):591-7.

17. Petit Y, Aubin CE, Labelle H. Patient-specific mechanical properties of a flexible multi-body model of the scoliotic spine. Med Biol Eng Comput. 2004 Jan;42(1):55-60.

4.1.8 FIGURES AND TABLES

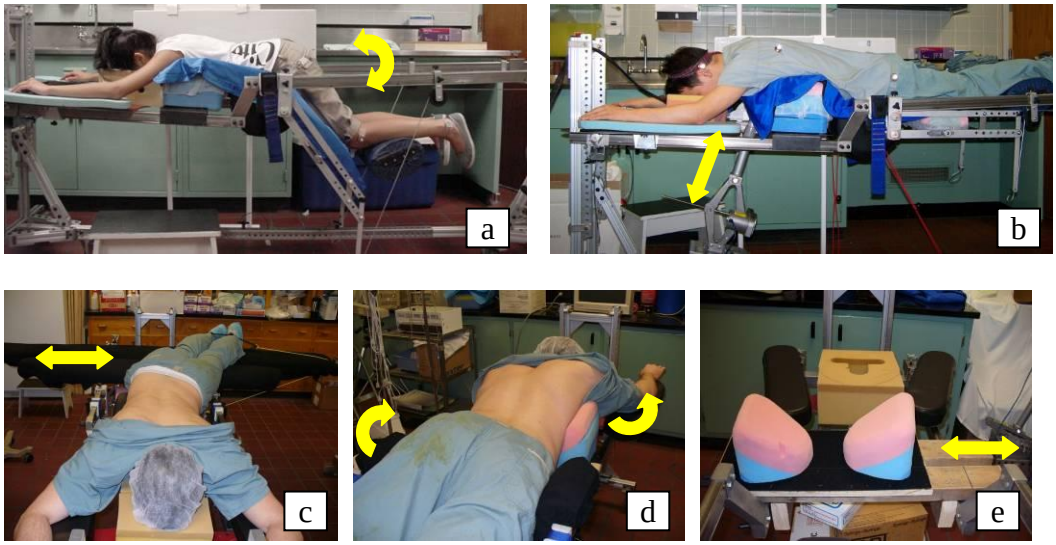

Figure 4.1 (A5F1): Multi-Functional Positioning Frame (MFPF) positioning features; a) lower limb positioned, b) thorax vertical displacer, c) lateral leg displacer, d) pelvic torsion device, and e) thorax lateral displacer.

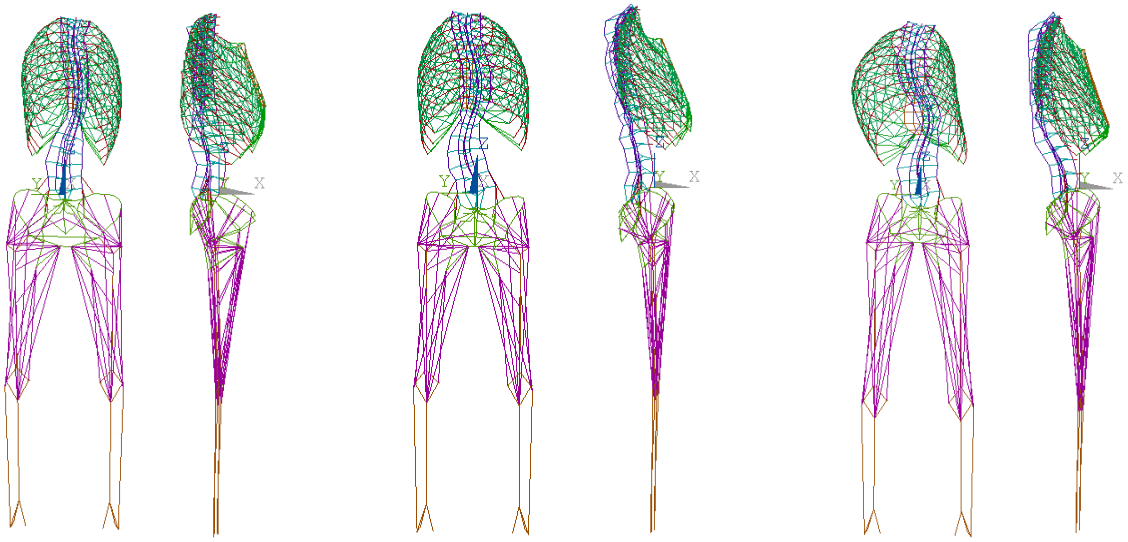

Figure 4.2 (A5F2): FEMs; from left to right: main thoracic, double major, and triple major cases.

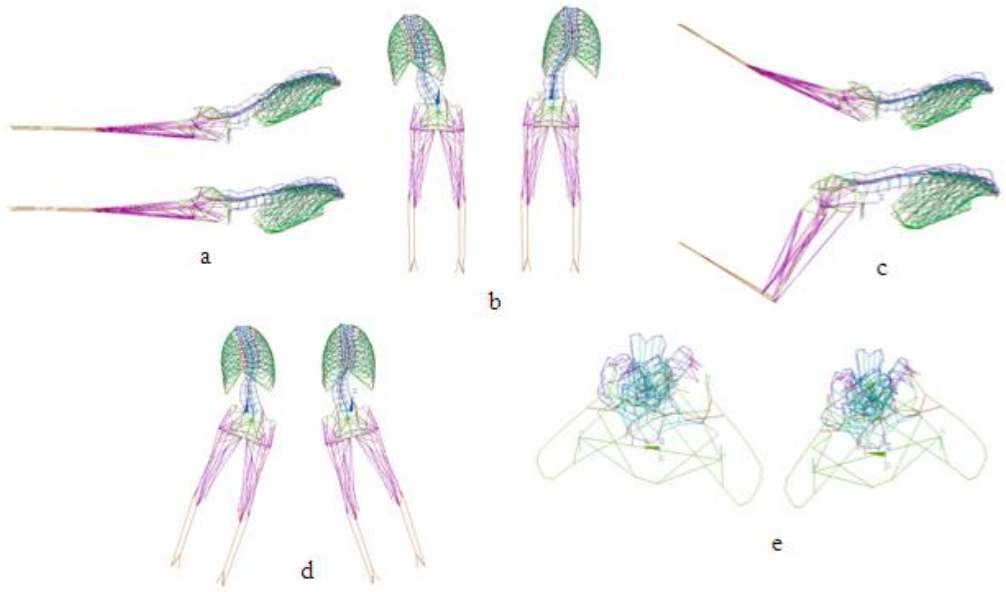

Figure 4.3 (A5F3): Limit phases of each positioning factor for the double major FEM; a) Thoracic Vertical Displacement (TVD),b) Thoracic Lateral Displacement (TLD), c) Hip Flexion Extension (HFE), d) Lateral Limb Displacement (LLD), and e) Pelvic Transverse plane Torsion (PTT). For visualization purposed only the pelvis and spine are shown for the PTT case.

Table 4.1 (A5T1): Spinal geometry following optimization of individual parameters on the MFPF (distances in mm; angles in degrees).

Spinal Geometrical Parameters		Desired Value	Case 1 (Single Thoracic)			Case 2 (Double Major)			Case 3 (Triple Major)		
			MFPF Prone	Optimal	1 MFPF Feature	MFPF Prone	Optimal	1 MFPF Feature	MFPF Prone	Optimal	1 MFPF Feature
Sagittal Curves	Lordosis	56	40	56	56	39	55	51	51	56	56
	Kyphosis	38	13	31	25	20	38	28	29	38	33
Cobb Angles	PT	Min	n/a	n/a	n/a	n/a	n/a	n/a	47	16	38
	MT	Min	38	20	27	34	17	25	46	23	32
	TL/L	Min	n/a	n/a	n/a	40	24	31	32	3	22
Balance	SB	Min	1	0	0	8	0	0	43	0	0
	CB	Min	23	0	0	22	0	0	10	0	0
Disc Space	T4-T8	Max	6	6	6	7	12	8	6	7	6
	T9-T12	Max	7	8	8	8	10	9	7	8	7
	L1-S1	Max	8	9	9	10	14	11	10	10	10
AVR	MT	Min	19	11	14	13	0	1	n/a	n/a	n/a

Table 4.2 (A5T2): MFPF configuration for optimization of individual spinal geometrical parameters along with significance of feature ability to manipulate spinal geometry (* for $p < 0.05$ and † for most influential MFPF feature) (TVD and TLD values in cm; HFE, LLD, and PTT values in degrees).

Spinal Geometrical Parameters		Case 1 (Single Thoracic)					Case 2 (Double Major)					Case 3 (Triple Major)				
		TVD	TLD	HFE	LLD	PTT	TVD	TLD	HFE	LLD	PTT	TVD	TLD	HFE	LLD	PTT
Sagittal Curves	Lordosis	9*	-9	-17†	-15	0*	10*	-10*	-20†	-20*	-29*	0*	0*	-1†	-16*	0*
	Kyphosis	10†	-10*	50	-1	-30*	10†	-10*	50*	-2	-30*	3†	-4	47*	-16*	0*
Cobb Angles	PT	n/a	n/a	n/a	n/a	n/a	n/a	n/a	n/a	n/a	n/a	10*	-10†	-20	-20*	15
	MT	10	-10*	-20*	20†	-30*	10	10†	-20	20*	-26	10*	-10*	-20	20†	-30*
	TL/L	n/a	n/a	n/a	n/a	n/a	10*	10*	-20	-20†	30*	0	10*	-20	-20†	30*
Un-balance	SB	4†	10	50	-20	8*	1†	-4	31	16	16*	0†	-10	50	-20*	-23*
	CB	1	2†	-17	-16	1*	6	0†	-15	16*	0	9	0†	50	16	0*
Disc Space	T4T8	1*	-10†	50	0	-15	5*	10†	31	-20	30	0	-9†	50	20*	-30*
	T9T12	0†	10*	50*	-20	-5	0*	10†	50*	-20	-30	0†	-10	40*	1	-22
	L1S1	7	10†	1*	20*	0	10*	-10†	-20	0	-30	0	8†	33	-10	-30
AVR	MT	8	10*	-20	20*	-30†	7	10*	-20	20	-30†	n/a	n/a	n/a	n/a	n/a
	TL/L	n/a	n/a	n/a	n/a	n/a	6	-10*	-20	-20*	30†	n/a	n/a	n/a	n/a	n/a

Table 4.3 (A5T3): Spinal geometry a) and combined surgical positions b) in the globally optimized position using two different cost functions (Φ1 and Φ2) over three example cases (W = geometrical parameter weighting; GD = geometrical parameter desired value; GI = geometrical parameter initial value).

a)

Spinal Geometrical Parameters		GI	Example Case 1 pedicle screw insertion in the lower thoracic region				Example Case 2 rod insertion and rotation				Example Case 3 set-screw tightening and fusion			
			W	GD	Optimization		W	GD	Optimization		W	GD	Optimization	
					Φ_1	Φ_2			Φ_1	Φ_2			Φ_1	Φ_2
Sagittal Curves	Lordosis	46	3	0	31	32	3	56.1	41	46	4	56.1	35	48
	Kyphosis	23	5	49	27	30	3	37.5	25	21	4	37.5	26	21
Cobb Angles	MT	40	4	0	28	29	5	0	29	23	5	0	43	39
	TL/L	46	2	0	29	27	5	0	29	27	4	0	34	32
Balance	SB	12	0	0	-97	-92	2	0	-123	-143	4	0	0	-32
	CB	22	0	0	115	91	2	0	83	126	5	0	0	0
Disc Space	T4-T8	6	2	8	8	8	2	6	7	8	0	6	8	5
	T9-T12	7	5	9	7	9	2	7	7	7	0	7	8	8
	L1-S1	10	2	13	9	8	2	10	9	10	0	10	7	8
AVR	MT	13	5	0	0	0	5	0	0	0	4	0	2	0
	TL/L	-5	2	0	0	8	5	0	0	0	4	0	0	3

b)

Positioning features	Example Case 1		Example Case 2		Example Case 3	
	Φ_1	Φ_2	Φ_1	Φ_2	Φ_1	Φ_2
TVD	10	10	10.0	10	1.0	0.0
TLD	8	7	5.3	10	-4.2	-3.0
HFE	50	50	4.9	-13.4	30.3	-19.0
LLD	-16.5	-19.9	-16.1	-13.3	-20.0	-20.0
PTT	2.6	-27.9	1.0	3.3	-5.4	-16.0

CHAPTER 5 DESIGN AND STUDY OF COMPLEMENTARY FEATURES OF PATIENT POSITIONING

5.1 Design details of the Lateral Leg Positioner, Pelvic Torsion Device, and Lateral Thoracic Displacer accessories

The design details of the Lateral Leg Positioner (LLP), Pelvic Torsion Device (PTD), and Lateral Thoracic Displacer (LTD) accessories for the MFPF will be presented. They have been fabricated as proof of concepts using inexpensive materials. Suggestions to improve the designs for future use will also be given in the discussion section of chapter 6.

The LLP (figure 5.1) is composed of two distinct parts; a proximal one which supports the thigh and a distal one which supports the tibia. They have been designed to fit over the existing MFPF frame and do not interfere with any of its components. The base support has lateral stoppers designed to fit within the MFPF rails. The longitudinal positions of the two LLP components is adjustable as well as their relative positions to each others. This adjustment is important to deal with patients of different statures; base supports should be placed below the middle portion of the femur and tibia. The base support top surfaces and proximal sides (not shown for clarity) are covered with a 1.5” thick layer of memory foam. This thickness resulted in adequate comfort levels during experimental testing. The most important sizing feature was the width of the components in order to ensure proper support once the lower limbs have been laterally displaced. The proximal component is 60” wide and the distal component is 96” wide. This allows up to 60° lateral rotation of the legs with a fair margin of safety which is independent of leg length. The length of the components is 10” to allow for sufficient contact area in order to limit interface pressures. Lateral leg displacement is achieved by placing the patient’s ankles in the ankle loop and pulling on the chord which is passed through a loop fixed to either end of the distal component. The legs can then be fixed in place by tying the chord to the surgical frame rail.

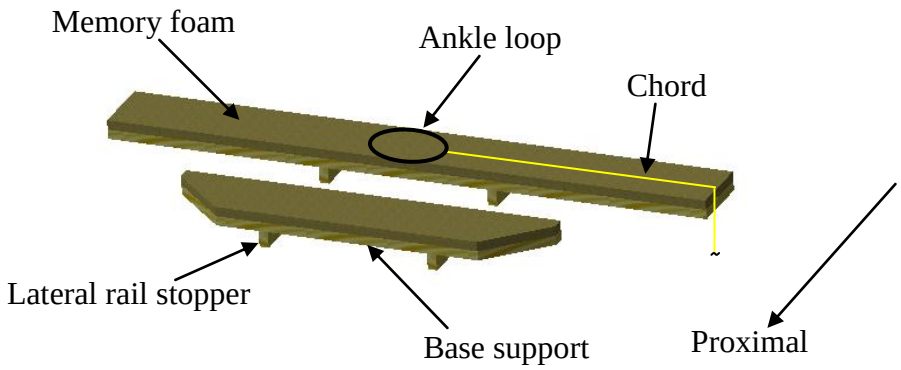

Figure 5.1: LLP CAD Representation

The PTD (figure 5.2) is composed of a single part designed to replace the existing MFPF pelvic cushion which must be removed. It is reversible so that either the left or right sides of the pelvis may be raised. Width is such that it fits within the MFPF rails and its longitudinal position is adjustable. Angle of the base support is fixed at 30° which was selected based on volunteer testing of maximum pelvic rotation. It is believed that above 30° the portion of the pelvis which is lowered would not be in contact with the base support. A length of 7" and memory foam thickness of 1.5" insure comfort and low interface pressures. Foam on the vertical section connecting the lower portion of the base support is necessary since there is a tendency for some lateral sliding of the pelvis down the incline.

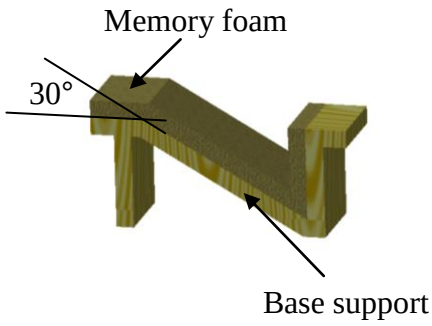

Figure 5.2: PTD CAD Representation

The LTD (figure 5.3) is composed of two distinct parts; a base support and a lateral slider. The base support is designed to fit within the MFPF rails and its longitudinal position is adjustable. It contains a slot which allows movement of the lateral slider. The lateral slider is covered with a sheet of Velcro for attachment of the MFPF thoracic cushions. It can be displaced

5.5” to the left or right and friction forces are sufficient to hold it in place. The vertical position of the lateral slider can be incrementally increased 2” or 4” by the insertion of specially designed spacers between it and the base support.

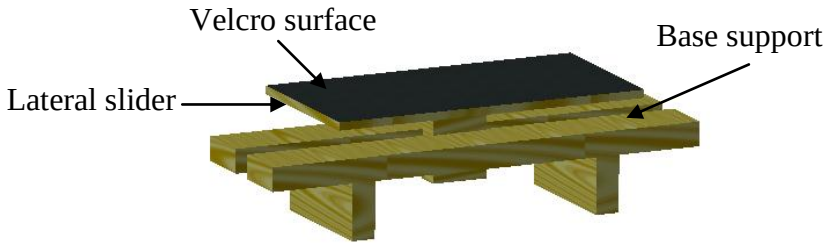

Figure 5.3: LTD CAD Representation

5.2 Experimental results for combined positioning

Some experimental testing was performed following the optimization study with the FEM. These preliminary tests, involving multiple surgical positioning parameters, were the first step of experimental validation of the optimization methodology developed for the MFPF. The results of these preliminary tests are presented here as they have not been covered elsewhere.

A surgical position which is close to the lateral bending position and possible on the MFPF is one in which the lower limbs and thorax are laterally displaced in the same direction. This position was tested on a scoliotic patient as shown in figure 5.4.

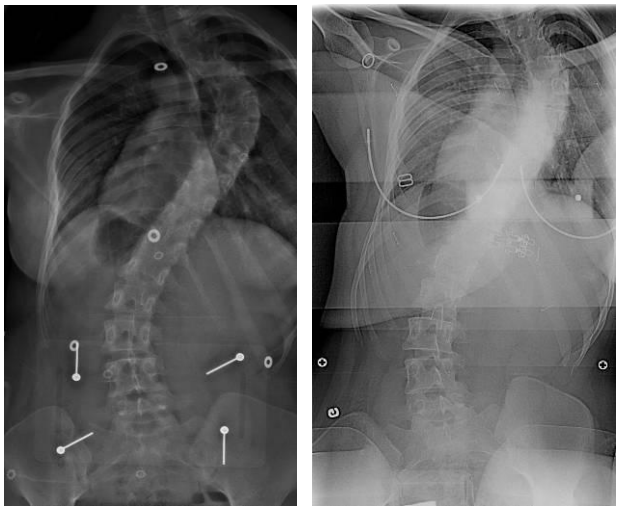

Figure 5.4: Scoliotic patient in the standing position (left) and combined lateral displaced torso and lower limb position (right)

In this position, their standing MT deformation of 65° Cobb and 33° AVR was reduced to 52° Cobb and 24° AVR. A surprising result of the optimization study was that the thoracic lateral displacer is more effective when the thorax is displaced towards the MT concavity. As such the simulated lateral bending position is not as effective. An ideal would be to laterally displace the thorax towards the MT concavity while at the same time rotating it in the same directions as the lower limbs to achieve both the lateral bending and lateral displaced positions.

A scoliotic patient was placed in two different optimized positions which would be useful intra-operatively; the first, maximum lumbar disc space which would facilitate pedicle screw insertion and the second, maximum sagittal balance and standing sagittal curves which would be good for final instrumentation and fusion. The lateral radiographs of each position are presented in figure 5.5.

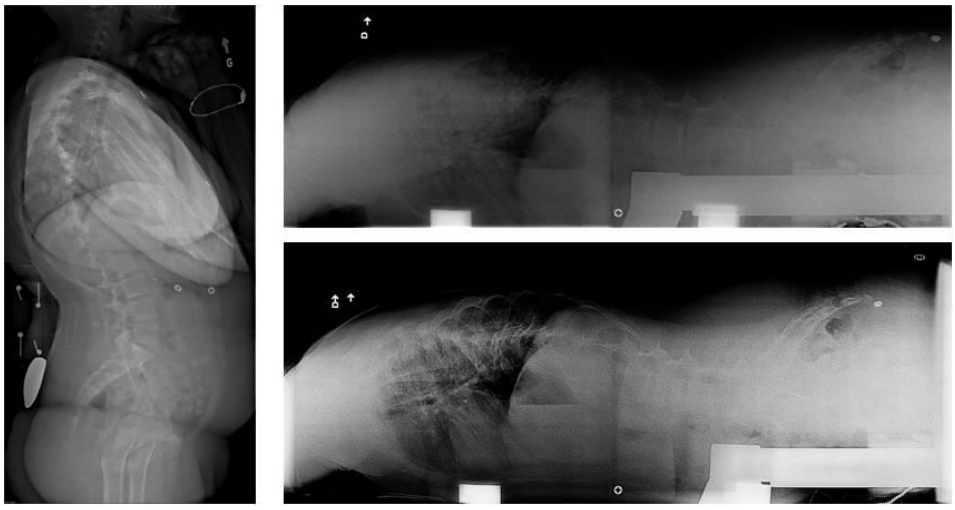

Figure 5.5: Lateral radiographs of scoliotic patient in the standing position (left), maximum disc space (top right) and maximum sagittal balance and standing sagittal curves (bottom right)

In this case, initial standing values were lordosis = 35°, kyphosis = 37°, sagittal unbalance = - 95 mm, average L1L5 space = 5 mm, and average L1L5 angles = 8°. For the maximum lumbar disc space position, lordosis was reduced to 22° with average L1L5 disc space increased to 7 mm and average L1L5 disc angles decreased to 2°. For the maximum sagittal balance and standing sagittal curves position (a compromise between the two), lordosis increased to 31°, kyphosis was increased to 41°, and sagittal unbalance reduced to -11 mm. This is a demonstration of the MFPF's ability to provide various spinal geometries intra-operatively depending on the phase of the operation. This is an advantage over frames in which the patient must remain stationary (e.g. Relton Hall) and thus compromises in positioning made.

CHAPTER 6 GENERAL DISCUSSION

Surgical frames such as the MFPF are evolving the conventional roles of surgical frames to include facilitation of surgical manoeuvres with potential improvement of post-operative results by allowing intra-operative manipulation of spinal geometry. The impact of patient positioning capabilities on spinal geometry could be done through extensive experimental testing, however, as demonstrated in this projects FEMs can be exploited in order to limit the amplitude of experimental testing required especially with regards to optimization of combined positions which would be virtually impossible without the FEM. In addition, FEMs such as the one utilized in this project can be used in order to test the impact of new operative positions prior to their construction thus saving time and money, as well as resulting in improved surgical frame performance.

A simplified global FEM type was selected for this study due to the fact that its primary objective was to study how patient positioning on a surgical frame impacts global spinal geometry. An FEM which had been previously utilised by Duke (2005) and Clin (2007) was chosen as a starting point because it allowed for personalized geometry reconstruction based on radiographs available at Sainte-Justine Hospital and it has shown good behaviour to force/displacement applications similar to those envisioned for the MFPF positioning simulations. Inclusion of the lower limbs and their associated muscles into the FEM yielded an extremely complete model well suited for the study of patient positioning on the MFPF. It contained all the necessary anatomy to accurately simulate the movement of the MFPF's positioning features and support cushions. In addition, the spine is represented in enough detail to allow for calculation of a wide range of spinal geometrical parameters. Besides the study of surgical positioning the FEM, especially with inclusion of the lower limbs, could be used for the study of the impact of other types of positioning on spinal geometry such as orthopaedic bed/chair design, distraction therapy, or even physical therapy (e.g. stretches).

The FEM developed has both patient-specific geometry and an estimate of patient-specific material properties. This specificity allows not just general patterns of surgical positioning to be

studied but also the unique behaviour of a given patient. As was shown throughout the project, in both the experimental testing and FEM simulations, different patients reacted differently to surgical positioning. Specificity becomes extremely important if positioning optimization is going to be performed for a given patient. Examples of this are the variability of optimized positions for different curve types in chapter 4 and the variability of sagittal curve changes due to hip flexion for different hamstring flexibilities in section 3.4. Thus far research in finite element modelling of humans has been much more successful in terms of geometrical accuracy than material property accuracy. Geometrical accuracies are in the mm range (Delorme 2003, Benameur 2003) while soft tissue material properties can only be approximated in a global fashion and can only be verified through behaviour reproduction (e.g. spinal reaction to outside loads) but not in absolute terms. The methods of material property personalization utilized in this study (e.g. hip flexion extension for lower limb muscles and prone positioning for intervertebral discs) yield good results (<5°) for specific movements but may be difficult to translate to other movements not utilized for the personalization.

Although the original intention was to validate the FEM using previous studies available in literature in addition to the experimental testing performed on the MFPF, it was determined that only experimental testing would be suitable due to the subject-specific nature of the FEM and the limited subject data available in published studies. Validation of the FEM was only presented in this thesis for prone positioning and lower limb positioning on the MFPF (sections 3.2 and 3.4 respectively). In fact, all the experimental testing presented in this study (sternum raising, lateral limb displacement and pelvic torsion) was utilized to validate the FEM. This was required in order to ensure the accuracy of the results presented in the final optimization study presented in chapter 4.

Although the FEM chosen and its subsequent inclusion of the lower limbs proved to be well suited for this project, it had the following limits. The intervertebral disc and ligament material properties were considered to be linear elastic while in reality they exhibit visco-elastic properties. This did not allow study of the impact of intervertebral disc and ligament stress relaxation and creep on simulation results. It is possible that leaving a patient in a MFPF position

such as sternum raised or legs laterally displaced will have a time dependant impact on spinal geometry resulting in progressive kyphosis increase or Cobb reduction. There is also the possibility that the rate of position displacement could have an impact of spinal geometrical changes, however, since sharp and sudden intra-operative movements should be avoided it may be a moot point. Muscles of the back were not represented. In most surgical positions, especially under anaesthesia, the back muscles are not in tension. However, during the lateral bending and the lateral leg displacement simulations it is possible that the back muscles would become under tension and impact the results in a passive manner. The back muscles could be included, in future studies, using their origins and insertions. The specific ones which become strained during positioning on the MFPF can then be identified and then attributed personalized initial strains based on flexibility testing such as was done with the lower limb muscles in section 3.4. The simplified global nature of the FEM developed allows for only some information on anatomical internal stress/strain to be calculated. A more detailed model could provide additional insight on the impacts of various patient positions such as intervertebral disc pressures or localized stress concentrations within the vertebrae. Of course, this added detail would increase computational time and may lead to non-convergence issues.

Hypothesis 1 was that the FEM would be able to simulate prone positioning with a coronal and sagittal plane Cobb angle accuracy of 5° for a segmental curve. With subject-specific geometry and baseline material properties the FEM was able to do this for lordosis, kyphosis and lumbar Cobb angles with respective average errors of 5°, 4° and 5° but unable to do it for thoracic Cobb angles with an average error of 14°. This was because the baseline intervertebral disc material properties, which were taken from literature for a healthy spine, did not account for the deformity stiffening effects. An intervertebral disc elastic modulus optimization procedure based on lateral bending tests managed to reduce the thoracic Cobb error to within 10°, however, this method is limited due to reproducibility issues with the lateral bending test. When the intervertebral disc elastic moduli were optimized based on the prone position radiographs, the 5° hypothesized value threshold was met for all curves. A way to improve the predictive value of the FEM is to use the average intervertebral disc elastic modulus distribution obtained in the optimization process as baseline values. Doing this would increase values within a thoracic scoliotic curve by a factor of about 2.5 (10.8 vs 4.2 MPa).

The prone positioning simulation process could be avoided if the patient's geometries could be reconstructed while on the MFPF. While this is possible using one radiograph as done by Novosad 2004, this would require additional radiograph acquisitions pre-operatively which were not possible in the current project due to ethical reasons. Further, while previous studies have demonstrated how scoliotic Cobb angles are reduced due to prone positioning on surgical frames such as the Relton-Hall or Jackson, this project required information about the specific impact of MFPF prone positioning on complete spinal geometry.

The study of prone positioning yielded some practical knowledge not just on the impact of MFPF prone positioning but on prone positioning in general as a result of the sensitivity study on patient and surgical frame influential factors. Specifically, the results showing decreases in sagittal curves influenced by the relative position between the thoracic and pelvic cushions clarified previously contradictory results stated in literature (Guanciale et al. 1996, Tan et al. 1994; Jackson et al. 2005 and Marsicano et al. 1998). The prone positioning study also highlighted the unsuitability in utilizing un-calibrated lateral bending radiographs as a means to personalize intervertebral disc mechanical properties which in this case resulted in FEM errors up to 10° which is twice the conventionally accepted value for clinical relevance.

There was a large inter-subject variability in additional decreases in all spinal segmental curves due to soft tissue relaxation; comparing the prone position radiographs on the MFPF and intra-operative radiographs on the RH frame. This raises some questions, particularly on how to predict a given patient's spine modification to anaesthesia and surgical opening. A compromise would be to determine an average soft tissue relaxation factor for intra-operative simulations and apply it as a baseline. For the 5 patients in the prone positioning study presented in section 3.2 (excluding the one who was operated on several months after the experimental testing) subsequent analysis showed an average 1.7 MPa (± 2.4) or 15% reduction in elastic modulus.

Study of the MFPF's two original features, the leg positioner and the sternum raiser, showed that it was efficient at manipulating sagittal curves but less efficient at manipulating coronal curves. Relative to hypothesis 2, the MFPF's leg positioner movement of 13° in extension and 48° in flexion modified lordosis an average of +12%, -44% and kyphosis an

average of +5%, -13%; which met targets for reduction but was below targets for increases. Study of enhanced lower limb positioning with the FEM, 30° in extension and 90° in flexion, lordosis could be modified an average of +18%, -76% and kyphosis an average of +10%, -28%. This far exceeds the targets for reductions but still falls below targets for increases. This shortcoming, although unfortunate considering the losses in sagittal curves that result from prone positioning and prevalence of hypo-kyphosis in scoliosis patients, can be directly addressed by use of the sternum vertical displacer. The sternum vertical displacer proved to be effective at increasing the sagittal curves with an average 53% increase in kyphosis and 24% increase in lordosis.

One result not discussed in previous chapters is the impact of knee flexion on the degree of sagittal curve modulation during lower limb positioning. As described in appendix A, having the knees straight as compared to flexed 90° resulted in an additional 14% loss of lordosis during 30° hip flexion simulations in simulations of an FEM of a healthy subject. This means that in order to get the greatest impact out of a surgical frame lower limb positioner, the patient's legs should be kept as straight as possible; positions such as the Andrew's 90°/90° one are less efficient. Of course there are other considerations such as ensuring patient stability on the frame but these could be addressed through retaining straps or at least a compromise between the two obtained.

The second part of hypothesis 2 was that lower limb positioning on the MFPF could be used to manipulate Cobb angles. Testing with the FEM showed that this was not the case (changes to be $< \pm 4°$ for PT, MT, and TL/L curves) and thus no experimental tests were performed. Instead, the FEM was used to study new lower limb positions that could be effective at manipulating Cobb angles and vertebral rotations. Lateral limb displacement and pelvic torsion prove to be suitable. Both simulation and experimental testing of these positions showed that the hypothesized value of 10° decrease could be achieved after some design modifications to the MFPF which were done by the introduction of "add-on" features; the LLD and PT. An additional new position which could manipulate Cobb angles and sagittal balance was also conceived during this process; lateral thoracic displacement with its own "add-on" feature the LTD.

Hip flexion/extension on the lower limb positioner, sternum raising on the sternum vertical displacer, lateral leg displacement on the lateral leg displacer (LLD) and pelvic torsion on the pelvic torsion device (PTD) have been shown to be respectively best suited for modifying lordosis, kyphosis, Cobb, and AVR as per their design intention. What was also shown is that changes in spinal geometries are coupled. Previous studies have shown the correlation between Cobb and AVR (Kuklo 2005), this current project demonstrated that on the MFPF changes to one sagittal curve result in corresponding changes in the other sagittal curve. Increasing kyphosis by 14° (53%) with the SVD led to a 10° (24%) increase in lordosis and reducing lordosis by 35° (52%) with hip flexion led to a 6° (14%) reduction in kyphosis. Compensatory action would have to be taken in order to modify one sagittal curve while maintaining the other (e.g. flexing the lower limbs when the sternum is raised to maintain lordosis). Also notes was that manipulating the lowest structural scoliotic curve with either the LLD or PTD has an impact on the other coronal plane curves.

The following proposed improvements can be made to the three prototype accessories developed for the MFPF based on their experimental evaluation.

An improved design for the LLD would be to have a narrower lower limb support which could swivel to either side and be locked in place. This way it would take up less room and could possibly be adapted to allow flexion/extension motion avoiding the need for an additional accessory. A proposed design improvement for the PTD would be to have a pelvic cushion with an adjustable tilt and strap around the buttocks to hold the pelvis in place. This would allow variable tilt positions, including the straight position, thus avoiding the swap out the baseline pelvic support cushions to achieve tilt. Felt cloth was used to cover the wood and foam on the LLD and PTD, this would have to be changed to a material better suited to cleaning and sterilization. PA radiographs taken with patients on the PTD and LTD have shown them to be sufficiently radio-transparent but a material with an improved strength to weight ration such as aluminum would lighten the accessories and possibly improve radiographic transparency. If the width of the surgical frame is adjustable, as with the adult MFPF prototype (not discussed in this current project – Canet 2008), the accessories described or future design iterations would have to

allow for this adjustment. The LTD design can be improved by allowing for continual adjustment in heights (as opposed to 2” increments).

The idea behind the LLD came from observing the Cobb angle reductions obtained from the lateral bending radiographs. The lateral leg displacer was able to reproduce the distal portion of the lateral bending position (hip rotation) but was unable to reproduce the proximal one (torso curvature). This is believed to be the reason for which the LLD was more efficient reducing Cobb angles in the lumbar region. An improved design would be one which combines hip rotation and torso curvature such as depicted in figure 6.1. This could be accomplished by inclusion of a hinge on the surgical frame rails at the pelvic level allowing bending of the surgical frame (similar to the Jackson axis only in the coronal plane instead of the sagittal one). This was not possible using the current MFPF frame design and would also required freedom of pivot motion between the support cushions and MFPF rails. This position could be used to facilitate certain stages of a spinal instrumentation procedure such as rod insertion

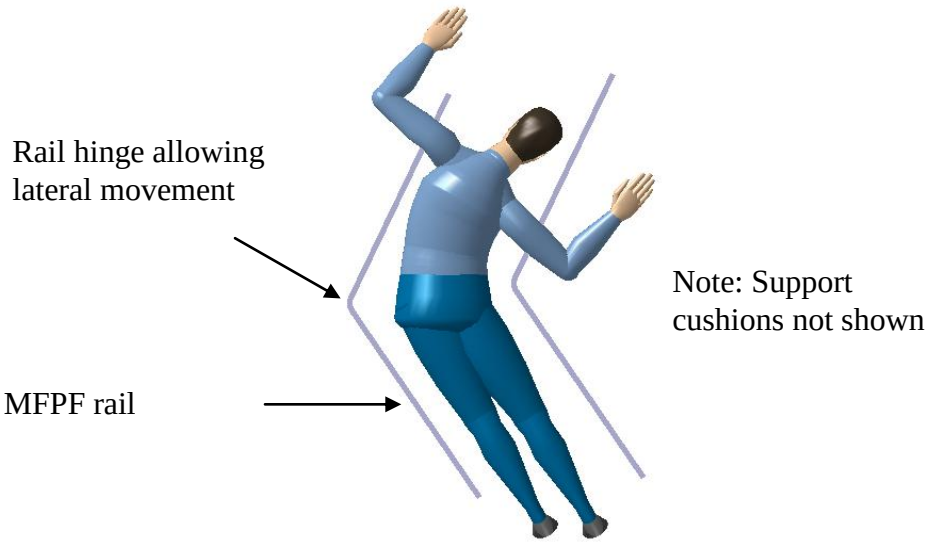

Figure 6.1: Top view of patient in prone position on MFPF in the lateral bending position

All the knowledge and tools gained in the previous steps were used for the study of patient position optimization on the MFPF. One of the main advantages that the MFPF has over previous surgical frames such as the Jackson, Andrews, or Wilson is its multiple positioning features which can be used simultaneously. Using a single positioning feature is much easier to relate to

subsequent changes in spinal geometry than combining them. However, as was shown in chapter 4, much more benefit can be obtained by the combined use of multiple features (average 22% percent closer to desired values for 11 spinal geometrical parameters). The difficulty lies in determining the optimal combination of features which is not evident and requires use of the optimization process developed.

Hypothesis 3 was based on the performance of global optimization on the MFPF. Average results (across the three different curve types studied) showed average manipulation of lordosis by +32%, -56% and kyphosis by +55%, -52%. The hypothesis was verified for increasing lordosis and reducing kyphosis while loss of lordosis and increase in kyphosis where close to the hypothesized values. Minimization of Cobb angles showed average results of 19%, 29% and 27% respective decrease in PT, MT, and TL/L curves. This was better than the hypothesized values for MT and TL/L curves but below for the PT case. The PT Cobb can be subsequently manipulated by the inclusion of a head positioned which has been proposed but not tested due to possible concerns about intra-operative strain on the neck muscles.

An effort must be made to clarify the distinction between desirable post-operative spinal geometry following instrumentation procedures and desirable intra-operative spinal geometry. One of the major advantages of a surgical frame such as the MFPF is that it allows for patient position to be adjusted during the surgery with relative ease. That means that depending on the given stage of surgery the patient can be placed in a certain manner which offers an advantageous spinal geometry. This advantageous geometry does not have to coincide with what is desired post-op because the patient's position can then be changed for the next stage of surgery. In fact patient positioning, and the spinal geometry it can offer, should be thought of as a tool to facilitate surgical interventions.

The global optimization process presented in chapter 4 assumes that it is possible to combine the proposed positions of the LLP, PTD, and lower limb positioner as discussed in the article. The following provides more details on a universal feature design which allows all three positions to be combined.

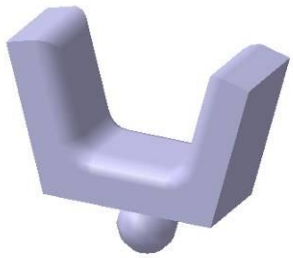

Figure 6.2: Universal Feature Allowing Combined Lower Limb Positions

The universal lower limb positioning feature (figure 6.2) can rotate in all directions due to the universal joint at its base. With the pelvis secured in place it can provide both incremental pelvic tilt (impact of lateral leg displacement) and pelvic torsion while still allowing the lower limbs to be flexed and extended if the current MFPF lower limb positioner can be secured to the universal feature (rotating and tilting with it).

CHAPTER 7 CONCLUSIONS AND RECOMMENDATIONS

Patient positioning on the MFPF has proven to be effective at manipulating a wide range of spinal geometrical parameters. This manipulation can be used to facilitate instrumentation procedures such as for scoliosis by providing improved intra-operative spinal geometries and potentially yield improved global corrections.

Lower limbs including muscles were added to an existing FEM of the spine, thoracic cage and pelvis which yielded it suitable for the study of patient positioning on the MFPF.

Experimental testing was performed on the original MFPF which yielded several results. Prone positioning on the MFPF has an important impact on both the sagittal and coronal curves of the vertebral column which are all reduced relative to the standing position. Lower limb positioning on the MFPF has an important impact on both lordosis and kyphosis; both sagittal curves can be increased with hip flexion and reduced with hip flexion. Sternum vertical displacement on the MFPF can significantly increase kyphosis, lordosis, and apical thoracic segment intervertebral disc space.

The FEM was validated based on experimental testing on the MFPF. It was able to reproduce experimental prone positioning (hypothesis 1) and hip flexion/extension within 5° through the utilization of both patient-specific geometry and material properties.

The validated FEM was exploited to further study some of the MFPF's original positioning capabilities. Simulations demonstrated that prone positioning spinal geometrical change are dependent on standing sagittal and coronal segmental curves and the relative vertical position of thoracic and pelvic support cushions. Simulations demonstrated that the relationship between hip flexion/extension and sagittal curve changes is linear and that additional modulation

capabilities can be achieved by increasing the range of motion of the MFPF's leg positioner. The changes in sagittal curves due to hip flexion/extension were very close to or surpassed hypothesized values however they were not able to manipulate Cobb angles.

The FEM was exploited to develop three new surgical positions for the MFPF: lateral leg displacement, pelvic torsion, and lateral thoracic displacement. Prototype MFPF features were fabricated to allow for these positions and they were experimentally tested. Experimental lateral leg displacement on the MFPF results in a significant reduction of Cobb angle and AVR in the lowest structural curve by lateral bending of the lower limbs towards the scoliotic spine convexity. Experimental pelvic torsion on the MFPF results in a significant reduction in Cobb angles and important reductions in AVR by raising the pelvis on the concave side of their lowest structural curve and opposite thoracic cushion.

The FEM was exploited to develop a method for the optimization of individual spinal geometrical parameters and global spinal geometry based on the combined use of all the MFPF's positioning features. This optimization is based on surgeon-specific input and can be used for the different stages of an instrumentation procedure. The combined use of multiple surgical positioning features on the MFPF offered a wider range of spinal geometries than their individual use. The efficiency of combined positioning on manipulating sagittal and coronal curves were very close to or surpassed hypothesized values.

FEMs should be incorporated into the design process of surgical frames. The FEM presented in this project permit to study the impact of a wide range of surgical positions and it would seem much more logical to first study these positions with the FEM, select the desirable ones, and then use them as the basis for surgical frame design. The lateral leg positioner and pelvic torsion device presented in section 5.1, as well as the lateral thoracic positioner presented in section 5.1 were developed using this method however they are only surgical frame accessories.

Better knowledge should be acquired on what spinal geometries would be desirable to surgeons throughout the different stages of a spinal instrumentation procedure. Questionnaires, such as the one in appendix b (asking surgeons what spinal geometries they would prefer during different stages of an operation), could be sent to surgeons which would not only emphasize the importance of varied intra-operative spinal geometry but also get input on their preferences. This would allow general recommendations for intra-operative positioning on the MFPF to be made.

If the MFPF or subsequent iteration is brought to market, it is recommended that a resource be provided along with it which indicates what impact its various positioning parameters will have on spinal geometry along with recommendations on how to use it. This resource could be in the form of a manual which contains graphs on how a given spinal geometrical parameter will respond to a given positioning such as the graph provided in section 3.4 relating lordosis to hip flexion/extension. Of course due to inter-subject variability some input from the patient would be required such as a spinal flexibility rating scale. The ultimate would be to have an integrated unit to the MFPF positioning controls which based on some input from the surgeon (e.g. curve type, apex, etc.) would have simple one touch controls which would automatically reconfigure the patient's position to offer a variety of pre-determined spinal geometries such as minimum Cobb, maximum disc space in a given region, maximum kyphosis, etc.

The next step in development of the FEM presented in this project would be inclusion of soft tissue such as skin, muscle, and adipose tissue along with volumetric representation of surgical frame cushions. This would allow for more realistic boundary condition representation as well as calculation of interface pressures which could be used to optimize cushion design. A volumetric FEM for the study of patient positioning was developed during the course of this project (figure 7.1). The model was able to reproduce experimentally obtained average interface pressures fairly accurately, however, due to simulation convergence issues and the project objectives it was not pursued further. The details on how this model was developed are presented in appendix c.

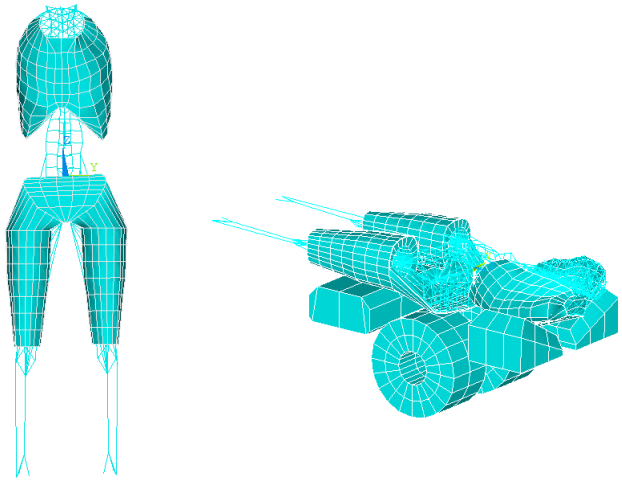

Figure 7.1: Volumetric FEM for the Study of Patient Positioning on the MFPF

FEM simulations of surgical positioning should be included in spinal surgical simulators. Firstly, the spinal geometry used in the simulators is based upon standing radiographs and thus does not represent the intra-op reality; at the very least the impact of prone positioning should also be included. Secondly, the simulators could be used in order to validate the usefulness of MFPF positioning. Surgeries could be simulated twice, once with a constant spinal geometry and once with the varied spinal geometries which are possible on the MFPF. A comparison could then be made on forces applied during the surgery as well as post-operative results.

The final recommendation would be that the design of any future iteration of the MFPF would consider the inclusion of a simplified traction feature such as those available on commercially available decompression therapy machines (design would have to be adapted to accommodate for spinal procedures). Traction is still one of the most efficient manners in which to increase spine length. While not as invasive as halo traction methods, this simplified traction would allow increase in intervertebral disc heights and reduction of various spinal deformities along with the potential to be used in conjunction with other positions.

REFERENCES

Asher MA, Lai SM, Burton DC. Analysis of instrumentation/fusion survivorship without reoperation after primary posterior multiple anchor instrumentation and arthrodesis for idiopathic scoliosis. Spine J. 2010 Jan;10(1):5-15.

Aubin CE, Labelle H, Chevrefils C, Desroches G, Clin J, Eng AB. Preoperative planning simulator for spinal deformity surgeries. Spine (Phila Pa 1976). 2008 Sep 15;33(20):2143-52.

Benameur S, Mignotte M, Parent S, Labelle H, Skalli W, de Guise J: A hierarchical statistical modeling approach for the unsupervised 3D reconstruction of the scoliotic spine. *ICIP* (1) 2003: 561-564

Behairy YM, Hauser DL, Hill D, Mahood J, Moreau M. Partial correction of Cobb angle prior to posterior spinal instrumentation. *Ann Saudi Med*. 2000 Sep-Nov;20(5-6):398-401.

Benfanti PL, Geissele AE. The effect of intraoperative hip position on maintenance of lumbar lordosis: a radiographic study of anesthetized patients and unanesthetized volunteers on the Wilson frame. Spine. 1997 Oct 1; 22(19):2299-303.

Blount WP, Schmidt AC, Keever ED, Leonard ET. The Milwaukee brace in the operative treatment of scoliosis. J Bone Joint Surg Am. 1958 Jun;40-A(3):511-25.

Böhler L (1972) [Conservative treatment of fractures of the thoracic and lumbar spine]. Z Unfallmed Berufskr 65(2):100-4.

Canet. Masters thesis. Conception et Évaluation d'un Système de Positionnement Dynamique pour les Chirurgies du Rachis. École Polytechnique 2008.

Chaffin, D. B., Redfern, M. S., Erig, M., Goldstein, S. A. (1990/02). Lumbar muscle size and locations from CT scans of 96 women of age 40 to 63 years. Clinical Biomechanics 5(1): 9-16.

Cheh G, Lenke LG, Lehman RA Jr, Kim YJ, Nunley R, Bridwell KH. The reliability of preoperative supine radiographs to predict the amount of curve flexibility in adolescent idiopathic scoliosis. Spine. 2007 Nov 15;32(24):2668-72.

Cheriet F, Laporte C, Kadoury S, Labelle H, Dansereau J. A novel system for the 3-D reconstruction of the human spine and rib cage from biplanar x-ray images. IEEE Trans. Biomed. Eng. 2007; 54:1356-8.

Cho KJ, Rah UW. Study of the lumbar curvature with various factors of pelvic inclination. Change of radiographic lumbar curvature according to hip joint flexion. Yonsei Med J. 1995 May;36(2):153-60.

Clin J, Aubin CE, Labelle H. Virtual prototyping of a brace design for the correction of scoliotic deformities. Med Biol Eng Comput. 2007 May;45(5):467-73.

Cotrel Y, Dubousset J (1984) Nouvelle technique d'osteó-synthése rachdienne segmentaire par voie postérieure. Rev Chir Orthop 70:489–494

Delisle A, Gagnon M, Sicard C. Effect of pelvic tilt on lumbar spine geometry. IEEE Trans Rehabil Eng. 1997 Dec;5(4):360-6.

Delorme S, Labelle H, Poitras B, Rivard CH, Coillard C, Dansereau J. Pre-, Intra-, and Postoperative Three-Dimensional Evaluation of Adolescent Idiopathic Scoliosis. Journal of Spinal Disorders. 2000 13(2):93-101.

Delorme S, Petit Y, de Guise JA, Labelle H, Aubin CE, Dansereau J. Assessment of the 3-d reconstruction and high-resolution geometrical modeling of the human skeletal trunk from 2-D radiographic images. IEEE Trans Biomed Eng. 2003 Aug;50(8):989-98.

Driscoll C, Aubin CE, Labelle H, Dansereau J. The relationship between hip flexion/extension and the sagittal curves of the spine. Stud Health Technol Inform. 2008;140:90-5.

Driscoll CR, Aubin CE, Canet F, Labelle H, Dansereau J. The Impact of Intra-Operative Sternum Vertical Displacement on the Sagittal Curves of the Spine. Eur Spine J. 2010 Mar;19(3):421-6.

Driscoll C, Aubin CE, Labelle H, Horton W, Dansereau J. Biomechanical Study of Patient Positioning: Influence of Lower Limb Positioning on Spinal Geometry. J Spinal Disord Tech. (Accepted December 2010).

Driscoll C, Aubin CE, Labelle H, Dansereau J. Assessment of Two Novel Surgical Positions for the Reduction of Scoliotic Deformities: Lateral Leg Displacement and Hip Torsion. Eur Spine J. (Submitted June 2010).

Driscoll CR, Aubin CE, Canet F, Labelle H, Dansereau J. Biomechanical Study of the Impact of Prone Surgical Positioning on the Scoliotic Spine. J Spinal Disord Tech. (submitted November 2010).

Duke K, Aubin CE, Dansereau J, Labelle H. Biomechanical simulations of scoliotic spine correction due to prone position and anaesthesia prior to surgical instrumentation. Clin Biomech (Bristol, Avon). 2005 Nov;20(9):923-31.

Duke K, Aubin CE, Dansereau J, Koller A, Labelle H. Dynamic positioning of scoliotic patients during spine instrumentation surgery. J Spinal Disord Tech. 2009 May;22(3):190-6.

Duke K, Aubin CE, Dansereau J, Labelle H. Computer simulation for the optimization of patient positioning in spinal deformity instrumentation surgery. Med Biol Eng Comput. 2008 Jan;46(1):33-41.

Duke. PhD thesis. The design and biomechanical analysis of a dynamic positioning frame for scoliosis surgery. École Polytechnique 2006.

Edmondston SJ, Allison GT, Althorpe BM, McConnell DR, Samuel KK. Comparison of ribcage and posteroanterior thoracic spine stiffness: an investigation of the normal response. Man Ther. 1999 Aug;4(3):157-62.

Edwards CC, Levine AM. Complications associated with posterior instrumentation in the treatment of thoracic and lumbar injuries. In: Garfin SR, ed. Complications of Spine Surgery. Baltimore: Williams and Wilkins, 1989:164-99.

Gardner-Morse MG, Laible JP, Stokes IA. Incorporation of spinal lexibility measurements into finite element analysis.J Biomech Eng. 1990 Nov;112(4):481-3.

Gharbi H. Étude biomécanique de la spondylolyse et du spondylolisthésis chez l'enfant : étude de cas. Master's thesis. École polytechnique de Montréal. Institut de génie biomédical. 2008.

Glassman SD, Bridwell K, Dimar JR, Horton W, Berven S, Schwab F. The impact of positive sagittal balance in adult spinal deformity. Spine. 2005 Sep 15;30(18):2024-9.

Goel, K., Weinstein J., *Biomechanics of the Spine: Clinical and Surgical Perspective,* CRC Press, Inc, Boca Raton, Florida, 1990.

Gray, Henry. Anatomy of the Human Body. Philadelphia: Lea & Febiger, 1918; Bartleby.com, 2000.

Gréalou L, Aubin CE, Labelle H. Rib cage surgery for the treatment of scoliosis: a biomechanical study of correction mechanisms. J Orthop Res. 2002 Sep;20(5):1121-8.

Guanciale AF, Dinsay JM, Watkins RG. Lumbar lordosis in spinal fusion. A comparison of intraoperative results of patient positioning on two different operative table frame types. Spine. 1996 Apr 15;21(8):964-9.

Harrison DE, Cailliet R, Harrison DD, Janik TJ, Troyanovich SJ, Coleman RR. Lumbar coupling during lateral translations of the thoracic cage relative to a fixed pelvis. Clin Biomech (Bristol, Avon). 1999 Dec;14(10):704-9.

Harrison DE, Cailliet R, Harrison DD, Janik TJ. How do anterior/posterior translations of the thoracic cage affect the sagittal lumbar spine, pelvic tilt, and thoracic kyphosis? Eur Spine J. 2002 Jun;11(3):287-93.

Heart RF Albert TJ. Spinal deformities the essentials. Thieme New York; 2007.

Hirabayashi Y, Igarashi T, Suzuki H, Fukuda H, Saitoh K, Seo N. Mechanical effects of leg position on vertebral structures examined by magnetic resonance imaging. Reg Anesth Pain Med. 2002 Jul-Aug;27(4):429-32

Ho EK, Upadhyay SS, Chan FL, Hsu LC, Leong JC. New methods of measuring vertebral rotation from computed tomographic scans. An intraobserver and interobserver study on girls with scoliosis. Spine (Phila Pa 1976). 1993 Jul;18(9):1173-7

Horsman K, Koopman HF, van der Helm FC, Prosé LP, Veeger HE. Morphological muscle and joint parameters for musculoskeletal modelling of the lower extremity. *Clin Biomech (Bristol, Avon).* 2007 Feb;22(2):239-47. Epub 2006 Nov 28.

Hosman AJ, de Kleuver M, Anderson PG, van Limbeek J, Langeloo DD, Veth RP, Slot GH. Scheuermann kyphosis: the importance of tight hamstrings in the surgical correction. *Spine*. 2003 Oct 1;28(19):2252-9

Hukins DWL, Meakin JR. Relationship Between Structure and Mechanical Function of the Tissues of the Intervertebral Joint. American Zoologist. 2000 40(1):42-52.

Jackson R, Behee K, McManus A. Sagittal spinopelvic alignments standing and in an intraoperative prone position. *Spine J*. 2005 Sept; 4(5) : S5.

Jhaveri SN, Zeller R, Miller S, Lewis SJ. The effect of intra-operative skeletal (skull femoral) traction on apical vertebral rotation. Eur Spine J. 2009 Mar;18(3):352-6.

de Jonge T, Dubousset JF, Illés T (2002) Sagittal plane correction in idiopathic scoliosis. Spine 27(7):754-60

Kadoury S, Cheriet F, Laporte C, Labelle H. A versatile 3D reconstruction system of the spine and pelvis for clinical assessment of spinal deformities. Med. Biol. Eng. Comput. 2007; 45:591-602.

Klepps SJ, Lenke LG, Bridwell KH, Bassett GS, Whorton J. Prospective comparison of flexibility radiographs in adolescent idiopathic scoliosis. *Spine.* 2001 Mar 1;26(5):E74-9.

Knight RQ, Jackson RP, Killian JT, Stanley EA. White paper on sagittal plane alignment. Scoliosis Research Society.

Kovanen V, Suominen H, Heikkinen E. Collagen of slow twitch and fast twitch muscle fibres in different types of rat skeletal muscle. *Eur J Appl Physiol Occup Physiol.* 1984;52(2):235-42.

Kuklo TR, Potter BK, Lenke LG. Vertebral rotation and thoracic torsion in adolescent idiopathic scoliosis: what is the best radiographic correlate? J Spinal Disord Tech. 2005 Apr;18(2):139-47.

Kumar MN, Baklanov A, Chopin D. Correlation between sagittal plane changes and adjacent segment degeneration following lumbar spine fusion. Eur Spine J. 2001 Aug;10(4):314-9.

Lafage V, Dubousset J, Lavaste F, Skalli W. 3D finite element simulation of Cotrel-Dubousset correction. Comput Aided Surg. 2004;9(1-2):17-25.

Lamarre ME, Parent S, Labelle H, Aubin CE, Joncas J, Cabral A, Petit Y. Assessment of spinal flexibility in adolescent idiopathic scoliosis: suspension versus side-bending radiography. Spine (Phila Pa 1976). 2009 Mar 15;34(6):591-7.

Lee SM, Suk SI, Chung ER. Direct vertebral rotation: A new technique of three-dimensional deformity correction with segmental pedicle screw fixation in adolescent idiopathic scoliosis. Spine (Phila Pa 1976) 2004;29:343-9.

Legaye J, Duval-Beaupere G, Hecquet J, et al. Pelvic incidence: a fundamental pelvic parameter for three-dimensional regulation of spinal sagittal curves. *Eur Spine J* 1998; 7: 99–103.

Lenke LG, Betz RR, Harms J, Bridwell KH, Clements DH, Lowe TG, Blanke K. Adolescent idiopathic scoliosis: a new classification to determine extent of spinal arthrodesis. J Bone Joint Surg Am. 2001 Aug;83-A(8):1169-81.

Li M, Zhao YC, Zhu XD, He SS, Wang CF, Yang CW. [Analysis of posterior pedicle screw-only constructs in surgical treatment of adolescent idiopathic scoliosis with a minimum three-year follow-up]. Zhonghua Wai Ke Za Zhi. 2010 Mar 15;48(6):410-4.

Lin H, Aubin CE, Parent S, Villemure I. Mechanobiological bone growth: comparative analysis of two biomechanical modeling approaches. Med Biol Eng Comput. 2009 Apr;47(4):357-66.

Lord MJ, Small JM, Dinsay JM, Watkins RG. Lumbar lordosis. Effects of sitting and standing. Spine. 1997 Nov 1;22(21):2571-4.

Luk KD, Chow DH, Holmes A. Vertical instability in spondylolisthesis: a traction radiographic assessment technique and the principle of management. Spine. 2003 Apr 15;28(8):819-27.

Mac-Thiong JM, Labelle H, Poitras B, Rivard CH, Joncas J. The effect of intraoperative traction during posterior spinal instrumentation and fusion for adolescent idiopathic scoliosis. *Spine.* 2004 Jul 15;29(14):1549-54. Review.

Mac-Thiong JM, Labelle H, Petit Y, Aubin CE. The effect of the Relton-Hall operative frame on trunk deformity in adolescent idiopathic scoliosis. Eur Spine J. 2002 Dec;11(6):556-60. Epub 2002 Aug 7

Majdouline Y, Aubin CE, Robitaille M, Sarwark JF, Labelle H. Scoliosis correction objectives in adolescent idiopathic scoliosis. *J Pediatr Orthop.* 2007 Oct-Nov;27(7):775-81.

Marsicano JG, Lenke LG, Bridwell KH, Chapman M, Gupta P, Weston J. The lordotic effect of the OSI frame on operative adolescent idiopathic scoliosis patients. *Spine.* 1998 Jun 15;23(12):1341-8.

Mayo AE, Labrom RD, Askin GN, Adam CJ. A biomechanical study of top screw pullout in anterior scoliosis correction constructs. Spine (Phila Pa 1976). 2010 Jun 1;35(13):E587-95.

Mazel C, Zrig M, Antonietti P, de Thomasson E. [Impaction posterior wedge osteotomy for the treatment of postsurgical flatback: 22 cases]. Rev Chir Orthop Reparatrice Appar Mot. 2005 Oct;91(6):530-41.

Mokhbi Soukane D, Shirazi-Adl A, Urban JP. Investigation of solute concentrations in a 3D model of intervertebral disc. Eur Spine J. 2009 Feb;18(2):254-62.

Nash CL Jr, Moe JH. A study of vertebral rotation. J Bone Joint Surg Am. 1969 Mar;51(2):223-9.

Novosad J, Cheriet F, Petit Y, Labelle H. Three-dimensional (3-D) reconstruction of the spine from a single X-ray image and prior vertebra models. IEEE *Trans Biomed Eng.* 2004 Sep;51(9):1628-39.

O'Brien MF, Kuklo TR, Blanke KM, et al. Spinal Deformity Study Group–Radiographic Measurement Manual. Minneapolis, MN: Medtronic Sofamor Danek, Inc; 2005.

Panjabi M, Brand R and White A, Three-dimensional flexibility and stiffness properties of the human thoracic spine. *Journal of Biomechanics* (1976), pp. 185–192.

Papini M, Zdero R, Schemitsch EH, Zalzal P. The biomechanics of human femurs in axial and torsional loading: comparison of finite element analysis, human cadaveric femurs, and synthetic femurs. *J Biomech Eng.* 2007 Feb;129(1):12-9.

Pearsall DJ, Reid JG, Livingston LA. Segmental inertial parameters of the human trunk as determined from computed tomography. Ann Biomed Eng. 1996 Mar-Apr;24(2):198-210.

Penning L. Acceleration injury of the cervical spine by hypertranslation of the head. Eur Spine J. 1992 June;1(1): 13-19.

Petit Y, Aubin CE, Labelle H. Patient-specific mechanical properties of a flexible multi-body model of the scoliotic spine. Med Biol Eng Comput. 2004 Jan;42(1):55-60.

Polly Jr., D.W., Sturm, P.F, 1998. Traction versus supine side bending. Which technique best determines curve flexibility? *Spine* 23, 804-808.

Price CT, Scott DS, Reed FE Jr, Riddick MF. Nighttime bracing for adolescent idiopathic scoliosis with the Charleston bending brace. Preliminary report. Spine. 1990 Dec;15(12):1294-9.

Relton JE, Hall JE. An operation frame for spinal fusion. A new apparatus designed to reduce haemorrhage during operation. J Bone Joint Surg Br. 1967 May;49(2):327-32

Rinella A, Lenke L, Whitaker C, Kim Y, Park SS, Peelle M, Edwards C 2nd, Bridwell K. Perioperative halo-gravity traction in the treatment of severe scoliosis and kyphosis. Spine (Phila Pa 1976). 2005 Feb 15;30(4):475-82.

Roberts SB, Chen PH. Elastostatic analysis of the human thoracic skeleton. J Biomech. 1970 Nov;3(6):527-45.

Sadiq S, Meir A, Hughes SP. Surgical management of spondylolisthesis overview of literature. Neurol India. 2005 Dec;53(4):506-11.

Scaglietti O, Frontino G, Bartolozzi (1976) Technique of anatomical reduction of lumbar pondylolisthesis and its surgical stabilization. Clin Orthop Relat Res (117):165-75.

Schoberth H. Sitzhaltung, sitzschaden, sitzmobel. Berlin: Springer Verlag; 1962.

Schonauer C, Bocchetti A, Barbagallo G, Albanese V, Moraci A. Positioning on surgical table. Eur Spine J. 2004 Oct;13 Suppl 1:S50-5.

Schultz AB, Miller JAA. Biomechanics of the human spine. In: Mow VC, Hayes WC, editors. Basic orthopedic biomechanics. New York: Raven Press; 1991.

Shirazi-Adl A, Ahmed AM, Shrivastava SC. A finite element study of a lumbar motion segment subjected to pure sagittal plane moments. J Biomech. 1986;19(4):331-50.

Shultz, A. Galante, J. A mathematical Model for the Study of the Mechanics of the Human Vertebrae. 1970 J Biomech 1970;3:405.

Skalli W, Robin S, Lavaste F, Dubousset J. A biomechanical analysis of short segment spinal fixation using a three-dimensional geometric and mechanical model. Spine (Phila Pa 1976). 1993 Apr;18(5):536-45.

Sobottke R, Siewe J, Hokema J, Schlegel U, Zweig T, Eysel P. Scoliosis surgery: correction not correlated with instrumentation, quality of life not correlated with correction or instrumentation. Acta Orthop Belg. 2010 Aug;76(4):536-42.

Stagnara P, De Mauroy JC, Dran G, Gonon GP, Costanzo G, Dimnet J, Pasquet A. Reciprocal angulation of vertebral bodies in a sagittal plane: approach to references for the evaluation of kyphosis and lordosis. Spine. 1982 Jul-Aug;7(4):335-42.

Stephens GC, Yoo JU, Wilbur G. Comparison of lumbar sagittal alignment produced by different operative positions. Spine. 1996 Aug 1;21(15):1802-6; discussion 1807.

Stewart DG Jr, Skaggs DL. Consultation with the specialist: adolescent idiopathic scoliosis. Pediatr Rev. 2006 Aug;27(8):299-306.

Stokes IA, Abery JM. Influence of the hamstring muscles on lumbar spine curvature in sitting. *Spine*. 1980 Nov-Dec;5(6):525-8.

Stokes IA, Laible JP. Three-dimensional osseo-ligamentous model of the thorax representing initiation of scoliosis by asymmetric growth. J Biomech. 1990;23(6):589-95.

Sucato DJ, Agrawal S, O'Brien MF, Lowe TG, Richards SB, Lenke L (2008) Restoration of thoracic kyphosis after operative treatment of adolescent idiopathic scoliosis: a multicenter comparison of three surgical approaches. Spine 33(24):2630-6

Tafazzoli F, Lamontagne M. Mechanical behaviour of hamstring muscles in low-back pain patients and control subjects. Clin Biomech (Bristol, Avon). 1996 Jan;11(1):16-24.

Takemura Y, Yamamoto H, Tani T. Biomechanical study of the development of scoliosis, using a thoracolumbar spine model. J Orthop Sci. 1999;4(6):439-45.

Tan SB, Kozak JA, Dickson JH, Nalty TJ. Effect of operative position on sagittal alignment of the lumbar spine. Spine. 1994 Feb 1;19(3):314-8.

Tarlov I. The knee-chest position for lower spinal operations. J Bone Joint Surg [Am] 1967;49:1193-4.

Torell G, Nachemson A, Haderspeck-Grib K, Schultz A. Standing and supine Cobb measures in girls with idiopathic scoliosis. *Spine*. 1985 Jun;10(5):425-7.

Van Deursen DL, Lengsfeld M, Snijders CJ, Evers JJ, Goossens RH. Mechanical effects of continuous passive motion on the lumbar spine in seating. J Biomech. 2000 Jun;33(6):695-9.

Van Herp G, Rowe P, Salter P, Paul JP. Three-dimensional lumbar spinal kinematics: a study of range of movement in 100 healthy subjects aged 20 to 60+ years. Rheumatology (Oxford). 2000 Dec;39(12):1337-40.

Vialle R, Levassor N, Rillardon L, Templier A, Skalli W, Guigui P. Radiographic analysis of the sagittal alignment and balance of the spine in asymptomatic subjects. J Bone Joint Surg Am. 2005 Feb;87(2):260-7.

Viceconti M, From: The BEL Repository, "http://www.tecno.ior.it/VRLAB/".

Viceconti, M, International Congress on Computational Bioengineering, M. Doblaré, et al, Eds., Zaragoza, Sept. 24-26,(2003) and: http://www.tecno.ior.it/VRLAB/researchers/repository/BEL_repository.html

Villemure I, Aubin CE, Dansereau J, Labelle H. Biomechanical simulations of the spine deformation process in adolescent idiopathic scoliosis from different pathogenesis hypotheses. Eur Spine J. 2004 Feb;13(1):83-90.

Voor MJ, Roberts CS, Rose SM, Glassman SD. Biomechanics of in situ rod contouring of short-segment pedicle screw instrumentation in the thoracolumbar spine. J Spinal Disord. 1997 Apr;10(2):106-16.

Voutsinas SA, MacEwen GD. Sagittal profiles of the spine. Clin Orthop Relat Res. 1986 Sep;(210):235-42.

Whelan, B.M., McBratney, A.B., and Minasny, B., 2001. Vesper – Spatial prediction software for precison agriculture. In: ECPA 2001. Third European Conference on Precision Agriculture. (G. Grenier, S. Blackmore Eds.) pp. 139-144. Agro Montpellier, Ecole Nationale Agronomique de Montpellier.

White SC, Yack HJ, Winter DA. A three-dimensional musculoskeletal model for gait analysis. Anatomical variability estimates. *J Biomech.* 1989;22(8-9):885-93.

White, A. A. and Panjabi M.M. *Clinical Biomechanics of the Spine* – 2nd Edition. J.B. Lipincott Co. USA, 1990

Winter D.A., Biomechanics and Motor Control of Human Movement, Second edition. John Wiley & Sons, Inc., Toronto, 1990.

Xu RM, Sun SH, Ma WH, Liu GY, Gu YJ, Huang L, Ying JW, Jiang WY. Analysis of complications in scoliosis surgery. Zhongguo Gu Shang. 2008 Apr;21(4):245-8. Chinese.

Yazici M, Acaroglu ER, Alanay A, Deviren V, Cila A, Surat A. Measurement of vertebral rotation in standing versus supine position in adolescent idiopathic scoliosis. *J Pediatr Orthop*. 2001 Mar-Apr;21(2):252-6.

Zhang D, Song Y. The finite element analysis of lumbar fusions. Zhongguo Xiu Fu Chong Jian Wai Ke Za Zhi. 2006 Apr;20(4):400-3.

Zhang LQ, Nuber G, Butler J, Bowen M, Rymer WZ. In vivo human knee joint dynamic properties as functions of muscle contraction and joint position. J Biomech. 1998 Jan;31(1):71-6.

ANNEX 1 THE RELATIONSHIP BETWEEN HIP FLEXION/EXTENSION AND THE SAGITTAL CURVES OF THE SPINE

The Relationship Between Hip Flexion/Extension and the Sagittal Curves of the Spine

Published in: Stud Health Technol Inform. 2008;140:90-5.

Christopher DRISCOLL[1,2], Carl-Eric AUBIN[1,2], Hubert LABELLE[2], Jean DANSEREAU[1]

1 – Dept. of Mechanical Engineering, École Polytechnique de Montréal P.O. Box 6079, Station Centre-Ville Montréal, Québec, H3C 3A7, Canada
2 – Saint-Justine University Hospital Center 3175 Cote-Ste-Catherine Rd. Montreal, Quebec, H3T 1C5, Canada

Abstract. The objective of this study was to develop a finite element model in order to study the relationship between hip flexion/extension and the sagittal curves of the spine. A previously developed FEM of the spine, rib cage and pelvis personalized to the 3D reconstructed geometry of a patient using biplanar radiographs was adapted to include the lower limbs including muscles. Simulations were performed to determine: the relationship between hip flexion / extension and lumbar lordosis / thoracic kyphosis, the mechanism of transfer between hip flexion / extension and pelvic rotation, and the influence that knee bending, muscle stiffness, and muscle mass have on the degree to which sagittal spinal curves are modified due to lower limb positioning. Preliminary results showed that the model was able to accurately reproduce published results for the modulation of lumbar lordosis due to hip flexion; which proved to linearly decrease 68% at 90^o of flexion. Additional simulations showed that the hamstrings and gluteal muscles were responsible for the transmission of hip flexion to pelvic rotation with the legs straight and flexed respectively, and the important influence of knee bending on lordosis modulation during lower limb positioning. The knowledge gained through this study is intended to be used to improve operative patient positioning.

Keywords: surgical positioning, lower limbs, spine, scoliosis, biomechanics, finite element modeling.

Introduction

Patient positioning is increasingly being recognized as an important step in spinal surgeries[1,2,3]. One of the most important desired outcomes of spinal instrumentation surgeries is preservation / restoration of sagittal balance[4], which can improve long term fusion results[5,6]. The relationship between hip flexion and lumbar lordosis has been studied by Stephen et al.[7] on the Andrews frame and Befanti et al.[8] on the Wilson frame who concluded that that hip flexion results in a loss of lumbar lordosis and that the correlation between the two is subject to inter-patient variability. As a general rule hips should not be flexed greater than 30^o in order to maintain sufficient lumbar lordosis to avoid flat back symptoms. The influence of lower limb positioning on thoracic kyphosis has received little attention. The mechanism of transfer between lower limb positioning and resulting geometrical changes to the spine has not been properly defined. Stokes et al.[9] have reported on the influence of the hamstring muscles on lumbar lordosis in sitting while others have reported on the possible contribution of the gluteal muscles with knees flexed[10]. Finite element modeling (FEM) has been previously used to study the impact of patient positioning on the geometry of the vertebral column. Duke et al.[2] looked at the impact of dynamic positioning parameters on the geometry of the vertebral column using a FEM, the impact of lower limb positioning was simulated through the modulation of pelvic inclination +/- 15^o.

The objective of this study is to develop a patient-specific FEM which is able to simulate the impact of lower limb positioning on the geometry of the spine. It is hypothesized that manipulation of lower limb position, hip and knee flexion/extension, can significantly impact lumbar lordosis and thoracic kyphosis. It is also hypothesized that the mechanism of transfer between lower limb positioning and pelvic angle modulation includes both the hamstring and gluteal muscles groups and is dependent on the degree of knee flexion.

Materials and Methods

A previously developed simplified global beam FEM of the spine, rib cage and pelvis[11] which uses a biplanar reconstruction technique[12] to obtain patient specific geometry was adapted to include the lower limbs. Complementary detailed geometry of the femur, tibia, and fibula was taken from Visible Human Project (VHP) data with scaling based on anthropological equations factoring height and sex[13]. A total of 31 muscles per leg were modeled with origins and insertions obtained by mapping of the coordinates defined by White et al.[14]. Lower limb muscle cross-sectional data and material properties were taken from literature[15,16]. Hip and knee joints were represented as well as ligaments. In all, the model contains 1790 nodes and 1247 elements (Figure A1).

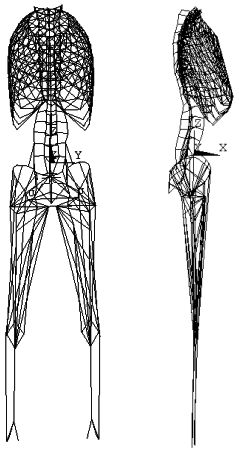

Figure A1.1: Frontal and Lateral Views of the FEM developed

Simulations were performed in order to evaluate the model's ability to reproduce published results for loss of lumbar lordosis due to hip flexion[5,6]. The geometric reconstruction of a healthy young male subject taken from the databases at Sainte-Justine University Hospital measuring 150 cm with an initial L1-S1 lordosis of 44° and a T4-T12 kyphosis of 31° was used for this and subsequent simulations. Hamstring muscle initial strains were uniformly adjusted such that the percent loss of lumbar lordosis obtained through FEM simulations matched the average results obtained by Befanti et al.[6] for 30° of hip flexion. These conditions were maintained and additional simulations performed for 60° and 90° hip flexion with the results compared to the averages obtained by Stephen et al.[5] in similar conditions.

A sensitivity study was performed in order to determine the relative impact that hamstring muscle initial strain (representing flexibility), cross-sectional area, and elastic modulus have on the degree to which hip flexion impacts the sagittal profile of the spine. 30° hip flexion simulations were performed while varying hamstring muscle initial strain 0-10%, doubling and halving cross-sectional area baseline values, and elastic modulus +/- 50% their baseline value.

In order to evaluate the muscles responsible for transmission of lower limb positioning to pelvic rotation and the impact of knee flexion on this relationship, hip flexion / extension simulations were performed, over their respective ranges of motion[17], at intervals of 20° while maintaining the knees different degrees of flexion 0°, 30°, 60°, and 90°. In each case, the resultant impacts on lordosis, kyphosis, and lower limb muscle strains were recorded.

Muscles with strains exceeding their initial strain were considered stretched and to contribute passively to the transfer of lower limb positioning to pelvic rotation.

Results

The results of the model validation based on published references are outlined in Table A1. They were obtained for a uniform hamstring initial strain of 4%.

Table A1.1: Validation of the relationship between hip flexion and loss of lumbar lordosis

	L1-S1 Lumbar Lordosis	
Hip Flexion	Simulated Results	Published values[5,6]
30°	33°	33°
60°	24°	23°
90°	14°	15°

The sensitivity study demonstrated that the most influential factor impacting the degree to which hip flexion impacts the sagittal profile of the spine is muscle flexibility; a 5% increase in hamstring initial strain caused an additional 9% reduction of lordosis at 30° of hip flexion. The impacts of muscle cross-sectional area and elastic modulus were less important; doubling cross-sectional area and elastic modulus respectively caused an additional 4% and 6% loss of lumbar lordosis.

The muscles found to be responsible for the transmission of straight leg hip flexion to pelvic rotation were the hamstrings (semimembranosus, biceps femoris long head). Once knee flexion reached approximately 60°, the gluteals (gluteus medius) started increasingly contributing. The primary muscles responsible for the transmission of hip extension to pelvic rotation are the anterior thigh muscles (rectus femoris, satorius, vastus medialis, tensor fasciae latae) up until the maximum hip range of motion. The degree of knee flexion (0° to 90°) for 30° hip flexion simulations contributed to additional modification of lordosis of 14%.

The impact of lower limb positioning (90° of flexion to 30° of extension, while maintaining the knees at 30° of flexion) on lordosis (L) and kyphosis (K) is outlined in Figure A2.

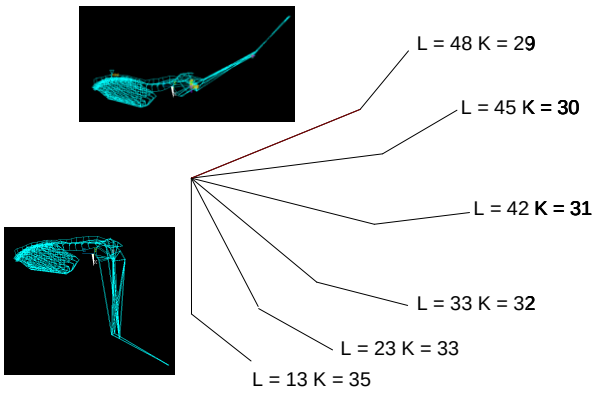

Figure A1.2: Impact of Lower Limb Positioning on a Newly Developed Surgical Frame

Discussion

One aspect of the model, which remains to be validated, is its ability to accurately reproduce the impact of hip extension on spinal geometry. Since no literary data was available, anterior thigh muscles were given the same initial strain determined for the hamstring muscles. Due to the nature of beam FEMs not all origin and insertion

coordinates coincided with an anatomical representation, specifically with regards to the un-represented ilium, and had to be translated to the nearest available element. However, this factor was assumed to negligibly impact the results as the translation distances did not exceed 4 cm.

The results obtained for the mechanism of transfer between hip flexion and pelvic rotation is in agreement with those proposed in literature. This study was able to show which muscles of the hamstring and gluteal groups are responsible for this transmission and at what degree of knee flexion does the transmission from the hamstrings to gluteals take place.

The inter-patient variability found in literature with regards to lumbar lordosis modulation with hip flexion can be attributed to individual lower limb flexibilities. It is proposed that any attempt made to predict patient specific modulation of spinal geometry due to lower limb positioning incorporate clinical flexibility testing data into personalized FEMs.

Conclusion

The FEM developed has shown good agreement with published results in its ability to reproduce the impact of lower limb positioning on spinal geometry in a patient-specific manner. Its exploitation has allowed for a more detailed study of the mechanisms of transfer and influential factors between lower limb positioning and spinal geometry than has been previously reported in literature. It is believed that the use of surgical frames which allow lower limb positioning in conjunction with knowledge of how lower limb positioning impacts patient specific spinal geometry can be used in order to facilitate an improve upon current operating procedures.

References

[1] Schonauer C, Bocchetti A, Barbagallo G, Albanese V, Moraci A. Positioning on surgical table. Eur Spine J. 2004 Oct;13 Suppl 1:S50-5. Epub 2004 Jun 22. Review.
[2] Duke K, Aubin CE, Dansereau J, Labelle H. Computer simulation for the optimization of patient positioning in spinal deformity instrumentation surgery. Med Biol Eng Comput. 2008 Jan;46(1):33-41.
[3] Delorme S, Labelle H, Poitras B, Rivard CH, Coillard C, Dansereau J. Pre-, intra-, and postoperative three-dimensional evaluation of adolescent idiopathic scoliosis. J Spinal Disord. 2000 Apr;13(2):93-101.
[4] Majdouline Y, Aubin CE, Robitaille M, Sarwark JF, Labelle H. Scoliosis correction objectives in adolescent idiopathic scoliosis. J Pediatr Orthop. 2007 Oct-Nov;27(7):775-81.
[5] Edwards CC, Levine AM. Complications associated with posterior instrumentation in the treatment of thoracic and lumbar injuries. In: Garfin SR, ed. Complications of Spine Surgery. Baltimore: Williams and Wilkins, 1989:164-99.
[6] Herkowitz HN. Lumbar spinal stenosis: Indications for arthrodesis and spinal instrumentation. Instructional Course Lectures 1994:43:425-33.
[7] Stephens GC, Yoo JU, Wilbur G. Comparison of lumbar sagittal alignment produced by different operative positions. Spine. 1996 Aug 1;21(15):1802-6; discussion 1807.
[8] Benfanti PL, Geissele AE. The effect of intraoperative hip position on maintenance of lumbar lordosis: a radiographic study of anesthetized patients and unanesthetized volunteers on the Wilson frame. Spine. 1997 Oct 1;22(19):2299-303.
[9] Stokes IA, Abery JM. Influence of the hamstring muscles on lumbar spine curvature in sitting. *Spine*. 1980 Nov-Dec;5(6):525-8.
[10] Tafazzoli F, Lamontagne M. Mechanical behaviour of hamstring muscles in low-back pain patients and control subjects. Clin Biomech (Bristol, Avon). 1996 Jan;11(1):16-24.
[11] Clin J, Aubin CE, Labelle H., Virtual prototyping of a brace design for the correction of scoliotic deformities. Med Biol Eng Comput. 2007 May;45(5):467-73.
[12] Delorme S, Petit Y, de Guise JA, Labelle H, Aubin CE, Dansereau J. Assessment of the 3-D reconstruction and high-resolution geometrical modeling of the human skeletal trunk from 2-D radiographic images. IEEE Trans Biomed Eng. 2003 Aug;50(8):989-98.
[13] Bhasin MK, Malik SL. Anthropology: Trends and Applications. New Delhi: Kamala-Raj Enterprises, 2002. p.141-147.
[14] White SC, Yack HJ, Winter DA. A three-dimensional musculoskeletal model for gait analysis. Anatomical variability estimates. J Biomech. 1989;22(8-9):885-93.
[15] Klein Horsman MD, Koopman HF, van der Helm FC, Prosé LP, Veeger HE. Morphological muscle and joint parameters for musculoskeletal modelling of the lower extremity. Clin Biomech (Bristol, Avon). 2007 Feb;22(2):239-47. Epub 2006 Nov 28.
[16] Kovanen V, Suominen H, Heikkinen E. Collagen of slow twitch and fast twitch muscle fibres in different types of rat skeletal muscle. Eur J Appl Physiol Occup Physiol. 1984;52(2):235-42.
[17] Luttgens, Kathryn and Hamilton, Nancy. Kinesiology : Scientific Basis of Human Motion. Madison, WI : Brown & Benchmark, 1997

Acknowledgements

Project funded by the Natural Sciences and Engineering Research Council of Canada (Industrial Research Chair Program, with Medtronic).

ANNEX 2 SPINAL GEOMETRY QUESTIONNAIRE

Desired Spinal Geometry for Surgical Procedures (18 Questions)

Background: The following questionnaire is meant to identify what would be the desired spinal geometry for different surgical procedures. That is to say, for various surgical procedures (e.g. pedicle screw insertion, diskectomy, etc.) how would you want the patient's spine to look (sagittal and coronal curves) to facilitate the procedure and/or benefit the patient. For example, in a diskectomy procedure Surgeon Sean wanted lumbar lordosis to be minimized in order to have better access through greater intervertebral disc angles and he didn't really care about the degree of kyphosis. In another example, in a bone grafting procedure on an instrumented scoliotic spine, Surgeon Sean wanted both lordosis and kyphosis to be in a natural state and Cobb angle to be minimized in order to ensure a good post-operative spinal balance. The context of the questionnaire is in the development of a new surgical frame which can modify the patient's spinal geometry intra-operatively. By knowing how surgeons would like the spinal geometry to look like in different situations, we will then be able to recommend how to adjust the surgical frame in order to achieve those geometries.

Note: A visualization tool has been provided at the end of the questionnaire.

1. Scoliosis

1.1 Pedicle Screw / Hook Insertion

1.1.1 What would be the desired sagittal profile of the spine during pedicle screw / hook insertion?

☐ Minimize both kyphosis and lordosis
☐ Maximize both kyphosis and lordosis
☐ Maximize kyphosis and minimize lordosis
☐ Minimize kyphosis and maximize lordosis
☐ Maintain patient's natural kyphosis and lordosis
☐ Sagittal profile does not impact pedicle screw / hook insertion
☐ Other, specify: _____

1.1.2 What would be the desired coronal profile of the spine during pedicle screw / hook insertion?

☐ Minimize Cobb angle
☐ Maximize Cobb angle
☐ Maintain patient's Cobb angle
☐ Cobb angle does not impact pedicle screw / hook insertion
☐ Other, specify: _____

1.2 Rod Insertion / correction maneuver

1.2.1 What would be the desired sagittal profile of the spine during rod insertion?

☐ Minimize both kyphosis and lordosis
☐ Maximize both kyphosis and lordosis
☐ Maximize kyphosis and minimize lordosis
☐ Minimize kyphosis and maximize lordosis
☐ Maintain patient's natural kyphosis and lordosis
☐ Sagittal profile does not impact rod insertion
☐ Other, specify: _____

1.2.2 What would be the desired coronal profile of the spine during rod insertion?

☐ Minimize Cobb angle
☐ Maximize Cobb angle
☐ Maintain patient's Cobb angle
☐ Cobb angle does not impact rod insertion
☐ Other, specify: _____

1.3 Grafting

1.3.1 What would be the desired sagittal profile of the spine during bone grafting?

☐ Minimize both kyphosis and lordosis
☐ Maximize both kyphosis and lordosis
☐ Maximize kyphosis and minimize lordosis
☐ Minimize kyphosis and maximize lordosis
☐ Maintain patient's natural kyphosis and lordosis
☐ Sagittal profile does not impact bone grafting
☐ Other, specify: _____

1.3.2 What would be the desired coronal profile of the spine during bone grafting?

☐ Minimize Cobb angle
☐ Maximize Cobb angle
☐ Maintain patient's Cobb angle
☐ Cobb angle does not impact bone grafting
☐ Other, specify: _____

2. Lumbar Spondylolisthesis

2.1 Pedicle Screw / Hook Insertion

2.1.1 What would be the desired sagittal profile of the spine during pedicle or lamina screw / hook insertion?

☐ Minimize lordosis
☐ Maximize lordosis
☐ Maintain patient's natural lordosis
☐ Lordosis does not impact pedicle or lamina screw / hook insertion
☐ Other, specify: _____

2.2 Rod /wiring / plate Insertion

2.2.1 What would be the desired sagittal profile of the spine during rod / wiring / plate insertion (if performed)?

☐ Minimize lordosis
☐ Maximize lordosis
☐ Maintain patient's natural lordosis
☐ Lordosis does not impact rod / wiring / plate insertion
☐ Other, specify: _____

2.3 Reduction

2.3.1 What would be the desired sagittal profile of the spine during vertebral reduction (if performed)?

☐ Minimize lordosis
☐ Maximize lordosis
☐ Maintain patient's natural lordosis
☐ Lordosis does not impact vertebral reduction
☐ Other, specify: _____

2.4 Grafting

2.4.1 What would be the desired sagittal profile of the spine during bone grafting?

☐ Minimize lordosis
☐ Maximize lordosis
☐ Maintain patient's natural lordosis
☐ Lordosis does not impact bone grafting
☐ Other, specify: _____

3. Hyperkyphosis

3.1 Pedicle Screw / Hook Insertion

3.1.1 What would be the desired sagittal profile of the spine during pedicle screw / hook insertion?

☐ Minimize kyphosis and lordosis

☐ Maximize kyphosis and lordosis
☐ Maximize kyphosis and minimize lordosis
☐ Minimize kyphosis and maximize lordosis
☐ Maintain patient's natural kyphosis and lordosis
☐ Sagittal profile does not impact pedicle screw / hook insertion
☐ Other, specify: _____

3.2 Rod Insertion

3.2.1 What would be the desired sagittal profile of the spine during rod insertion?

☐ Minimize kyphosis and lordosis
☐ Maximize kyphosis and lordosis
☐ Maximize kyphosis and minimize lordosis
☐ Minimize kyphosis and maximize lordosis
☐ Maintain patient's natural kyphosis and lordosis
☐ Sagittal profile does not impact rod insertion
☐ Other, specify: _____

3.3 Grafting

3.3.1 What would be the desired sagittal profile of the spine during bone grafting?

☐ Minimize kyphosis and lordosis
☐ Maximize kyphosis and lordosis
☐ Maximize kyphosis and minimize lordosis
☐ Minimize kyphosis and maximize lordosis
☐ Maintain patient's natural kyphosis and lordosis
☐ Sagittal profile does not impact bone grafting
☐ Other, specify: _____

4. Lumbar Herniated/Slipped/Degenerative disk

4.1 Discectomy

4.1.1 What would be the desired sagittal profile of the spine during the discectomy procedure (if performed)?

☐ Minimize lordosis
☐ Maximize lordosis
☐ Maintain patient's natural lordosis
☐ Lordosis does not impact discectomy procedure
☐ Other, specify: _____

4.2 Laminectomy

4.2.1 What would be the desired sagittal profile of the spine during the laminectomy procedure (if performed)?

☐ Minimize lordosis
☐ Maximize lordosis
☐ Maintain patient's natural lordosis
☐ Lordosis does not impact laminectomy procedure
☐ Other, specify: _____

4.3 Pedicle Screw / Hook Insertion

4.3.1 What would be the desired sagittal profile of the spine during pedicle screw / hook insertion (if performed)?

☐ Minimize lordosis
☐ Maximize lordosis
☐ Maintain patient's natural lordosis
☐ Lordosis does not impact pedicle screw / hook insertion
☐ Other, specify: _____

4.4 Rod / Wiring / Plate Insertion

4.4.1 What would be the desired sagittal profile of the spine during rod / wiring / plate insertion (if performed)?

☐ Minimize lordosis
☐ Maximize lordosis
☐ Maintain patient's natural lordosis
☐ Lordosis does not impact rod / wiring / plate insertion
☐ Other, specify: _____

4.5 Grafting

4.5.1 What would be the desired sagittal profile of the spine during bone grafting (if performed)?

☐ Minimize lordosis
☐ Maximize lordosis
☐ Maintain patient's natural lordosis
☐ Lordosis does not impact bone grafting
☐ Other, specify: _____

Visualization tool

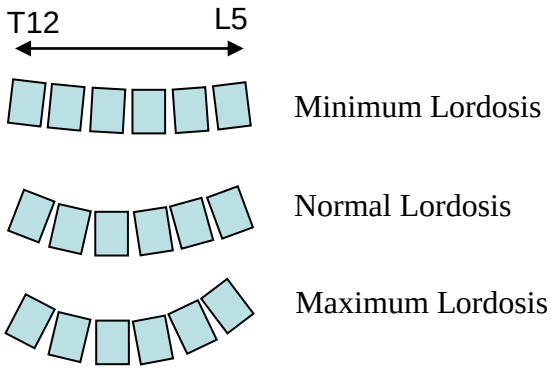
T12
L5
Minimum Lordosis
Normal Lordosis
Maximum Lordosis

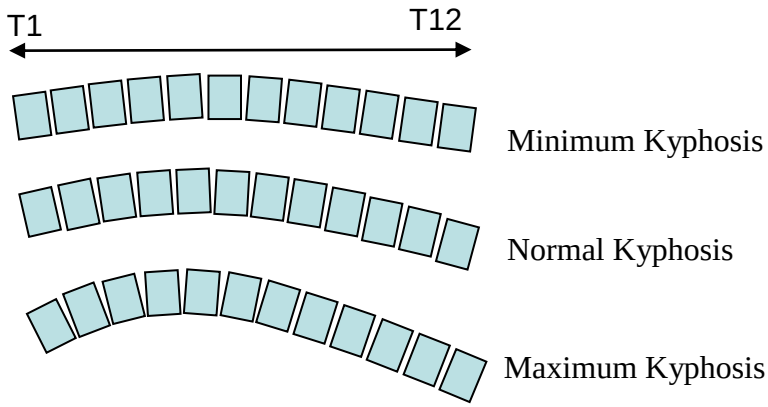
T1
T12
Minimum Kyphosis
Normal Kyphosis
Maximum Kyphosis

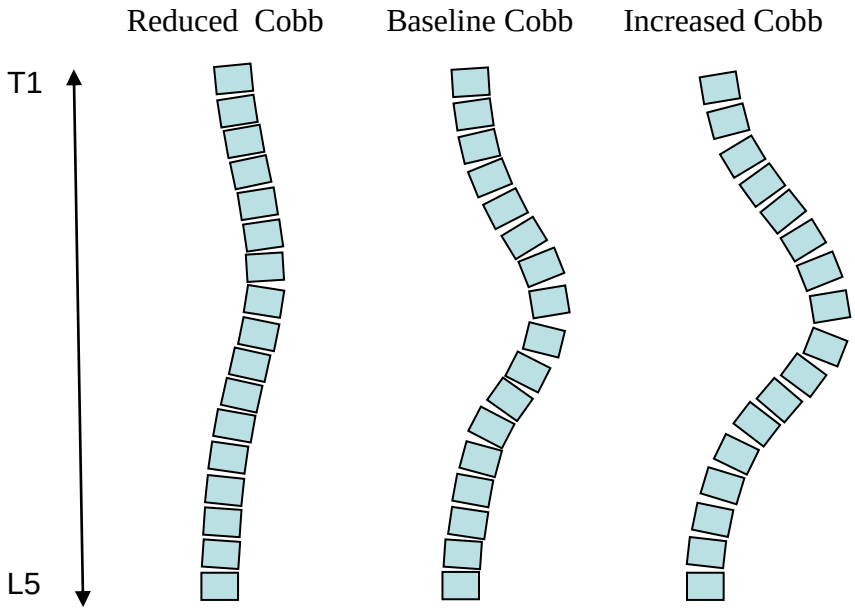
Reduced Cobb
Baseline Cobb
Increased Cobb
T1
L5

ANNEX 3 VOLUMETRIC FEM FOR THE STUDY OF PATIENT POSITIONING

Soft tissue was modeled over areas of possible contact with the surgical frame which included the anterior thoracic region, anterior pelvic/abdomen region, and anterior thigh region. Two layers of interconnected brick elements were used: a soft layer representing the dermis and hypodermis over a rigid substrate representing subcutaneous tissue such a muscle. The epidermis was not represented as it was assumed that it did not influence the skin's global mechanical behaviour. Dermis/hypodermis elastic modulus of 0.00625 N/mm^2 was taken from the work of Pailler-Mattei et al.[1] and substrate elastic modulus of 0.018 N/mm^2 was taken from an average literary muscle shear value[2,3,4]. An isotropic linear elastic behavior[5] was assumed over the limited deformation experienced during surgical positioning and both layers were given a Poisson's ratio of 0.425 from average published values[6,7,8] for soft tissue. Soft tissue distribution relative to bony landmarks was obtained from VHP transverse slices (Figure-C1) and linearly scaled such that the circumferences of the chest, pelvis, and thighs matched those measured for a given subject using a measuring tape. Thickness of the outer dermis/hypodermis layer was set based on the work of Agache et al.[9] (Table C1) who has tabulated data according to location and patient sex. The resultant substrate layer was limited to a maximum thickness of 50 mm which if exceeded was linked to bones with a matrix of undeformable beams in order to reduce computational cost (Figure-C2). While this approximation does not allow the calculation of deep tissue pressure levels, it is assumed that at the limited levels of skin deformation under investigation that the interface pressures obtained will be negligibly impacted.

Volumetric FEMs of the Relton-Hall frame and newly developed Multi-Functional Positioning Frame (MFPF) were developed. Geometry of the Relton-Hall cushions was directly measured and geometry of the MFPF cushions was taken directly from the CAD drawings. In all cases cushions were modeled using layered brick elements with elastic moduli obtained via indentation test for the Relton-Hall frame and directly from the cushion material manufacturer for the MFPF. Poison ratios were attributed a literary values for the given materials.

Surface-to-surface contact elements were modeled between the top surface of the surgical frame cushions and the corresponding possible contact zones on the outer layer of the patient model's skin. Static friction coefficients between the various surgical frame cushions and a hospital gown (typically worn during spinal surgeries) as well as between human skin and a hospital gown were experimentally measured using a sliding test (Figure-C3) with the lower of the two, skin-gown coefficient of 1.16 in all cases, applied to the model.

A scoliotic patient was placed in the prone position on the MFPF and the resultant cushion interface pressures measured using a force sensing array. A personalized FEM was then created for that patient and the prone position simulated. A comparison of the results can be visualized in Figure-C4. The FEM average pressures were within 10 mmHg of the experimental results, however, it predicted higher pressure peaks than were measured.

REFERENCES

1. Pailler-Mattei C, Bec S, Zahouani H. In vivo measurements of the elastic mechanical properties of human skin by indentation tests. Med Eng Phys. 2007 Sep 12; [Epub ahead of print].

2. Fujii K, Sato T, Kameyama K, Inoue I, Yokoyama K, Kobayashi K. Imaging hardness distribution in soft tissue in vivo using forced vibration and ultrasonic detection. *Acoust Imag Proc* 1994;21:253–8.

3. Levinson SF. Ultrasound propagation in anisotropic soft tissues: the application of linear elastic theory. *J Biomech* 1987;20:251–60.

4. Dresner MA, Rose GH, Rossman PJ, Muthupillai R, Manduca A, Ehman RL. Magnetic resonance elastography of skeletal muscle. *J Magn Reson Imaging* 2001;13:269–76.

5. Zhang M, Turner-Smith AR, Roberts VC. The reaction of skin and soft tissue to shear forces applied externally to the skin surface. *J Eng Med* 1994;208:217–22.

6. Kathyr F, Imberdis C, Vescovo P, Varchon D, Lagarde JM. Model of the viscoelastic behaviour of skin in vivo and study of anisotropy. Skin Res Technol 2004;10:93–103.

7. Hendriks FM, Brokken D,Van Eemeren J, Oomens CWJ, Baaijens FPT, Horsten JBAM. A numerical–experimental method to characterize the non linear mechanical behaviour of human skin. Skin Res Technol 2003;9:274–83.

8. Choi APC, Zheng YP. Estimation of Young's modulus and Poisson's ratio of soft tissue from indentation using two different-sized indentors: finite element analysis of the finite deformation effect. Med Biol Eng Comput 2005;43:258–64.

9. Agache P. Physiologie de la peau et exploitations fonctionnelles cutanees. Paris: Editions Medicales Internationales; 2000.

FIGURES AND TABLES

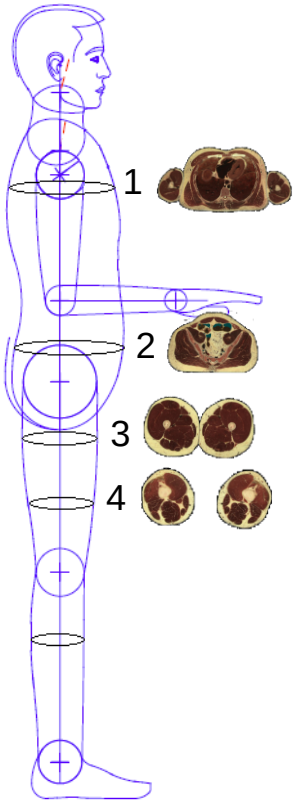

Figure A3.1: Experimental testing geometrical measurements with corresponding VHP slices (only male CS slices shown). Human figure modified from ergoforms.com & VHP slices modified from meddean.luc.edu/lumen/MedEd/GrossAnatomy/vhp/visible.htm)

Table A3.1: Dermis / Hypodermis Thicknesses

Location	Thickness (mm)	
	Male	Female
Anterior Chest	1.92	1.77
Abdomen	1.88	1.62
Anterior Thigh	1.59	1.42

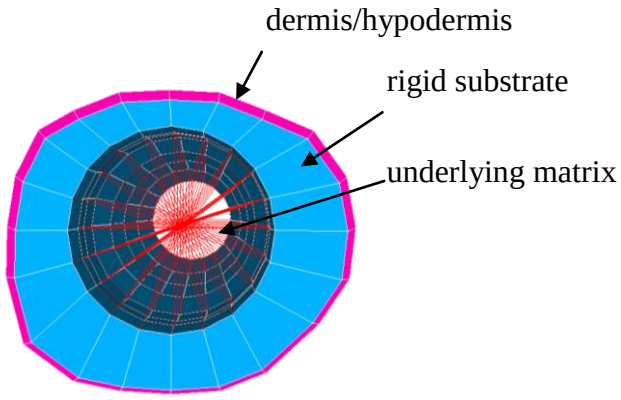

Figure A3.2: Cross-section of the FEM thigh showing the different layers of soft tissue representation

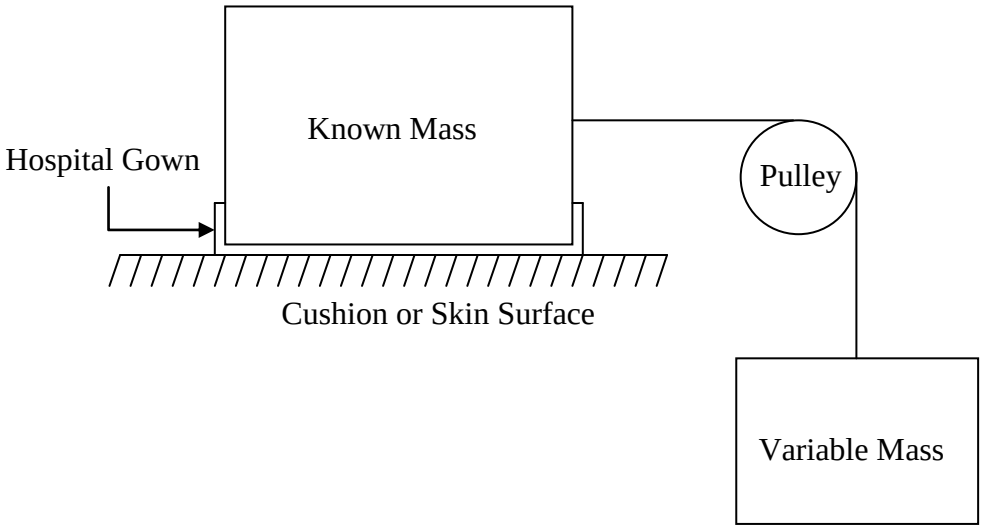

Figure A3.3: Friction coefficient Experimental Setup

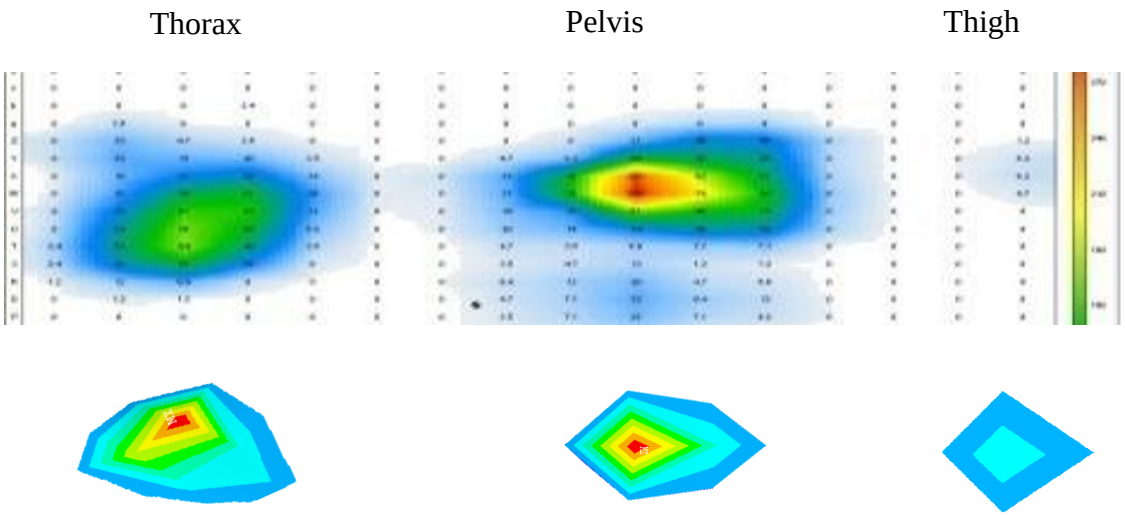

Figure A3.4: Comparison of interface pressures measured with a force sensing array (top) and simulated with the FEM (bottom)